ISTANBUL TECHNICAL UNIVERSITY ★ GRADUATE SCHOOL

COMPREHENSIVE ASSESSMENT OF DECENTRALIZED STORMWATER SYSTEMS IN URBANIZED AREAS UNDER CLIMATE CHANGE AND WATERSHED CHARACTERISTICS

Ph.D. THESIS

Sina SAM

Department of Civil Engineering

Hydraulics and Water Resources Engineering Programme

DECEMBER 2024

ISTANBUL TECHNICAL UNIVERSITY ★ GRADUATE SCHOOL

COMPREHENSIVE ASSESSMENT OF DECENTRALIZED STORMWATER SYSTEMS IN URBANIZED AREAS UNDER CLIMATE CHANGE AND WATERSHED CHARACTERISTICS

Ph.D. THESIS

Sina SAM
(501192502)

Department of Civil Engineering

Hydraulics and Water Resources Engineering Programme

Thesis Advisor: Prof. Dr. Mehmet ÖZGER

DECEMBER 2024

ISTANBUL TEKNİK ÜNİVERSİTESİ ★ LİSANSÜSTÜ EĞİTİM ENSTİTÜSÜ

ŞEHİRLEŞMİŞ BÖLGELERDE İKLİM DEĞİŞİKLİĞİ VE HAVZA ÖZELLİKLERİ ALTINDA MERKEZİ OLMAYAN YAĞMUR SUYU SİSTEMLERİNİN KAPSAMLI DEĞERLENDİRMESİ

DOKTORA TEZİ

Sina SAM
(501192502)

İnşaat Mühendisliği Anabilim Dalı

Hidrolik ve Su Kaynakları Mühendisliği Programı

Tez Danışmanı: Prof. Dr. Mehmet ÖZGER

ARALIK 2024

Sina SAM, a Ph.D. student of İTU Graduate School student ID 501192502, successfully defended the thesis/dissertation entitled "COMPREHENSIVE ASSESSMENT OF DECENTRALIZED STORMWATER SYSTEMS IN URBANIZED AREAS UNDER CLIMATE CHANGE AND WATERSHED CHARACTERISTICS", which he prepared after fulfilling the requirements specified in the associated legislations, before the jury whose signatures are below.

Thesis Advisor : **Prof. Dr. Mehmet ÖZGER** ....
İstanbul Technical University

Jury Members : **Assoc. Prof. Dr. Mahmut Ekrem KARPUZCU** ....
Istanbul Technical University

Assist. Prof. Dr. Mustafa NURİ ....
Istanbul Gelişim University

Assoc. Prof. Dr. Tarkan ERDIK ....
Istanbul Technical University

Prof. Dr. Hayrullah AĞAÇCIOĞLU ....
Yıldız Technical University

Date of Submission : 10 December 2024
Date of Defense : 30 December 2024

To my beloved wife,

FOREWORD

Flooding in urbanized watersheds poses significant challenges, disrupting daily life, damaging infrastructure, and threatening public safety. Addressing these issues demands sustainable and innovative approaches to mitigate the risks effectively and adapt to changing environmental conditions. This thesis delves into such solutions, contributing to the growing body of knowledge in sustainable urban flood management.

In this foreword, I take the opportunity to extend my deepest gratitude to my advisor, Prof. Dr. Mehmet ÖZGER, for his support, contributions, and insightful guidance throughout my PhD journey. His welcoming attitude has always made it easier to seek advice, exchange ideas, and grow as a researcher. I am also sincerely thankful to the jury members of my thesis, Assoc. Prof. Dr. Mahmut Ekrem KARPUZCU and Assist. Prof. Dr. Mustafa NURİ, for their constructive comments and valuable guidance. I would also like to thank Prof. Dr. Abdüsselam ALTUNKAYNAK for his consistent support during my graduate studies.

A special thanks goes to my beloved wife, Deniz SAM, whose support and companionship have made reaching this milestone possible. I am deeply grateful for her dedication, patience, and encouragement, which enabled me to persevere and complete this chapter in my academic life.

I would also like to thank Dr. Sara SAMUEI and Dr. Peyman ANSARİ for generously sharing their academic and professional experiences, which enriched my understanding and approach. Finally, I owe a great debt of gratitude to my parents, who have always been my pillars of support, providing love, motivation, and encouragement in all my endeavors.

Lastly, I would like to acknowledge and appreciate the scholarship support provided by the Coordination Unit for Scientific Research Projects at Istanbul Technical University (BAP, Project ID: 45103).

December 2024 Sina SAM

TABLE OF CONTENTS

Page

ABBREVIATIONS

AHP	: Analytic Hierarchy Process
CORINE	: Coordination of information on the environment
CR	: Consistency Ratio
CSO	: Combined Sewer Overflow
DEM	: Digital Elevation Model
DSI	: Directorate General for State Hydraulic Works
EPA	: Environmental Protection Agency
GCOP	: General Purpose Constrained Optimization Platform
GI	: Green Infrastructure
GIS	: Geographic Information Systems
IBB	: Istanbul Metropolitan Municipality
IPCC	: Intergovernmental Panel on Climate Change
ITA	: Innovative Trend Analysis
LID	: Low Impact Development
MCDA	: Multi-Criteria Decision Analysis
MK	: Mann-Kendall test
OSTRICH	: Optimization Software Tool for Research Involving Computational Heuristics
SuDS	: Sustainable Drainage Systems
SWMM	: Storm Water Management Model

SYMBOLS

A_x	: Area of the subcatchment
α	: Significance level
β	: Sen's slope estimator value
C	: Hazen-Williams coefficient
CR	: Consistency Ratio
D	: Trend Indicator in the ITA method
d	: Pipe diameter
d_s	: Subcatchment depression storage
e	: Evaporation rate
F	: Cumulative infiltration
f	: Infiltration to the sub-soil rate
(Ha)	: Alternative hypothesis
(H0)	: Null hypothesis
h_f	: Friction loss
i	: Rainfall or snowmelt rate
K_s	: Saturated hydraulic conductivity
L	: Pipe length
Ψ_s	: Capillary suction head along the wetting front
Q, q	: Volumetric flow rate
RI	: Random index
R_x	: Hydraulic radius
S	: Trend existence indicator in the MK method
s	: Subcatchment slope
τ	: Time of the change point in time series
θ_d	: Initial moisture deficit
$U_{t,T}$	: The change point in time series
W	: Subcatchment width
Z	: Indicator of the significance of the trend in the MK method

LIST OF TABLES

Page

LIST OF FIGURES

Page

COMPREHENSIVE ASSESSMENT OF DECENTRALIZED STORMWATER SYSTEMS IN URBANIZED AREAS UNDER CLIMATE CHANGE AND WATERSHED CHARACTERISTICS

SUMMARY

This PhD thesis comprehensively assesses decentralized stormwater management systems within a highly urbanized and flood-prone watershed in Istanbul. Although decentralized systems occupy a vast range of measures in different types, this research focuses on the performance of three kinds of these systems including Rain Barrels, Cisterns, and Drywells in urban runoff mitigation under the climate change and physical characteristics of the subjected watershed. The aforementioned systems are denoted in this thesis with capital initial letters as RB, CI and DW respectively. The study is structured into two main phases: climate assessment and model development, each contributing vital insights into sustainable urban water management.

The climate assessment phase analyzed precipitation and temperature trends in Istanbul using data from a ground-based meteorological station, MERRA-2 temperature reanalysis, and IMERG precipitation estimations. Three non-parametric methods including the Mann-Kendall (MK) test, Sen's slope estimator, and Innovative Trend Analysis (ITA) were employed to identify the magnitude and direction of the possible trends.

The reason for using different data sources and methods is to provide a comprehensive comparison between ground-based meteorological data with space-based weather observatory products and different methods that are used in trend analysis of hydrometeorological variables. This comparison is believed to provide valuable insights toward trend analysis of hydrometeorological variables and assist the transition process from traditional toward more novel data sources and methods in this field of study.

Results of the first phase of the study revealed significant upward trends in temperature on seasonal and annual scales, with summer exhibiting the strongest increase followed by the spring, fall, and winter seasons. Conversely, multi-duration analysis using the ITA method identified intervals of decreasing trends, particularly between 1980 and 1999, except during summer. A distinctive upward trend re-emerged in the 2000–2019 interval.

Precipitation trends were less consistent compared to the temperature, with single-duration analysis indicating significant increases during fall and summer but insignificant decreases during winter and spring. Annual analysis also resulted in significant increases in the precipitation trend. The multi-duration analysis uncovered more nuanced trends, including significant seasonal variations in specific intervals.

The compliance against ground-based data was at a higher level in MERRA-2 data compared to the IMERG data. Especially weak results were observed in the trend analysis of precipitation in the spring season and high-value group of the fall season

based on the IMERG data. In the same vein, the ITA method proved to be particularly effective for detecting sub-trends in temperature and precipitation data across different value groups, offering a graphical advantage over MK and Sen’s slope methods. This capacity is critical for analyzing short-term variations and hydrometeorological extremes in densely populated megacities like Istanbul.

In the model development phase, the highly urbanized Ayamama watershed in Istanbul which is known for its dreadful flood history in 2009, was selected as the study area. In this phase of the study, based on the climate assessment findings, Rain Barrel (RB), Cistern (CI), and Drywell (DW) units were selected for implementation in the hydrologic model of the study area due to their retention and infiltration capabilities. These systems can assist in addressing the water shortage due to increasing temperature and evaporation and also act as an auxiliary tool for mitigating runoff due to increasing precipitations in the city. A robust framework then was developed to integrate the design, implementation, and simulation of the aforementioned decentralized stormwater management units in the Ayamama watershed, using a combination of geospatial data, hydrologic-hydraulic modeling, and expert-driven decision-making.

First, a physically based model was constructed using the Storm Water Management Model (SWMM), calibrated and validated through an auto-calibration process with OSTRICH optimization software. For calibration, water level data from the main drainage channel in the study area for different rainfall events were obtained from the Istanbul Metropolitan Municipality (IBB). These data were compared with the channel water levels generated by the simulation of the same rainfall events in the SWMM model. The automatic calibration process minimized the difference between the water level obtained from the simulation and the actual water level measured in the channel, thereby significantly improving the model's accuracy. This process was fully automated and carried out using the OSTRICH optimization software. As a result of the calibration, the Nash-Sutcliffe Efficiency Coefficient (NSE) values of 0.77 and 0.67 were achieved for the calibrated and validated models respectively, indicating a good agreement between the simulated and measured water depth in the channel.

In this study, blind implementations without any logical reason are avoided. This means that a strict strategy is employed to determine the number, location, and type of decentralized stormwater management units to be implemented in the study area. To identify suitable locations for RB, CI, and DW implementation, a multi-criteria decision analysis was conducted by using the Analytical Hierarchy Process (AHP). In this process a survey was conducted with 10 participating experts to fill out three pairwise comparison matrices for RB, CI, and DW units based on a 1-9 Likert scale. This approach established practical thresholds for the number of units, balancing spatial, hydrological, and environmental constraints. Consequently, the initially defined maximum number of units to be implemented in the study area which was calculated only based on the available residential and industrial areas was reduced by 30.4%, 20%, and 57.2%, respectively for RB, CI, and DW units, ensuring optimal functionality and alignment with site conditions.

The key findings of the second phase of this study can be summarized below:

In the sensitivity analysis, model calibration, and validation stage, the most five sensitive parameters were found to be %imperviousness, conduit roughness, width of the subcatchment, N-imperviousness, and slope of the subcatchment. Which were introduced to the OSTRICH along with 5 other sensitive parameters to be calibrated automatically. The integration of SWMM and OSTRICH demonstrated a strong capability for handling large, complex models with numerous parameters, affirming OSTRICH's utility in calibration and optimization tasks.

In decision making process about determining the location and number of RB, CI, and DW units to be implemented in the study area, amoung various criteria, subcatchment runoff, occupied area by residential and industrial areas, sub-soil permeability, and proximity to seawater were identified as the most critical factors influencing the suitability. The obtained results at this stage highlight the importance of initial hydrologic modeling in prioritizing subcatchments for the implementation of decentralized stormwater management units.

In the assessment of the hydrologic response of the watershed under various designed storm events, implementing RB, CI, and DW units resulted in significant reductions in peak runoff (23.63%–54.03%) and runoff volume (11.17%–27.43%) under storm events with 2-hour durations and return periods ranging from 2 to 50 years. The time to peak also increased, indicating improved watershed response. However, it is noteworthy to mention that the reduction rate in urban runoff was inversely related to the storm's intensity or return interval.

The developed model also was assessed under a real case long-duration storm event as well. For prolonged or intermittent storms, such as the storm event experienced in September 2009 in the Ayamama watershed, the performance of RB, CI, and DW units in runoff reduction declined due to limited storage capacities and slow infiltration because of saturation of DW units, emphasizing the need for periodic recovery mechanisms or bigger storage volume of the units.

Finally, the water harvesting potential of the implemented decentralized stormwater management units was assessed. A year-long simulation using 2018 meteorological data showed that implemented RB and CI units could capture over 12 million m^3 of rainwater, equivalent to 5.15% and 7.46% of the storage capacities of the Ömerli and Terkos dams, respectively which are the first two biggest dams of Istanbul. This underscores their potential to address water scarcity challenges in the city which is intensified due to climate change and population growth.

This study contributes significantly to the body of knowledge in urban water management, offering scalable solutions for mitigating the dual threats of urbanization and climate change in megacities like Istanbul. The findings of this research provide valuable guidance for urban planners and decision-makers in designing sustainable runoff mitigation strategies tailored to local climate conditions. The proposed framework demonstrates how decentralized stormwater systems can be effectively integrated into urban environments, particularly in areas with limited groundwater resources and available space for large-scale implementations.

Future research should focus on evaluating the impacts of evolving climate conditions on the performance of LID systems and optimizing their implementation strategies under constraints such as budget, space, and competing land-use priorities. Expanding the application of advanced calibration tools and exploring hybrid approaches that combine centralized and decentralized stormwater solutions could further enhance urban resilience against climate-induced challenges.

ŞEHİRLEŞMİŞ BÖLGELERDE İKLİM DEĞİŞİKLİĞİ VE HAVZA ÖZELLİKLERİ ALTINDA MERKEZİ OLMAYAN YAĞMUR SUYU SİSTEMLERİNİN KAPSAMLI DEĞERLENDİRMESİ

ÖZET

Bu doktora tezi çalışmasında, İstanbul'un yoğun kentleşmiş ve taşkın riski yüksek olan bir havzası için merkezi olmayan yağmur suyu yönetim sistemlerinin kapsamlı bir değerlendirmesi ele alınmıştır. Merkezi olmayan sistemler, tüm havza alanına dağılarak, nispeten küçük boyutlardaki mekanizmalar yardımıyla taşkını kaynağında kontrol altına almak için tasarlanmış olup farklı türlerde birçok sistemi içermektedir. Bu sistemler genellikle yağmur suyunun toplanması, biriktirilmesi, sızdırılması veya buharlaştırılmasına yardımcı olarak taşkın riskini azaltmayı hedeflemektedir. Ancak, bu sistemlerin gerçekte ne derece etkili olduğu henüz tam olarak anlaşılamamış olup halen dünya çapında bir araştırma konusudur.

Bu araştırmada, merkezi olmayan yağmur suyu sistemlerinden olan Yağmur Varilleri, Sarnıçlar ve Drenaj Kuyularının taşkın kontrolündeki etkileri, iklim değişikliği ve havza özelliklerine bağlı olarak incelenmiştir. Sırasıyla uluslararası bilimsel literatürde Rain Barrel, Cistern ve Drywell olarak da bilinen bu sistemler, bu tez çalışmasında kısaca (RB), (CI) ve (DW) olarak anılmıştır. Bu çalışma iki ana aşamadan oluşmaktadır: iklim değerlendirmesi ve model geliştirme.

İklim değerlendirmesi, bu tez çalışmasının birinci aşamasını oluşturmaktadır. Bu aşamada, İstanbul'da yağış ve sıcaklık eğilimleri, çalışma alanına yakın mesafede bulunan bir yerel meteoroloji istasyonundan alınan veriler ile MERRA-2 sıcaklık modeli sonuçları ve IMERG yağış tahminleri kullanılarak analiz edilmiştir. Eğilimlerin büyüklüğünü ve yönünü belirlemek için Mann-Kendall (MK) testi, Sen's Slope Estimator ve Innovative Trend Analysis (ITA) yöntemleri dahil olmak üzere üç farklı parametrik olmayan istatistiksel yöntem kullanılmıştır.

Farklı veri kaynakları ve yöntemlerin kullanılmasının temel amacı, istasyon tabanlı veriler ile uzay tabanlı hava gözlem verileri arasındaki farkların kapsamlı bir şekilde karşılaştırılmasını sağlamaktır. Ayrıca, hidro-meteorolojik değişkenlerin eğilim analizinde kullanılan yöntemler arasındaki farklılıkları anlamak ve bu alanda gelenekselden yenilikçi veri kaynaklarına ve yöntemlere geçiş sürecine katkıda bulunmaktır.

İlk aşamanın sonuçları, sıcaklıkta mevsimsel ve yıllık ölçeklerde önemli artış eğilimlerini ortaya koymuştur. Özellikle yaz mevsiminde en güçlü artışlar gözlemlenmiştir. Sıcaklık artış oranında yaz mevsimini sırasıyla ilkbahar, sonbahar ve kış mevsimleri takip etmiştir. Ayrıca, ITA yöntemi kullanılarak yapılan 20 yıllık analizler, 1980-1999 yılları arasında azalma eğilimleri olduğunu göstermiş, ancak yaz mevsimi bu durumun istisnası olmuştur. 2000-2019 dönemi arasında ise belirgin bir artış eğilimi yeniden gözlemlenmiştir.

Sıcaklığa kıyasla, yağış eğilimleri daha az tutarlılık göstermiştir. Uzun süreli analizler, sonbahar ve yaz mevsimlerinde önemli artışlar, kış ve ilkbahar mevsimlerinde ise önemsiz azalmalar olduğunu ortaya koymuştur. Uzun dönemli yıllık bazda yapılan analizler, yağış eğiliminde önemli artışlar olduğunu göstermiştir. Ancak, 20 yıllık analizler, uzun vadede önemsiz eğilimlere sahip olan kış ve ilkbahar mevsimlerinin, 20 yıllık bazda önemli düşüş eğilimlerine sahip olduğunu ortaya koymuştur.

20 yıllık analizler, MERRA-2 verilerinin, IMERG'e kıyasla istasyon tabanlı verilere daha iyi uyum sağladığını göstermiştir. Özellikle, IMERG verilerine dayalı olarak ilkbahar mevsimindeki yağış eğilim analizlerinde ve sonbaharın yüksek değer grubunda zayıf sonuçlar gözlemlendiği tespit edilmiştir. Ek olarak, ITA yöntemi, sıcaklık ve yağış verilerindeki alt eğilimleri tespit etmek için özellikle etkili bulunmuş ve grafiksel avantajlar sağlamıştır. Bu özellik, İstanbul gibi yoğun nüfuslu mega kentlerde kısa süreli değişimleri ve hidro-meteorolojik aşırılıkları analiz etmek açısından kritik bir öneme sahiptir.

Model geliştirme aşamasında, 2009 yılında meydana gelen yıkıcı sel felaketi ile bilinen, yoğun kentleşmiş Ayamama Havzası çalışma alanı olarak seçilmiştir. Bu aşamada, iklim değerlendirmesi bulgularına dayanarak, yağmur varilleri (RB), sarnıçlar (CI) ve drenaj kuyuları (DW), su tutma ve sızdırma kapasiteleri nedeniyle çalışma alanının hidrolojik modeline taşkın kontrolü amacıyla uygulanmak üzere seçilmiştir. Bu sistemler, artan sıcaklık ve buharlaşma nedeniyle daha sık yaşanan su kıtlığı ile mücadelede yardımcı olabilir ve aynı zamanda, çalışmanın birinci aşama sonuçlarına göre İstanbul'da artan yağışlar nedeniyle oluşan yüzey akışını azaltmak için etkili bir araç olarak işlev görebilir.

Bu çalışmanın ikinci aşamasında, merkezi olmayan yağmur suyu yönetim sistemlerinin tasarımı, uygulanması ve simülasyonu için kapsamlı bir çerçeve geliştirilmiştir. Çalışma, coğrafi veri analizleri, hidrolojik-hidrolik modelleme ve uzman bilgisine dayalı karar verme süreçlerinin entegrasyonunu içermektedir. İlk olarak, çalışma alanı için fiziksel tabanlı bir model, Storm Water Management Model (SWMM) yazılımı kullanılarak oluşturulmuştur. Model, daha sonra Optimization Software Tool for Research Involving Computational Heuristics (OSTRICH) optimizasyon yazılımı ile gerçekleştirilen otomatik kalibrasyon süreci aracılığıyla kalibre edilmiş ve doğrulanmıştır.

Kalibrasyon için, çalışma alanında bulunan ana drenaj kanalındaki su seviye verileri, farklı yağış olayları için İstanbul Büyükşehir Belediyesi (İBB)'nden temin edilmiş ve aynı yağış olaylarının SWMM modelinde simülasyon sonucu oluşturduğu kanal su seviyeleri ile karşılaştırılmıştır. Yapılan otomatik kalibrasyon işlemi, simülasyon sonucu elde edilen su seviyesi ile gerçekte kanalda ölçülmüş olan su seviyesi arasındaki farkı en aza indirmiş ve dolayısıyla modelin doğruluğunu önemli ölçüde artırmıştır. Bu süreç tamamen otomatik olarak ve OSTRICH optimizasyon yazılımı kullanılarak gerçekleştirilmiştir. Kalibrasyon sonucunda Nash-Sutcliffe Efficiency Katsayısı (NSE), sırasıyla kalibre edilmiş ve doğrulanmış modeller için 0.77 ve 0.67 olarak elde edilmiştir. Bu yüksek değerler, modelin çalışma alanındaki farklı hidrolojik koşulları doğru bir şekilde temsil etme kapasitesini göstermektedir.

Daha sonra, RB, CI ve DW sistemlerinin Ayamama Havzası SWMM modeli içinde uygulama yerlerini belirlemek için uzman görüşlerinin yer aldığı bir anketle Analytic Hierarchy Process (AHP) yöntemi kullanılmıştır. Bu çok kriterli karar analizi yöntemi, mekansal, hidrolojik ve çevresel kısıtlamaları dikkate alarak pratik eşik değerler oluşturmuştur.

Farklı disiplinlerden 10 uzman katılımıyla gerçekleşen ankette, belirlenen kriterler arasında alt havza yüzey akışı (SWMM model sonucu), meskun ve sanayi alanları tarafından kaplanan alanlar, alt tabaka toprak geçirgenliği ve denize (tuzlu suya) olan mesafe gibi faktörler öne çıkmıştır. Bu yaklaşımla, önceden önerilen maksimum RB, CI ve DW birimlerinin sayısı sırasıyla %30,4, %20 ve %57,2 oranında azaltılmıştır. Bu azalma, sistemlerin işlevselliğinin optimize edilmesini ve saha koşullarıyla son derece uyumlu hale getirilmesini sağlamıştır.

Simülasyon ve sistem performans değerlendirmesi sonucu, merkezi olmayan sistemlerin uygulanmasının Ayamama Havzası'nda dikkate değer etkiler sağladığı tespit edilmiştir. İlk başta uygulanan RB, CI ve DW sistemleri, 5 farklı tasarlanmış yağış olayı altında test edilmiştir. Toplam süreleri 2 saat olan ve dönüş aralıkları 2, 5, 10, 25 ve 50 yıl olan bahse konu tasarlanmış yağış olaylarında, pik akışta %23,63 ila %54,03 arasında ve toplam akış hacminde ise %11,17 ila %27,43 arasında azalmalar sağlanmıştır. Ayrıca, 70 dakika toplam konsantrasyon süresi olan Ayamama Havzası'nda, pik akış süresinde 50 dakikaya kadar artışlar gözlemlenmiştir; bu da havzanın şiddetli yağış olaylarına karşı tepkisinde iyileşmeler olduğunu göstermektedir. Ancak, yağış şiddeti veya geri dönüş aralığı arttıkça, yüzey akışındaki azalma oranlarının ters orantılı bir şekilde düştüğü görülmüştür. Bu durum, yoğun yağışlar sırasında RB, CI ve DW sistemlerinin depolama kapasitesinin sınırlı olduğunu ve bu tür olaylar için daha büyük depolama hacimlerine veya düzenli bakım ve boşaltmaya ihtiyaç duyulduğunu ortaya koymuştur.

Tasarlanmış kısa süreli yağış olaylarına ek olarak, geliştirilen model ve uygulanan sistemlerin performansı, uzun süreli yağışlar ve gerçekte yaşanan taşkın olaylarına karşı da test edilmiştir. Elde edilen sonuçlara göre, Ayamama Havzası'nda, Eylül 2009'da yaşandığı gibi uzun süreli veya aralıklı yağışlarda, RB, CI ve DW sistemlerinin performansında belirgin bir düşüş gözlemlenmiştir. Bunun temel nedenleri arasında, depolama kapasitelerinin sınırlı olması ve zemin doygunluğu nedeniyle DW sistemlerinde infiltrasyonun yavaşlaması yer almaktadır. Bu sonuçlar, depolama birimlerinin periyodik olarak yenilenmesinin veya daha büyük hacimlerde birimler tasarlanmasının gerekliliğini vurgulamaktadır.

Yağmur suyu hasadı potansiyeli göz önünde bulundurulduğunda, 2018 yılı meteorolojik verileri kullanılarak gerçekleştirilen bir yıllık simülasyon, uygulanan RB ve CI birimlerinin toplamda 12 milyon m^3'ten fazla yağmur suyunu yakalayabileceğini göstermiştir. Bu miktar, İstanbul'un en büyük iki barajı olan Ömerli ve Terkos barajlarının depolama kapasitelerinin sırasıyla %5,15 ve %7,46'sına denk gelmektedir. Buna ek olarak uygulanan DW sistemleri yağmur suyunu toprağa sızdırmakla yer altı su kaynaklarını zenginleştirecek. Bu sonuçlar, merkezi olmayan sistemlerin, iklim değişikliği ve nüfus artışı nedeniyle yoğunlaşan su krizi gibi sorunların çözülmesinde iyi bir potansiyele sahip olduğunu açıkça ortaya koymaktadır.

Bu çalışma, merkezi olmayan yağmur suyu yönetim sistemlerinden RB, CI ve DW sistemlerinin, özellikle sınırlı yeraltı suyu kaynaklarına ve kısıtlı alanlara sahip bölgelerde etkili bir taşkın kontrolü ve yağmur suyu hasadı aracı olduğunu göstermektedir. İstanbul gibi hızlı kentleşme ve iklim değişikliği gibi çifte tehditlerle karşı karşıya kalan megakentlerde, bu sistemler şehir planlamacılarına ve karar verme makamında bulunanlara rehberlik ederek pratik ve sürdürülebilir çözümler sunabilmektedir.

1. INTRODUCTION

1.1 General

Over the past few decades, concerns about the adverse effects of climate change have grown significantly on a global scale. Naturally occurring phenomena are now more frequent and severe than in the past, and this is believed to be closely related to climate change and global warming (Chaudhary & Piracha, 2021). Hurricanes and floods are among the most frequently experienced types of climate-induced disasters, which directly threaten a great proportion of the world's population, especially those who live in coastal areas (Adshead et al., 2024).

Protecting the residents and infrastructure of coastal megacities from flooding has become increasingly urgent. However, this task is complicated by constant population growth (UN, 2022) and ongoing migration from rural areas to urbanization centers, driven by various socio-economic factors (Busso et al., 2021). These trends place immense pressure on urban planners and decision-makers to implement sustainable flood protection measures that keep pace with the expanding urban landscape.

Additionally, the complicated climate patterns and abrupt shifts in the current climate situation in various parts of the world create a great obstacle in following a sustainable development pattern, especially in large urbanization centers. For example, it is estimated that if global temperature rises by 4 °C by the year 2100, 72–187 million people may have to relocate because of sea level rise (Nicholls et al., 2011). In the same vein, it is outlined in research by (Thackeray et al., 2022) that by the year 2100, the frequency of extreme precipitations on a global scale may increase roughly between 32% and 55% depending on the probable emission scenarios. This highlights the importance of a profound evaluation of the climate condition on the regional scale and adopting appropriate measures or strategies such as structural protection (Wenger, 2015), employing Low Impact Development (LID) strategies, and Sustainable Drainage Systems (SuDS) (D'Ambrosio et al., 2023; Samouei & Özger, 2020), or managed retreat (Hino et al., 2017), especially in coastal communities (Dannenberg et al., 2019).

A common solution that was employed by many communities all over the world throughout history for managing the surface runoff generated by rainfall is the use of excessive and complex drainage networks constructed by pipes and connection nodes (manholes). Initial stormwater drainage systems were designed and constructed as primitive channels for conveying the excess surface water in early civilizations such as Mesopotamia and Rome. By the 19th century, industrialized cities developed more structured underground sewer systems to address urban flooding, improve sanitation, and separate stormwater from wastewater (Burian Steven & Edwards Findlay, 2012). Conventional stormwater drainage systems, which were designed primarily in the mid-20th century and are still the main stormwater management measures in many countries, focused on quickly removing stormwater from urban areas and discharging it into nearby water bodies, often without treatment employing a complex drainage network (Alves et al., 2018; Morris et al., 2018).

This approach which is introduced as "gray" infrastructure or centralized stormwater drainage systems in the literature (Chen et al., 2021; Tansar et al., 2024), is unsustainable in light of increasing urbanization and climate change, particularly in coastal areas where most rainwater is diverted directly to the sea, leads to the loss of substantial amounts of water that could otherwise be repurposed for irrigation, washing, or other uses. Additionally, in areas with combined sewer systems—where stormwater and wastewater share the same pipeline network—heavy rainfall can exceed system capacity, resulting in untreated wastewater being discharged into urban rivers or lakes. This occurrence, known as wet weather discharge or Combined Sewer Overflow (CSO), poses a significant environmental risk (Botturi et al., 2021; Gosset et al., 2016). Furthermore, centralized urban drainage systems are associated with high maintenance costs, inflexible infrastructure, and frequent pipeline blockages, all of which highlight the need to transition toward more sustainable, resilient, and efficient stormwater management strategies in urban watersheds (Butler et al., 2017).

On the contrary, green infrastructure (GI) or decentralized stormwater systems are introduced as an emerging solution for a sustainable development pattern in urbanized environments (Hesarkazzazi et al., 2022; Keeley et al., 2013; Zhang et al., 2017). In general GI or decentralized stormwater systems work based on mitigating the urban runoff and pollutants in the source through small units scattered across the watershed. Each unit in these systems tries to improve the existing retention or detention capacity or evaporation process of the subjected land by imitating the natural flow cycle (Ahiablame et al., 2013). Although this process is mutual among all types of GI systems incorporating urban runoff and pollutant control, they are introduced with various terminology in the literature, such as Best Management Practices (BMP) and Low Impact Development (LID) (Dietz, 2007; Liu et al., 2016), Sustainable Drainage Systems (SuDS) (Garcia et al., 2023), and sponge cities (Chikhi et al., 2023). Some of the prevalent examples of these systems that have been the focal point of researchers, designers, and city planners are green roofs (Zheng et al., 2021), rain gardens (Bąk & Barjenbruch, 2022), rain barrels (Lin et al., 2023), permeable pavement (Sambito et al., 2021), bio-retention cells (Su et al., 2024), infiltration trenches (Hanley et al., 2024), vegetated filter strips (Forgione et al., 2024), and stormwater wetlands (Malaviya & Singh, 2012). These units, depending on the site specifications, implementation feasibility, and stakeholder decisions, can be implemented as stand-alone units or in combination with varying types and ratios within an urbanized watershed.

The primary step in designing and evaluating the performance of different LID units and decentralized stormwater systems is developing a physically-based hydrologic model. The U.S. Environmental Protection Agency's (EPA) Storm Water Management Model (SWMM) is one of the most popular and reliable tools that is commonly used by researchers and engineers globally for evaluating the hydrologic response of urbanized watersheds under various land development and meteorological conditions. This model capably simulates different processes that take place in a hydrologic cycle, including precipitation, infiltration, flow routing, evaporation, and even simulating LID processes in an urbanized environment owing to its various modules (Rossman, 2010).

However, regardless of SWMM capabilities and advanced modules, because of the high number of variables that are involved in a hydrologic model of a complex urbanized watershed, developing a model for LID simulations can be challenging. This challenge is further intensified by the limited availability of open spaces in urbanized watersheds. City areas are predominantly occupied by residential, industrial, or governmental buildings, which are both highly valuable and densely structured. As a result, securing sufficient land for implementing large-scale Low Impact Development (LID) practices, such as rain gardens, permeable pavements, bioretention cells, infiltration trenches, or retention basins to reduce runoff, becomes increasingly difficult (Motovalibashi Naeini et al., 2024) and this creates a huge concern especially for policymakers and urban planners because implementations in large scales can be practically and financially challenging (Liu et al., 2021). Therefore, benefitting from those types of LIDs that comparatively occupy less area or placed underground along with employing comprehensive site evaluation methods for LID retrofitting is necessary.

Istanbul, as one of the world's largest cities with a population exceeding 15 million, continues to expand rapidly, with land transitioning daily from undeveloped to developed areas. This is while heavy rainfall events, which end with pluvial and flash floods, regularly hit the city and other locations in the Marmara region. In the aftermath of one of the most recent flood disasters in the Ayamama river basin in Istanbul, 32 people died and many were injured, which indicates the vulnerability of the watershed and city to floods and river basin overflows. In general, and based on historical records, illegal constructions in flood plains, poor drainage systems, and favorable meteorological conditions are some of the main reasons contributing to disastrous flooding events in the urbanized watersheds of Türkiye (Gülbaz et al., 2019; Kömüşcü & Aksoy, 2023). Therefore, it is crucial to thoroughly analyze the variation in local climate conditions and develop suitable strategies to cope with the adverse outcomes of climate-induced natural hazards in flood-prone watersheds of Istanbul like the Ayamama watershed.

From this perspective, this study tries to address the imperative need for adaptive and sustainable stormwater management strategies in Istanbul Metropolitan by initially offering a comprehensive analysis of long-term trends in hydrometeorological variables. Subsequently, it examines optimal measures to establish a resilient and sustainable urban flood control system within the watershed by employing decentralized stormwater management systems.

1.2 Purpose Of Thesis

The main purpose of this thesis is to evaluate the impacts of a decentralized stormwater management system on the hydrologic response of a densely populated and heavily urbanized watershed in Istanbul. This evaluation embraces three different types of decentralized stormwater management systems such as rain barrels, cisterns, and drywell units. Moreover, it is intended to conduct a comprehensive evaluation considering different aspects such as climate conditions and physical characteristics of the study area.

In this context, first, the climate condition of the study area was assessed by using various methods and data sources in different temporal intervals. To elaborate briefly, the temperature and precipitation data of the study area were obtained for a ground-based meteorological station, and compared with MERRA-2 model reanalysis temperature data and GPM IMERG precipitation estimations. Thereafter, the obtained data were analyzed using three different methods such as the Mann-Kendal test, Sen's slope estimator, and Innovative Trend Analysis (ITA) methods in 60 and 20-year intervals. Then, the most suitable decentralized stormwater management units based on the climate condition of the study area were determined to be implemented in the hydrologic model of the study area.

Later, the physically-based hydrologic model of the study area was developed. In the modeling stage, first, the study area was defined as the Ayamama Watershed because of the availability of data and its dreadful flooding history, and then a physically-based hydrologic-hydraulic model of the study area was developed using SWMM. In this step, various data were obtained from different sources and arranged as layers in the QGIS program to build the basis of the SWMM model.

In the next step, the developed model was auto-calibrated against measured data by using a newly developed Optimization Software Tool for Research Involving Computational Heuristics (OSTRICH) (Matott, 2017). Before the calibration, the most sensitive parameters were detected and entered into the calibration cycle to minimize computational time and effort.

Thereafter, an implementation strategy was developed for implementing three types of decentralized stormwater management units such as rain barrels, cisterns, and drywells, in the study area. These units were particularly considered for implementation because of their small occupation area and the dual benefits of runoff mitigation and rainwater harvesting. The implementation strategy in this step was developed based on a survey from experts and the Analytical Hierarchy Process

(AHP), and finally, the variation in the hydrologic response of the watershed was assessed under various synthetically designed and one real case storm scenarios, along with a year-long simulation.

The insights gained from this study provide a valuable resource for researchers, urban planners, and policymakers involved in urban runoff management. These findings can support assessments during the pre-development phase and guide the adoption of sustainable mitigation strategies to reduce runoff impacts in flood-prone urban watersheds. By applying these approaches, stakeholders can make informed decisions to enhance resilience and address long-term challenges associated with urban flooding.

1.3 Literature Review

1.3.1 Climate assessment

According to the latest report published by the Intergovernmental Panel on Climate Change (IPCC) (Lee et al., 2023) the global surface temperature increased by 0.99 (0.84 to 1.10) °C from 2001 to 2020, as a result of unsustainable and unequal land and energy use, coupled with the use of fossil fuels for over a century. In accordance with this, extensive studies have indicated a great variation in the precipitation patterns on a global scale due to climate change as well. For instance, Caloiero et al. (2018) in a study in southern Italy observed a decreasing trend in the annual precipitation while in the seasonal analysis, various regions demonstrated both increasing and decreasing trends at the same time. Despite locating in a relatively close location, opposite results were obtained in a study by Benabdelouahab et al. (2020) in the coastal regions of the western Mediterranean Sea. On the eastern side of the Mediterranean Sea extending to the Balkans and Anatolian Plateau Zittis (2018) noticed a significant variation in the spatio-temporal precipitation trends. Song and Park (2021) investigated temperature trends over 40 years in urban areas of South Korea, identifying a rise in daily mean temperatures ranging from 0.5°C to 2°C. They found this increase to be positively associated with intensified urbanization and shifts in land cover.

In a closer look at the temperature and precipitation trends in Tükiye, various studies appear in the literature with minor and major differences in the employed methodology, region or area of concentration, and obtained results. For instance, Ay and Kisi (2015) compared the monthly precipitation trends in six provinces of Tükiye in the north-south orientation by using 41 years of ground-based station data and they noticed substantial variation in the direction and magnitude of the trend along with better performance of Innovative Trend Analysis method (ITA) (Şen, 2012) compared to the other methods used. In the Aegean region of Türkiye, annual precipitation analysis showed an increase of up to 7.9 mm per year (Mersin et al., 2022). However, across the country, monthly precipitation has shown a downward trend over the past 50 years (Kömüşcü & Aksoy, 2023). In the temperature analysis, a positive trend was found by Aksu (2021) in 26 of the maximum temperature time series and 21 of the minimum temperature time series from a total of 50 time series.

Further to the aforementioned studies, significant increasing trends have also been observed in records of annual and extreme precipitation events with standard durations along Türkiye's northern and western coasts (Aksu & Şen, 2021; Hadi & Tombul, 2018; Touhedi et al., 2023; Yetik et al., 2024). This highlights the importance of conducting trend analysis at regional or even city scales in Türkiye's coastal areas.

Most of the previous studies in Türkiye have focused on the analysis of either precipitation or temperature trends, and studies to investigate the trends of both temperature and precipitation simultaneously are rare. Whilst, these two variables are intricately related and drive the hydrological cycle collaboratively together. Another limitation in the majority of the related studies and all of the studies cited above is that the data used in the trend analysis process is from ground-based meteorological stations, and the role of remote sensing data is minimal. However, a great part of the maritime and continental regions are deprived of meteorological stations or in situ recording equipment. This makes the studies incorporating remote sensing data or space-based weather observatory products in the trend analysis process extremely valuable (Nguyen et al., 2018; Tang et al., 2020).

Therefore, this study's first objective is to comprehensively analyze the temperature and precipitation trends in Istanbul by using a combination of various data sources and non-parametric methods to provide a basis for selecting the most suitable decentralized stormwater management system types for implementation in the Ayamama watershed.

In this vein, different statistical methods, such as the well-known Mann-Kendall (MK) test (Maurice G Kendall, 1938; Mann, 1945), Sen's slope estimator (Sen, 1968), and ITA method, were used in this study for discovering and interpreting seasonal and annual temperature and precipitation trends. The employed methods especially are famous and advantageous because of their beneficial characteristics, such as robustness against the non-normal distribution of data and outliers that commonly occur in environmental and meteorological data, flexibility in performing analysis in different time scales and intervals while avoiding restrictive assumptions about data, (Agbo et al., 2023; Andualem et al., 2024; Ashraf et al., 2021; Mohorji et al., 2017).

Furthermore, the precipitation and temperature trends based on a ground-based meteorological station in the study area were compared with those of temperature based on the second version of Modern-Era Retrospective Analysis for Research and Applications (MERRA-2) reanalysis (Gupta et al., 2020) and Global Precipitation Mission Integrated Multi-satellitE Retrievals (GPM IMERG) estimations (Huffman et al., 2020). The reason for providing this comparison was to test the applicability of MERRA-2 temperature reanalysis and IMERG precipitation estimations in trend analysis of the hydrometeorological variables which to the best of our knowledge has not been attempted in previous studies in Istanbul.

Beyond the undeniable importance of climate assessments for determining the most suitable types of decentralized stormwater management units in the study area, the results of this part of the study can serve as a valuable reference and assist researchers who focus solely on climate assessments in Istanbul or the Marmara region.

1.3.2 Hydrologic model development and LID implementation

The beneficial impacts of LID practices or different decentralized stormwater management systems in mitigating urban stormwater runoff have been outlined by different researchers so far in the literature. For example, Samouei and Özger (2020) developed a physically based hydrologic model of the Istanbul Technical University main campus and replaced the existing impermeable surfaces with different combinations of permeable pavement, bio-retention cells, and green roofs in 5% to 20% and noticed the implemented LID practices resulted in 2.74% to 24.73% peak runoff reduction and 2.89% to 16.97% runoff volume reduction under different synthetic storm events with return intervals of 2 to 50 years.

Another type of LID system that is recognized as an efficient and effective solution for managing urban stormwater is stormwater wetland. These engineered nature-based systems harness biological and physico-chemical processes to enhance water quality and regulate urban runoff. Numerous studies have documented the effectiveness of stormwater wetlands in mitigating runoff impacts. For instance, Stefanakis (2019) underscored their critical role in urban stormwater and wastewater management. Kabenge et al. (2018) evaluated the performance of stormwater wetlands as upstream watershed interventions, demonstrating their capability to treat runoff from impervious surfaces such as roads and parking lots. Their study reported reductions in total runoff volume and pollutant concentrations by up to 37% and 81%, respectively.

Shokri et al. (2021) investigated the hydraulic performance and nutrient removal capabilities of vegetated filter strips installed at the roadsides in an experimental site in Orlando, Florida, over various rainfall and runoff conditions. They observed significant reductions both in the generated runoff and the amount of adverse nutrients such as ammonium and nitrate compounds. However, they outlined that the actual performance highly depends on the design and site specifications.Kasprzyk et al. (2022) explored technical characteristics and beneficial aspects of rain gardens implemented in the Gdańsk city in Poland and noticed that the implemented rain gardens are capable of infiltrating 0.4 to 0.7 mm/day of rainwater to the soil and thereby can be used as an effective tool for flood prevention and even help to improve the microclimate by reducing the urban heat island effect.

Sheikh and Izanloo (2021), assessed six different LID scenarios in Bojnurd a growing city in northeast Iran by evaluating hydrological, social, and economic criteria by various Multi-Criteria Decision Analysis (MCDA) techniques. They surveyed experts and integrated the survey results with a hydrologic model of the study area developed by SWMM. Based on the geospatial and climate condition of the study area, which was reflected in the MCDA ranking results, they found rain barrels to be the most suitable and permeable pavement to be the least suitable scenario. Ghodsi et al. (2021), investigated the effects of rain barrels, cisterns, and downspout disconnections on urban runoff reduction in a small urban center in Buffalo USA, and observed up to 24% reduction in frequency and volume of CSO events depending on the configuration of implementations. Boroomandnia et al. (2021), concentrated on the performance of drywells as underground units for infiltrating the rainwater in a small district of Tehran city in Iran and indicated that by combining drywells with other LID facilities, a 10% additional reduction can be achieved in runoff within a pre-defined budget.

Although it is demonstrated in different research that the application of LID practices or decentralized stormwater management systems can assist in mitigating urban runoff up to a certain level, the application of these systems needs special attention to the technical and conceptual details and neglecting the contributing conditions such as site specifications, climate conditions, budget restrictions, and hydrologic characteristics of the watershed can significantly reduce the performance, lifetime, and reliability of the implemented LID units and cost a significant amount of time and budget (Xie et al., 2024).

For instance, drywells can act as a tool for groundwater recharge in arid environments or stormwater absorption units in urbanized environments due to their high infiltration capacity (Edwards et al., 2022). However, these units can also facilitate contamination of aquifers and groundwater resources in case of implementation without appropriate filtering chambers or in environmentally unsuitable places (Sasidharan et al., 2018). Similarly, permeable pavements can be subjected to frequent cloggings due to the sediments transported by surface waters (Razzaghmanesh & Beecham, 2018) and therefore are not suitable for implementation in steep slopes in the vicinity of nearby brownfields and also because of having a rough surface cannot be implemented in places with high-speed traffic (Weiss et al., 2019). While small rooftops are suitable for regular-size rain barrels, on large rooftops it's more convenient to use cisterns instead of rain barrels (Ghodsi et al., 2021). In general, and regardless of the type, to avoid harmful outcomes to the environment and improve the performance of LIDs or decentralized stormwater management systems some restrictions need to be considered in the site selection process (Gulshad et al., 2024).

Different methods were employed by researchers and engineers to take into account the contributing factors in the LID site selection process such as Index-Based Approaches which use topographic and hydrologic indices to determine the most suitable locations for implementations (Azari & Tabesh, 2022), a combination of Geographic Information Systems (GIS) and MCDA which is based on integrating different data layers to evaluate the suitability of different locations for implementation (Malczewski & Rinner, 2015) and Fuzzy Logic with MCDA which merges quantitative and qualitative information for selecting the optimal locations for LID implementations (Saadat Foomani & Malekmohammadi, 2020). Among the various techniques employed for evaluating the criteria influencing the performance of LID practices, the combination of GIS layers with different MCDA techniques such as the Analytic Hierarchy Process (AHP) seems to be advantageous considering the high number of criteria and multiple geospatial layers involved in the hydrologic model of the study area (Kaykhosravi et al., 2019). This approach can significantly streamline the complex process of finding the best combination of different implementation patterns in a relatively large urbanized watershed (Kaykhosravi et al., 2022).

Another major challenge that exists in the modeling process of LID systems further to the high number of contributing criteria and complex structure of the urbanized watershed is the absence of a rigorous approach for calibration and validation of the developed model. This shortage imposes a substantial level of uncertainty on the results and creates a barrier to applying these findings to comparable studies. Therefore, implementing an independent and reliable calibration and validation process is essential for effectively assessing hydrologic models in urbanized watersheds (Razavi & Tolson, 2013).

The majority of published research focuses on evaluating the performance of different LIDs or decentralized stormwater management units for urban runoff reduction by concentrating on only single or limited contributing aspects, making comprehensive studies that simultaneously evaluate multiple aspects quite rare. Some of the main aspects in this regard are model setup and calibration or optimization through various methods (Behrouz et al., 2020; Gao et al., 2023; Ghodsi et al., 2020; Perin et al., 2020; Zhuang et al., 2023), or taking into consideration the impacts of various criteria in the design and modeling process through MCDA process (Ahammed et al., 2012; Gogate et al., 2017; Li et al., 2017), climate change and imposed variation in the performance of LIDs (Alamdari et al., 2018; Zahmatkesh et al., 2015), implementation site selection process (Gulshad et al., 2024; Liu et al., 2016), etc. However, a more comprehensive approach is necessary for an accurate insight into all aspects of LID assessments.

In this context, this study provides a profound insight into the climate condition of the study area and based on the climate assessment results proceeds to selection, design, implementation, and simulation of RB, CI, and DW units as a part of a decentralized stormwater management system. The later part itself consists of several stages such as model development, calibration, and validation, integrating expert knowledge in LID retrofitting, and finally developing an implementation system based on the obtained results of MCDA analysis.

This will be a novel attempt with comprehensive phases for filling the gap in developing site-specific implementation strategies and also evaluation of the effectiveness of decentralized stormwater management systems particularly RB, CI, and DW units in large coastal catchments with high concentration of urbanization.

1.4 Hypothesis

Climate change and population increase have raised significant challenges in stormwater management, especially in big urbanization centers. Sustainable approaches are critically required to cope with the adverse outcomes of climate change and population growth. Decentralized stormwater management systems are known as an emerging solution in this context. However, these systems need to be analyzed and designed with special attention to detail and expertise.

In this study Ayamama watershed which is one of the most susceptible watersheds in Istanbul for flooding was selected as the study area. This watershed resembles a large and highly urbanized watershed in Istanbul. The change in the hydrologic response of the watershed for various hydrologic indicators after implementing three types of decentralized stormwater system measures such as Rain Barrel (RB), Cistern (CI), and Drywell (DW) was investigated thoroughly in this study. This assessment was carried on by developing a hydrologic model through SWMM and autocalibration of the developed model by OSTRICH. A unique implementation strategy was developed in accordance with the physical characteristics of the watershed through a survey from experts and the AHP method. Prior to the model development phase, a climate assessment was conducted by analyzing the seasonal and annual trends of the temperature and precipitation in Istanbul. This phase created the basis for selecting the type of decentralized stormwater management measures in this study.

Studies in the pertinent literature highlight the advantageous performance of RB, CI, and DW units in controlling the runoff generated from storm events in urbanized areas. However, differences in the scale of the study, methods, model development, calibration process, implementation strategy, and other aspects make it difficult to fully understand the capacity of these systems. Additionally, a lack of a proper assessment of the climate condition can result in implementing units that are not fully suitable for the subjected watershed and may lose functionality over time.

Hypothetically, incorporating various assessments, methods, data sources, and techniques can increase the comprehensiveness of the study and make it possible to extend the obtained results to other cases or geographic locations.

For instance, a multi-duration and multi-method trend analysis of the study area in advance of the model development and hydrologic assessment of the decentralized stormwater management measures will help in choosing more proper systems among many to be implemented in the subjected watershed.

Secondly, benefitting from auto-calibration tools in calibrating and validating the developed model will increase the accuracy and accountability of the obtained results. A substantial advantage that automatic calibration poses compared to manual calibration is that in auto-calibration it is possible to try a great number of different combinations for various parameter values in less amount of time. This is while in manual calibration for the same amount of calculation operation, a significant amount of time and computational effort is required. Another advantage is that in the automatic calibration process, it is possible to employ different search algorithms which minimize the chance of getting trapped in local minima which is highly probable in manual calibration.

Finally, the application of MCDA methods in evaluating the influencing criteria involved in the implementation of LID units or decentralized stormwater management measures can assist in finding the most suitable locations for implementation and remarkably increase the performance of the implemented units.

Therefore, it is assumed that the current study will justify the type of decentralized stormwater management units to be implemented in the study area based on the climate condition, develop an auto-calibrated hydrologic model resembling the actual condition of the study area, and provide a framework for implementing the selected units in the most suitable locations (subcatchments) in the study area. By this means a critical gap in the literature is addressed through various methods and novel tools.

2. DATA AND METHODOLOGY

2.1 Study Area

Istanbul, with geospatial coordinates of 41.0082° N, 28.9784° E, and a population of over 15 million, is located in the northwest of Türkiye. Known as the historical and cultural center of Türkiye due to its unique location and numerous ports, this city makes a major contribution to the national economy. The surface area of Istanbul is about 5400 km^2 (Ekmekcioğlu et al., 2021), which is split into two European and Asian parts. The city experiences an average of 837 mm of precipitation annually, with December seeing the highest total of 126 mm and July seeing the lowest amount of 35 mm. The average annual temperature of the city is about 14 °C, with August having the highest temperature of approximately equal to 23 °C and December having the lowest temperature of about 5.57 °C.

The Ayamama watershed, situated in the European part of Istanbul, extends southward to connect with the Marmara Sea and is bounded by geospatial coordinates ranging from 28° 21′ 18″ E to 28° 24′ 43″ E in longitude and 40° 58′ 14″ N to 41° 08′ 12″ N in latitude. Until the recent past, the Ayamama watershed was surrounded by fertile agricultural lands. The creek running through the center of the watershed from north to the Marmara Sea at the south had many tributaries and was an important water source for the surrounding orchards, gardens, and farms. However, with the immigration and population bloom in 1950 the surrounding lands turned to residential and industrial buildings to accommodate the needs of newcomers. This land use type still covers a chief part of the watershed today.

This watershed covers a significant area of approximately 65.792 km^2, encompassing 28 neighborhoods, and holds a critical place in Istanbul's hydrological landscape due to its vulnerability to flooding. In particular, the watershed gained attention for the devastating flood event of September 2009, which tragically claimed 32 lives and underscored the region's susceptibility to extreme weather conditions. (Nigussie & Altunkaynak, 2016) (Figure 2.1).

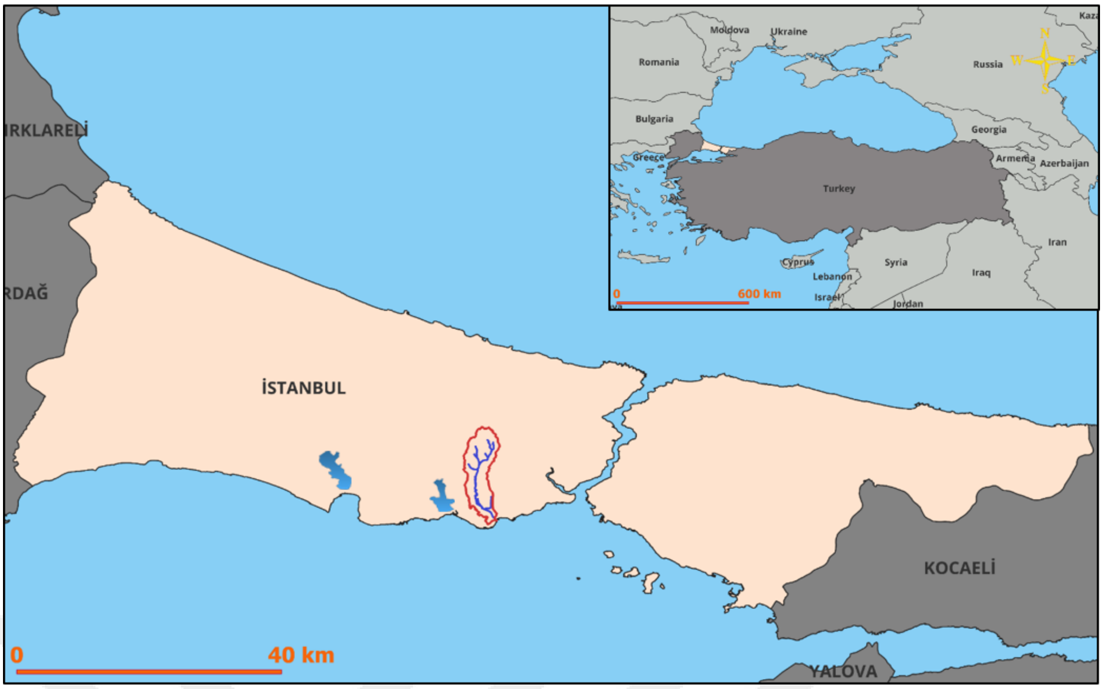

Figure 2.1 : Ayamama Watershed (study area) boundary and location.

2.2 Climate Analysis

Trend analysis of the precipitation and temperature in Istanbul city was carried out to determine the dominant seasonal and annual trends before the model development. The initial part of this step was acquiring long-term data from different sources such as a ground-based meteorologic station, MERRA-2 temperature reanalysis, and IMERG precipitation estimations. In the later part, various non-parametric methods including the Pettitt test, Mann-Kendal test, Sen's slope estimator, and Innovative Trend Analysis methods were used for detecting and interpreting the direction and magnitude of the trends on a seasonal and annual basis. The obtained results were important for decision-making about the type of decentralized stormwater management units to be implemented in the study area.

2.2.1 Long-term meteorologic data

Three types of data sources were used for acquiring the long-term precipitation and temperature data including ground-based station records, MERRA-2 temperature reanalysis, and IMERG precipitation estimations. Long-term meteorologic data were used in trend analysis of temperature and precipitation in Istanbul for understanding the general climate situation of the city before selecting the LID units supposed to be implemented in the Ayamama watershed.

2.2.1.1 Ground-based meteorological station data

Long-term daily precipitation and average daily temperature data were obtained from the Turkish State Meteorological Service (TSMS) for Sarıyer station (Station ID: 17061) to analyze the trends in temperature and precipitation in Istanbul city and to compare the findings based on satellite/model reanalysis data and ground-based meteorological station data in overlapping temporal intervals. This station was specifically selected since it provides a complete time series of precipitation and temperature data and is located at the center of Istanbul and at a relatively close distance to the Ayamama watershed. The location of the ground-based meteorologic station is presented in Figure 2.2. Both the temperature and precipitation data from ground-based meteorological stations have a temporal span of 60 years, starting from 1960 to 2019.

2.2.1.2 GPM IMERG data

The GPM IMERG program which is the short form of the Integrated Multi-SatellitE Retrievals for Global Precipitation Measurement, was initially launched by the Japan Aerospace Exploration Agency (JAXA) and NASA based on a constellation of connected satellites that offer enhanced worldwide monitoring of snow and rain. This program is the extension of the TRMM mission, which ended in 2015 (Liu, 2016). In comparison to its predecessor, IMERG's geospatial span has increased from 35° North-South to 65°. Moreover, because of the advanced imaging equipment that the core satellite carries, IMERG can successfully detect light and solid precipitation at a relatively high spatial ($0.1^{\circ}\times0.1^{\circ}$) and temporal (30 min) resolution (Hou et al., 2014; Huffman et al., 2020). IMERG not only offers the high spatial resolution essential for regional or city-scale studies, but it also shows superior performance in estimating precipitation on monthly and annual timescales compared to other satellite products (Pradhan et al., 2022).

IMERG-E, IMERG-L, and IMERG-F are the different types of IMERG products available, which vary depending on the run's latency and stand for early, late, and final runs, respectively. While early run is preferred for near-real-time processing or potentially forecasting objectives due to its swiftness, late run provides more accurate estimations based on refined data in a longer processing time.

Table 2.1 : Basic statistics of precipitation data.

	Ground-based station (ID: 17061) (1960-2019)					GPM IMERG (2000-2019)				
	Winter	Spring	Summer	Fall	Annual	Winter	Spring	Summer	Fall	Annual
Total number of values	60	60	60	60	60	20	20	20	20	20
Minimum (mm)	134.70	56.40	12.70	85.80	574.20	146.59	132.10	17.66	144.96	617.54
25% Percentile (mm)	244.13	109.18	60.80	208.28	714.50	257.02	158.44	74.10	197.39	781.31
Median (mm)	309.65	143.65	95.65	249.50	828.45	368.98	174.10	100.67	252.25	865.89
75% Percentile (mm)	378.45	190.18	155.63	311.38	944.68	405.21	213.67	167.70	292.12	966.75
Maximum (mm)	646.70	271.40	324.90	478.70	1218.80	529.97	253.71	210.17	346.62	1241.4
Mean (mm)	314.51	151.15	114.08	257.37	837.12	339.89	185.96	112.28	245.27	883.40
Std. Deviation (mm)	98.88	52.29	71.97	88.05	161.70	100.26	35.11	54.32	58.62	151.01
Std. Error of Mean (mm)	12.77	6.75	9.29	11.37	20.88	22.42	7.85	12.15	13.11	33.77
Lower 95% CI of mean (mm)	288.97	137.65	95.48	234.63	795.34	292.97	169.52	86.86	217.84	812.73
Upper 95% CI of mean (mm)	340.06	164.66	132.67	280.12	878.89	386.81	202.39	137.70	272.71	954.08

The final run, which provides the most accurate type of IMERG estimations, was chosen in this study. The version of the IMERG final data set that is used in this study is version 07, which, after broadening its temporal scope, includes the TRMM era and offers a data set spanning from June 2000 to May 2024 (Huffman et al., 2023). However, to overlap with the available ground-based meteorological data, only the first 20-year interval (2000 to 2019) was used.

Validation studies of IMERG data in Europe and the Middle East region are restricted (Pradhan et al., 2022). However, acceptable results were found in a recent study over Türkiye for all runs of IMERG estimations, outperforming the final run with KGE, BIAS, and R values of respectively 0.57, 18.63%, and 0.64 (Aksu et al., 2023). The spatial coverage of the used IMERG data is presented in Figure 2.2

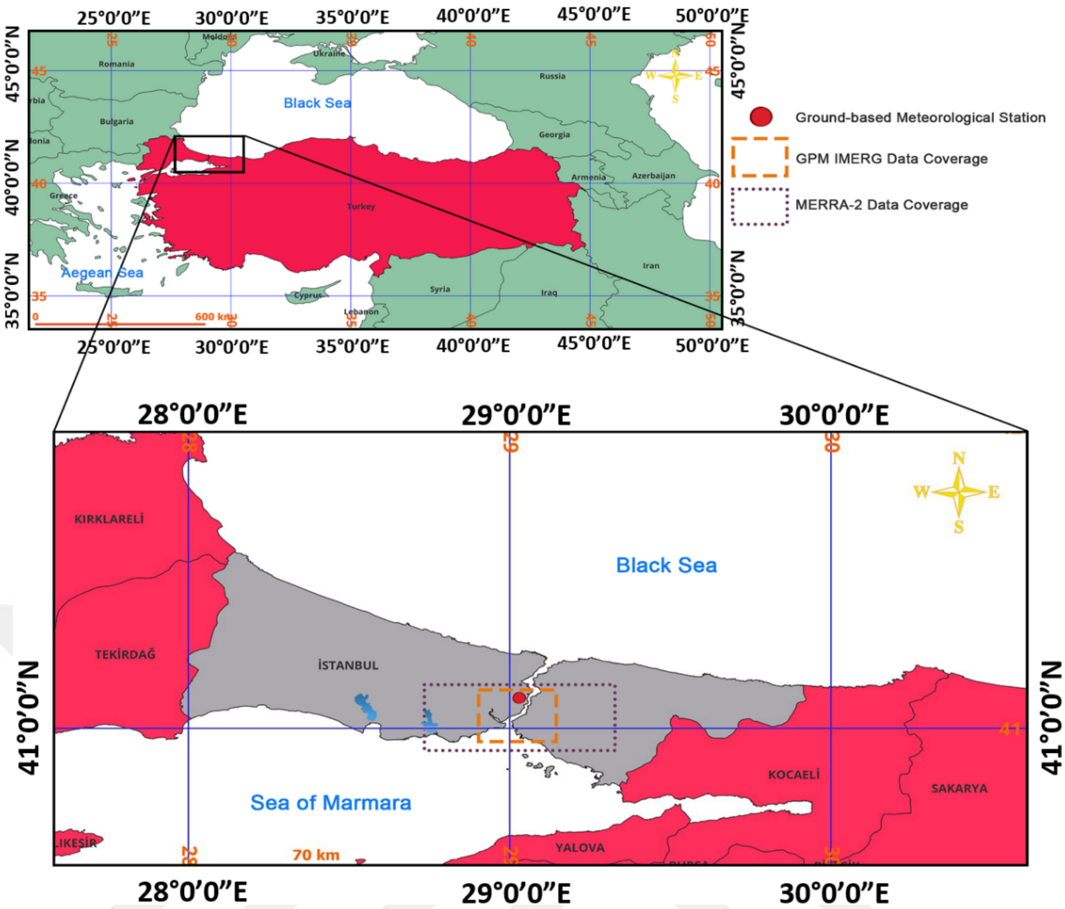

Figure 2.2 : Location of ground-based meteorological station, and spatial coverage of GPM IMERG and MERRA-2 data.

2.2.1.3 MERRA-2 data

The most recent version of Modern-Era Retrospective Analysis for Research and Applications (MERRA-2) is the latest atmospheric reanalysis of the modern satellite era produced by NASA’s Global Modeling and Assimilation Office (GMAO) and provides data beginning in 1980 (Gupta et al., 2020). Climate reanalysis creates a consistent time series of climate variables by combining historical observations with sophisticated earth system models. In the geophysical sciences, reanalysis is often used to acquire in-depth climate observations on 3D grids at sub-daily intervals (Gelaro et al., 2017). The MERRA-2 reanalysis replaced the original MERRA data set (Rienecker et al., 2011) by using an enhanced version of the Goddard Earth Observing System Model, Version 5 (GEOS-5) data assimilation system.

Despite new features such as the assimilation of modern hyperspectral radiance and microwave observations along with GPS-Radio occultation datasets, the spatial resolution of MERRA-2 is still the same as its predecessor MERRA and is equal to

0.5◦ (Lat) x 0.625◦ (Long) (Molod et al., 2015). MERRA-2 has demonstrated strong performance in capturing the temperature changes based on the validation studies over Türkiye with a correlation coefficient over 0.97, especially in the north, west, and northwest coasts, including Marmara and the Aegean regions, where the elevation variation is not as much as in the central, east, and northeast regions of the country (Hasan Karaman & Akyürek, 2023; Tulger Kara & Elbir, 2024). In this study, mean monthly air temperature at 2-meter height and for the 1980–20219 period from the MERRA-2 model reanalysis were used. The spatial coverage of the used MERRA-2 data is presented in Figure 2.2. Both MERRA-2 and GPM IMERG products are accessible through the NASA Goddard Earth Sciences Data Information Services Center (GES DISC).

Table 2.2 : Basic statistics of temperature data.

	Ground-based station (ID: 17061) (1960-2019)					MERRA-2 (1980-2019)				
	Winter	Spring	Summer	Fall	Annual	Winter	Spring	Summer	Fall	Annual
Total number of values	60	60	60	60	60	40	40	40	40	40
Minimum (°C)	4.32	9.18	20.32	13.77	12.66	4.09	9.38	21.83	14.67	13.42
25% Percentile (°C)	5.83	10.39	21.45	15.12	13.39	5.64	11.09	22.69	15.78	13.88
Median (°C)	6.42	11.55	22.17	15.84	13.93	6.23	12.12	23.52	16.58	14.50
75% Percentile (°C)	7.06	12.24	23.10	16.43	14.59	6.80	13.03	24.26	17.03	15.25
Maximum (°C)	8.78	14.36	24.62	18.34	15.68	8.66	14.35	25.62	18.89	15.92
Mean (°C)	6.45	11.48	22.23	15.84	14.00	6.24	12.15	23.57	16.43	14.60
Std. Deviation (°C)	0.91	1.27	1.06	1.00	0.78	0.88	1.23	0.93	0.98	0.77
Std. Error of Mean (°C)	0.12	0.16	0.14	0.13	0.10	0.14	0.19	0.15	0.15	0.12
Lower 95% CI of mean (°C)	6.21	11.15	21.96	15.58	13.80	5.96	11.75	23.28	16.12	14.35
Upper 95% CI of mean (°C)	6.68	11.81	22.50	16.10	14.20	6.52	12.54	23.87	16.74	14.84

Table 2.1 and Table 2.2, respectively, show the basic statistics of the temperature and precipitation data used in this study.

Seasonal and annual violin plots demonstrating the distribution of data points in each data group are shown in Figure 2.3 (Sam & Özger, 2025).

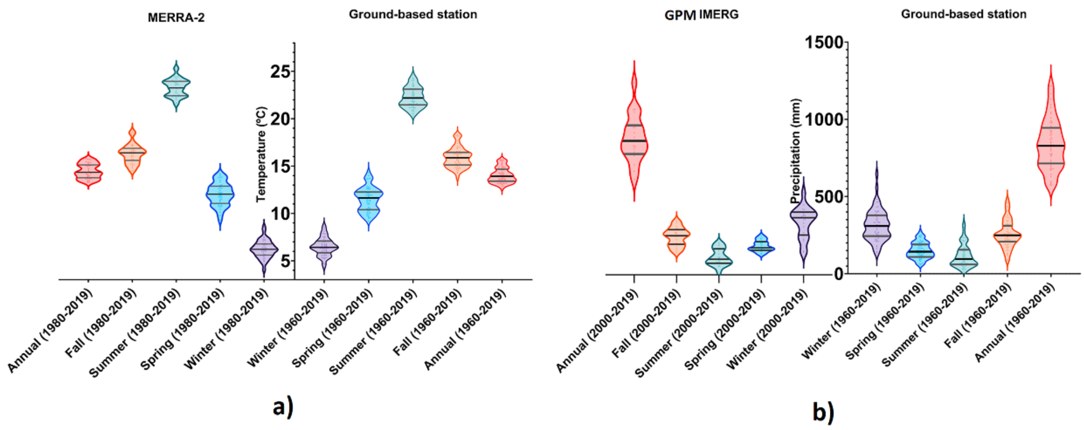

Figure 2.3 : Seasonal and annual violin plots of (a) temperature data and (b) precipitation data.

2.2.2 Statistic test and trend analysis methods

2.2.2.1 Pettitt test

The Pettitt test was used to assess the time series' homogeneity (Pettitt, 1979). This test is a rank-based, non-parametric test that is widely used in hydro-meteorological studies for the detection of a possible breaking point with an unknown occurring time within a given time series. This test does not require any assumptions about the distribution of the time series data and only assumes the data is continuous (Rybski & Neumann, 2011). The null hypothesis (H0) in the Pettitt test indicates that time series follow one or more distributions with the same location parameters, or simply that time series data is homogeneous, whereas the alternative hypothesis (Ha) indicates that a change point occurs in the time series. In the Pettitt test, a sequence of random variables $x_1,....,x_T$ with a change point at the time τ is divided into two sets with distribution functions of $F_1(X_t),\ t=1,2,...,\tau$ and $F_2(X_t),\ t=\tau+1,...,T$.

The change point is detected by using the statistic $U_{t,T}$ as below:

$$U_{t,T}=\sum_{i=1}^{t}\sum_{j=t+1}^{T} sign(X_i - X_j),\quad 1\leq \mathrm{t} \leq \mathrm{T} \tag{2.1}$$

whare,

$$sign(x_i - x_j) = \begin{cases} -1 & for\ (x_i - x_j) < 0 \\ 0 & for\ (x_i - x_j) = 0 \\ 1 & for\ (x_i - x_j) > 0 \end{cases} \tag{2.2}$$

If a break occurs in the year of τ, then the statistic is the maximal or minimal near year t = τ.

$$K_\tau \ = \ \mathrm{U}_{\tau,\mathrm{T}} = \max\left|\mathrm{U}_{\tau,\mathrm{T}}\right|,\ 1 \ \leq \ t \ \leq \ \mathrm{T} \tag{2.3}$$

For a given significance level of α if the p-value of the test as below satisfies $p < \alpha$, the null hypothesis (H0), is rejected.

$$p \approx 2\exp\left(\frac{-6k_\tau^2}{T^3 + T^2}\right) \tag{2.4}$$

2.2.2.2 Mann-Kendall test

The Mann-Kendal test is a non-parametric test for detecting variation trends mainly in hydrologic, climatologic, and meteorological time series. The data for this approach, which was first presented by M. G. Kendall (1938) and Mann (1945) do not have to follow a normal distribution pattern. In addition, the test exhibits minimal susceptibility to abrupt discontinuities in inhomogeneous time series (Jaagus, 2006; Tian et al., 2016). This method compares each data point with the subsequent data points in time after first ranking the data according to time.

If the data ($x_1, ..., x_n$) are randomly ordered and independent, and the null hypothesis H0 is accepted. Otherwise, the alternative hypothesis H1, which indicates that distributions of xi and xj are not identical for all i, j ≤ n with i ≠ j, is accepted and a monotonic trend exists in the time series.

The test statistic (S) for the time series $x_1, ..., x_n$ is given by the formula below:

$$S = \sum_{i=1}^{n-1} \sum_{j=i+1}^{n} sign(x_j - x_i) \tag{2.5}$$

where n is the number of data points, xi, and xj are respectively the i_{th} and j_{th} (j > i) data points, and "sign" is the sign function, as per the equation. (2.2).

For n > 10, the statistic S follows a normal distribution with a variance calculated as below:

$$Var(S) = \frac{n(n-1)(2n+5) - \sum_{k=1}^{m} t_k(t_k - 1)(2t_k + 5)}{18} \tag{2.6}$$

where n is equal to the total number of data points, m is the number of tied groups, and t is the extension of any given tie. For deciding if an existing trend is significant or not, test statistic Z, as below, is used:

$$Z = \begin{cases} \dfrac{S-1}{\sqrt{Var(S)}} & if \;\; S > 0 \\ 0 & if \;\; S = 0 \\ \dfrac{S+1}{\sqrt{Var(S)}} & if \;\; S < 0 \end{cases} \tag{2.7}$$

Z values that are positive or negative, respectively, show that the time series is trending upward or downward. In a two-tailed test, at the α significance level, if the obtained Z satisfies $|Z| > |Z_{1-\alpha/2}|$, then one should reject the null hypothesis and accept the alternative hypothesis (Modarres & da Silva, 2007). In this study, the precipitation and temperature trends were analyzed at two significance levels of α = 0.05 and α = 0.1.

2.2.2.3 Sen's slope estimator

If a time series including N data points exhibits a linear trend, Sen (1968) proposed a straightforward non-parametric method for estimating the trend's slope. The following formula can be used to estimate the slope for N pairs of data:

$$\beta = \frac{x_j - x_k}{j - k} \quad for \;\; i = 1, ..., N \tag{2.8}$$

where xj and xk are data values at times j and k (j > k), respectively. Sen's estimator of slope is equal to the median of the β_i values for the N pairs of data points. Over time, an increasing trend is indicated by a positive β_i value, and a decreasing trend is represented by a negative β_i number. Sen's estimator of the slope value for odd N integers is equivalent to:

For even N numbers, then Sen's estimator of slope can be calculated as:

$$\beta_{med} = \frac{1}{2}(\beta[n/2] + \beta[(n+2)/2]) \tag{2.9}$$

Then the β_{med} is assessed with a two-tailed test at the $100(1-\alpha)\%$ confidence level and the true slope can be calculated by the non-parametric test (Partal & Kahya, 2006; Tabari et al., 2011).

2.2.2.4 Innovative trend analysis (ITA):

The ITA method was first proposed by Şen in 2012 (Şen, 2012). Despite other commonly used approaches, in the ITA method, restrictive assumptions, including the existence of autocorrelation in the series, necessity for an independent data structure, distribution type, and extension of data, are avoided. Moreover, the ITA method has shown substantial advantages in detecting monotonic and non-monotonic trends over time, sub-trends, and various combinations of trends within different time spans due to its visualization capability (Das et al., 2021; Güçlü, 2018; Pour et al., 2020). In this method, the time series is divided into two or several parts with equal lengths, sorted in ascending order, and plotted on a Cartesian coordinate system (Figure 2.4).

If the data points appear around the 1:1 line, then it can be concluded that there is no trend in the time series. For an increasing trend, data points occupy the upper triangle, and for a decreasing trend, data points fall inside the lower triangle.

This method determines the size of an increasing or decreasing trend based on the distance, either horizontally or vertically, of data points from the 1:1 line. This is equivalent to the difference between a data point's y and x values expressed in absolute terms. A time series' overall trend may be determined by calculating the average difference of all of its data points. Normalizing the average differences is necessary to compare the magnitudes of any two separate time series. The average difference must be divided by the average of the first sub-series since the trend is detected based on that sub-series. The trend indicator produced by this approach must be multiplied by 10 in order to be on the same scale as the Mann-Kendall test for a direct comparison. Therefore, the ITA trend indicator can be calculated as below:

$$D = \frac{1}{n}\sum_{i=1}^{n}\frac{10(y_i - x_i)}{\bar{x}} \tag{2.10}$$

where D is the trend indicator, n represents the number of observations in each sub-series, and $\bar{x}$ is the average value of observations in the first sub-series. While D > 0 corresponds to the existence of an increasing trend, a D < 0 value represents a decreasing trend (Wu & Qian, 2017). ±5% and ±10% confidence bands were calculated as below and added to the graphs (Caloiero et al., 2018; Tosunoglu & Kisi, 2017).

$$\pm 5\% \text{ confidence band} = x \pm 0.05 * \bar{x} \tag{2.11}$$

$$\pm 10\% \text{ confidence band} = x \pm 0.1 * \bar{x} \tag{2.12}$$

where x and $\bar{x}$ represent the precipitation or temperature value and the average of precipitation or temperature values, respectively.

In the simplest form of ITA known as the single-duration method, the time series is divided into two sub-series with equal lengths. This approach is preferably used for analyzing the existence, direction, or magnitude of a trend in the entire length of the time series. In the multi-duration form of the ITA method, the time series is divided into multiple sub-series with equal lengths, and one of the sub-series is considered the referral interval for comparing the existence, direction, or magnitude of the trend in the remaining sub-series (Mohorji et al., 2017). This approach is beneficial, especially in uncovering nuanced trends that might not be detected with the conventional single-duration analysis method or for comparing the possible trends in specific intervals with shorter lengths. In this study, the single-duration ITA method was used along with the MK test and Sen’s slope for analyzing the trends in the entire length of data obtained from the ground-based meteorological station, and the multiple-duration ITA method was used for comparing the trends in time series obtained from the ground-based meteorological station, MERRA-2, and IMERG, in overlapping sub-series with 20-year intervals.

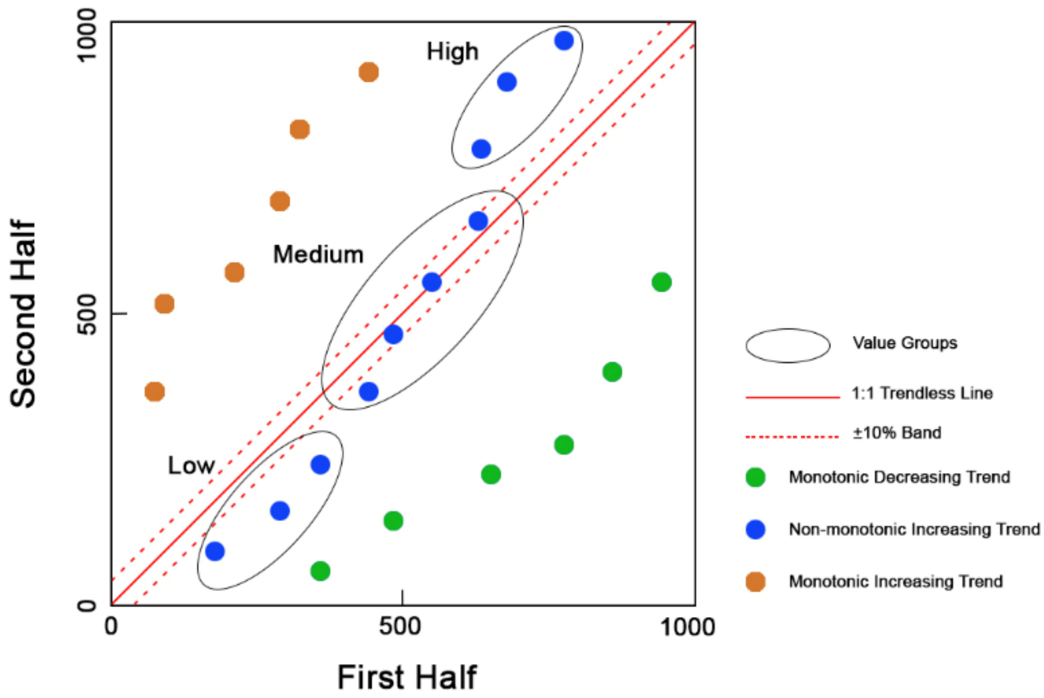

Figure 2.4 : Illustration of the ITA method.

2.3 Model Development

2.3.1 Meteorological and water depth data

Temperature and precipitation data for the temporal interval of 2005 to 2019 were obtained from the Turkish State Meteorological Service for the Olimpiyat station (ID: 20022) which is located at a close distance to Ayamama watershed. The obtained time series resolution was one data per minute. However sporadic intervals with missing data were evident in the entire span of the time series. Therefore, 13 rainfall events with a complete recorded value between the years 2012 and 2019 were randomly selected for carrying on the calibration and validation processes. Moreover, the meteorological data associated with the flooding event of September 2009 (9-10 September) in the Ayamama watershed was extracted from the obtained time series to be used in simulating the experienced flooding event of September 2009.

Further to the aforementioned events that were used in simulation and model calibration-validation phases, Intensity-Duration-Frequency curves from the same meteorological station were also used for designing 5 synthetic storm events with a 2-hour duration and return intervals of T = 2, 5, 10, 25, and 50 years to provide a comprehensive assessment of the performance of implemented RB, CI, and DW units against flooding events.

For long-term simulations, temperature and precipitation data for the year 2018 were extracted from the obtained data and were used in the developed model to evaluate the amount of rainwater captured by the RB, and CI units. The year 2018 was selected for the long-term simulation as a sample year for containing full data records with no missing entries.

In the Ayamama watershed, drained water is collected by an extensive centralized drainage system and conveyed through a main channel to the treatment facility at the southern end of the watershed, and from there, it is released to the Marmara Sea. The water depth in the channel has been measured every minute by a gauge installed in a measuring station in the vicinity of the Milli Gazete building between 2012 and 2019 and is used for calibration and validation processes of the developed SWMM model. Figure 2.5 shows the location of water depth gauge station in the channel.

Figure 2.5 : Location of water depth gauge station in the channel.

2.3.2 Land cover data

The coarse land cover and land use data of the study area was obtained from the Copernicus Land Monitoring Service's CORINE data set for the year 2018 with a 100 m^2 resolution (Copernicus Europe's Eye on Earth and Land Monitoring Service, 2020). This is the latest land cover data offered by CORINE. According to the coarse land cover map of the study area, while the central parts of the watershed are dominated by residential buildings, roads, and industrial facilities, the northern part of the watershed is mostly covered with pastures and natural grasslands. In this map layer different land cover types were specified and demonstrated such as continuous urban fabric, discontinuous urban fabric, industrial or commercial units, roads and rail networks and associated land, airports, construction sites, green urban areas, sport and leisure facilities, pastures and natural grasslands as shown in Figure 2.6.

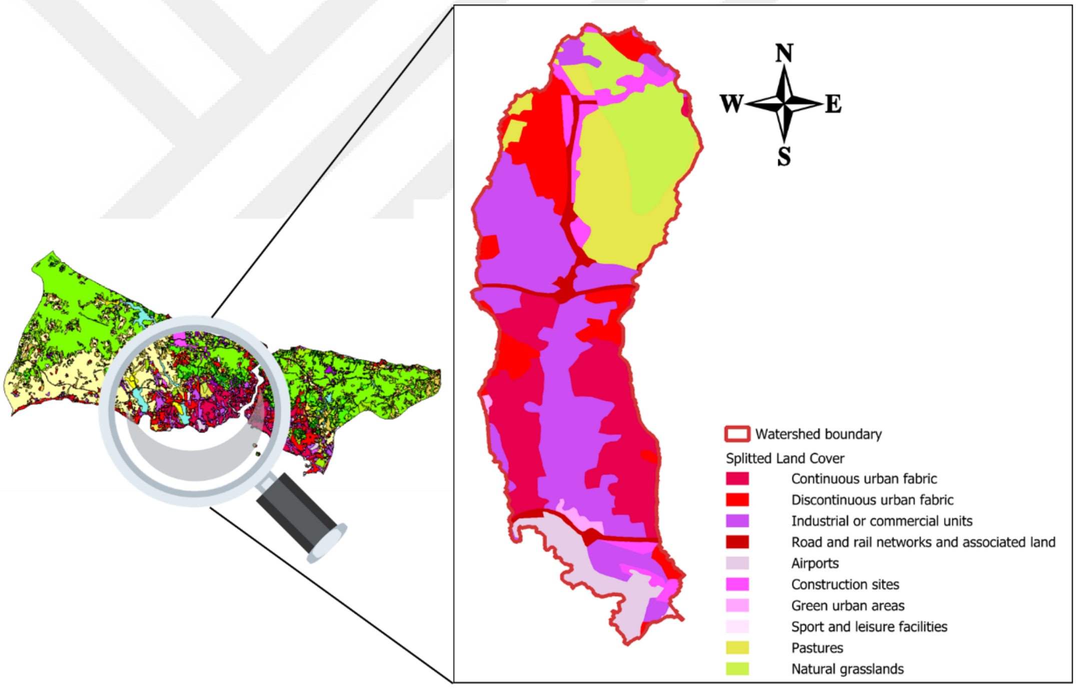

Figure 2.6 : Land cover map of the study area.

Once the study area is divided into several land cover types, essential information such as total area, percent of occupation, and impervious or perviousness were obtained using the QGIS V3.32 program and Microsoft Excell 2016. The obtained geospatial information later was used in the hydrologic model of the study area to calculate Manning's roughness, surface depression storage, etc.

In this study, to determine the most suitable locations and number of different decentralized stormwater management units (RB, CI, and DW) in the implementation process, it was necessary to create a high-resolution land cover map of the study area with a concentration on industrial and residential buildings. Therefore, a high-resolution land cover map for specifying the industrial and residential areas was created based on the aerial photos of the study area and the coarse land cover map in the QGIS program. In addition to the residential and industrial buildings, the main roads in the study area were determined and specified in the high-resolution land cover map. This was done to take into account the environmental concerns regarding contamination of the groundwater resources by suspended sediment pollutants from main roads through LID units (particularly cistern in this study). It is noteworthy to mention that, special attention was devoted to creating the most accurate high-resolution map of the residential and industrial buildings; however, due to the limited resolution of the aerial photos provided by QGIS or recent construction works in the study area, a slight amount of error in the area of residential and industrial buildings is possible.

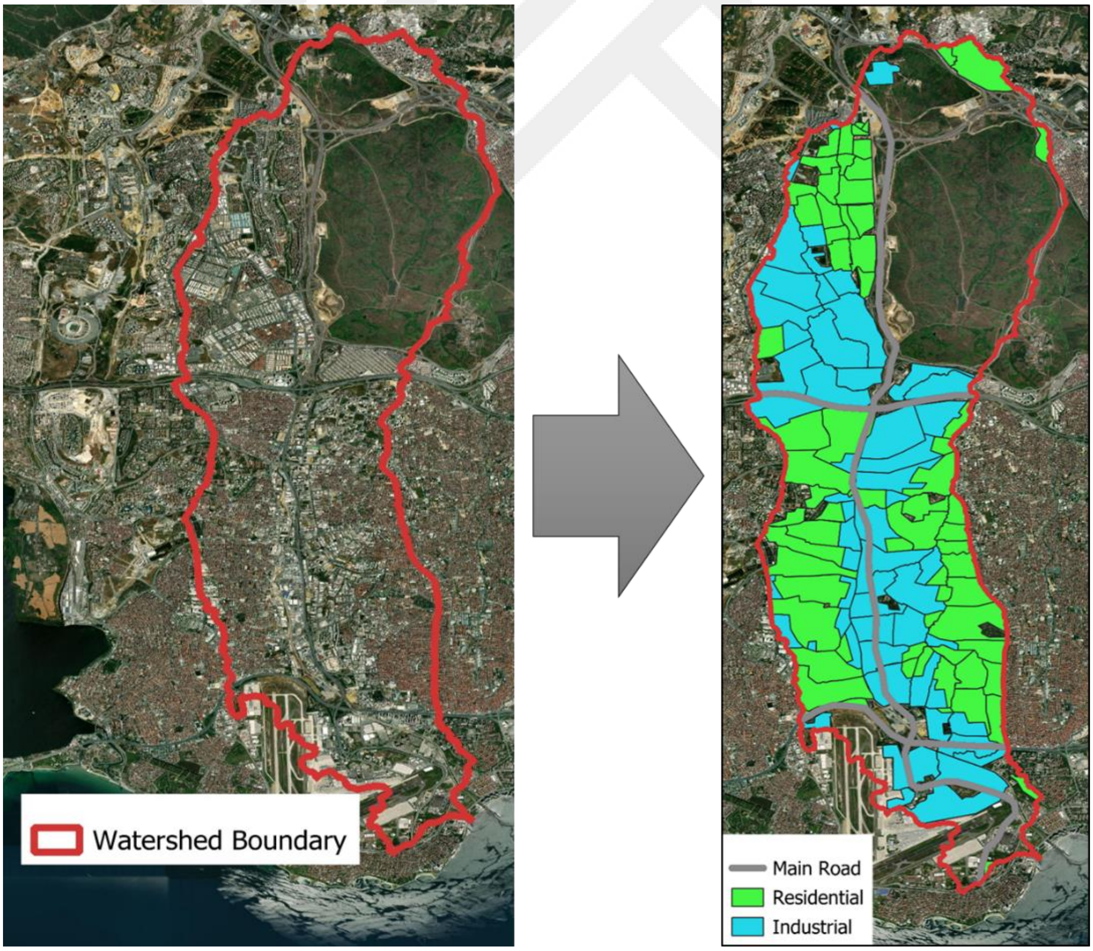

Figure 2.7 : High-resolution land cover map of main roads and residential and industrial buildings.

2.3.3 Topographic and soil data

The next important layers of data that were used prior to the model development were topographic and soil data. For the topographic data, a Digital Elevation Model (DEM) of the study area with a resolution of 5x5 m^2 was used. With a mean of 87.7 m, the elevation of the study area ranges from 0 at the south where it is connected to the Marmara Sea, and 219 m at the north. DEM of the study area was used for watershed boundary delineation, calculating the slope and flow directions, and also dividing the watershed into smaller sub-watersheds.

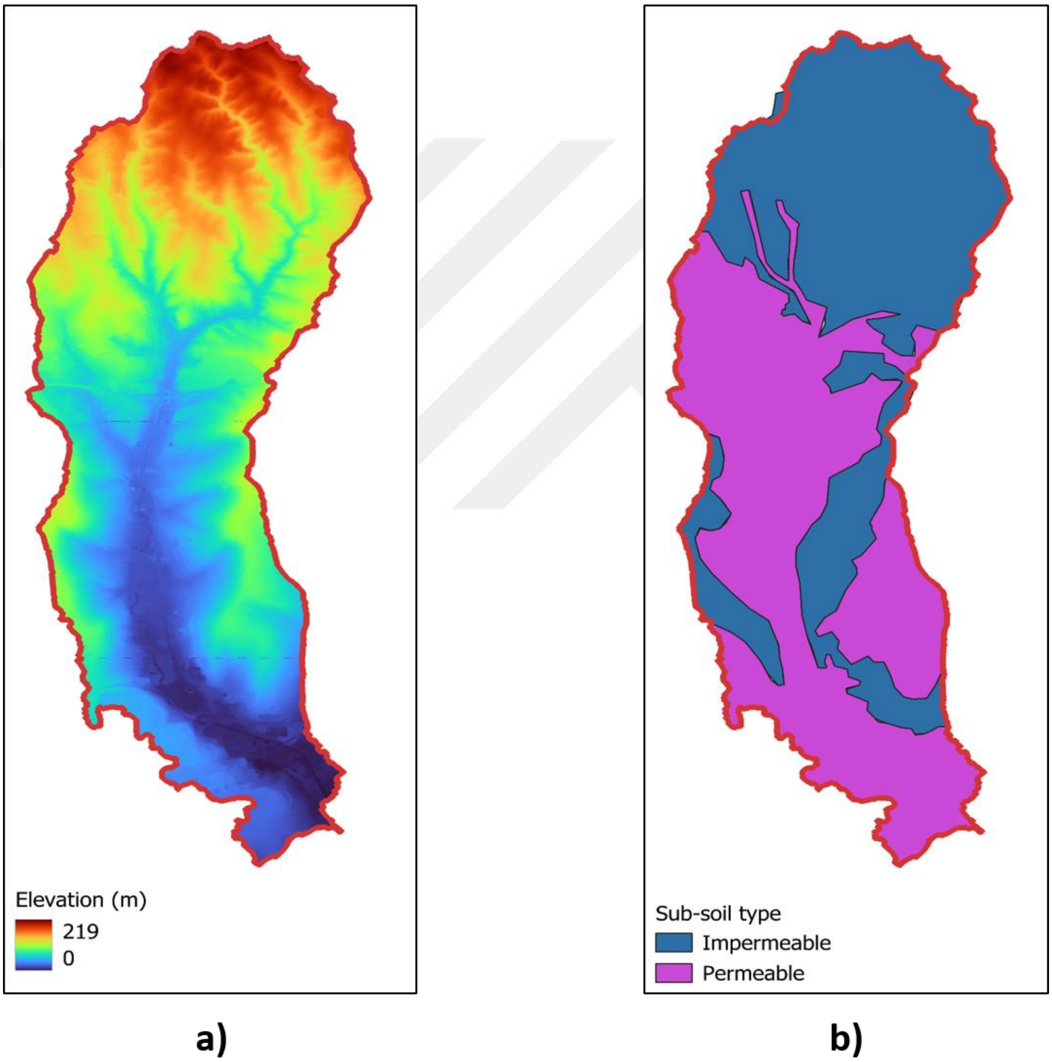

Figure 2.8 : DEM (a) and soil type (b) map of the study area.

Data associated with the soil characteristics of the study area and permeability of the sub-soil in the depth of 6 m and lower was obtained from studies that were conducted in the study area previously (Demiroglu, 2019; Gülbaz et al., 2019). A depth of 6 m was of special interest since it is equal to the depth of DW units that were supposed to be designed and implemented in the study area. Analysis of the study area watershed indicates the presence of only two sub-soil types: permeable (Qal (Alluvium), Tçç (Çukurçeşme Formation), Tcb (Bakırköy Formation), Tks (Soğucak Formation)) and impermeable (Ct (Trakya Formation), Tçg (Güngören Formation)). Impermeable sub-soils predominantly occupy the northern sections of the watershed, whereas the southern regions are largely characterized by permeable sub-soils (Demiroglu, 2019).

2.3.4 Infrastructure data

Drainage network data of the study area was obtained from Istanbul Metropolitan Municipality in Autocad file (.dwg) format. This file revealed substantially important information about the drainage network including dimensions of the pipeline, material of the pipeline, plan of the pipeline and manholes, location of inlet points, location of outlet points, bottom elevation and depth of the manholes along with the width, depth and plan of the main channel. Based on the infrastructure plan, drained water in the watershed is collected by an extensive centralized drainage system across the watershed, conveyed through a main channel to the treatment facility at the southern end of the watershed, and finally released to the Marmara Sea.

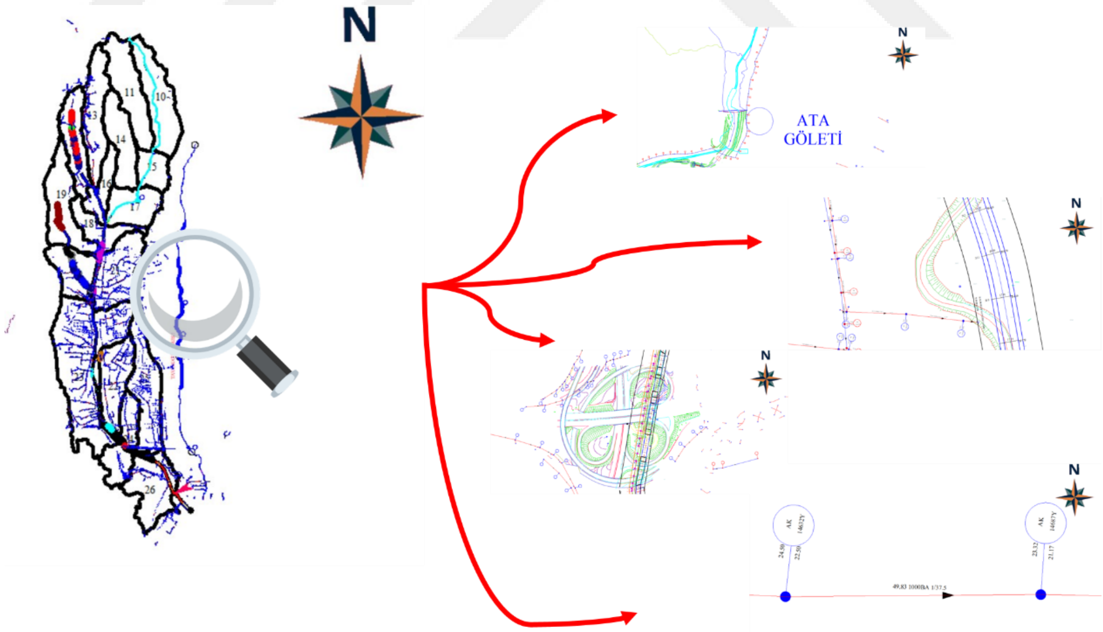

Figure 2.9 : Drainage network data of the study area.

A dam exists in the north of the watershed, creating a relatively small reservoir for storing the stormwater in the creek. This dam is located in a military base and is used mainly for military training and also flood retention in case of storm events. Reportedly this dam collapsed during the flooding event of September 2009 in Ayamama watershed and contributed to the scale of disaster happened. The reconstruction of the dam was finished by the Directorate General for State Hydraulic Works known as DSI in 2012. Details of the dam including the dimensions and location were obtained from a magazine with the name “Su Dünyası” published by DSI in September 2013 with the number 122 (DSI, 2013). The reservoir depth-storage area was calculated in the QGIS program and was prepared to be entered into the hydrologic model (SWMM) of the watershed.

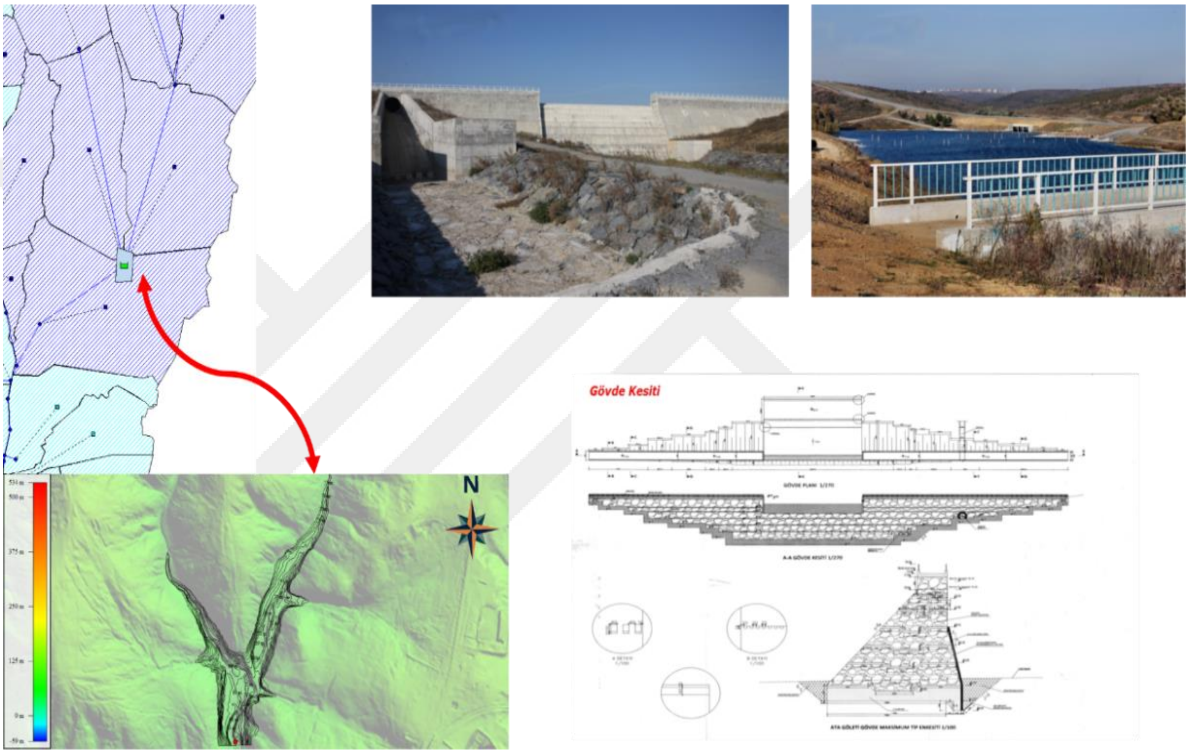

Figure 2.10 : Details of the dam and its reservoir in the north of the study area.

2.3.5 EPA SWMM model

The U.S. Environmental Protection Agency initially developed EPA SWMM in 1971, and it has since undergone multiple updates, steadily growing in popularity. EPA SWMM is a physically based, dynamic rainfall-runoff modeling program that operates in discrete time steps to simulate runoff quantity and quality for single or long-term events in both urban and rural settings. It applies the fundamental principles of mass, energy, and momentum conservation (Rossman, 2010). This program heavily depends on spatial information of the study area. SWMM monitors runoff quality and quantity by calculating evaporation and infiltration into the sub-soil within each sub-catchment, using the water mass balance equation as a basis.

To estimate surface runoff from each subcatchment, SWMM employs a non-linear reservoir model that works based on the precipitation amount. Although the number and shape of the subcatchments depend on user preferences; the general terms applied are based on the surface topography, land cover, and soil characteristics. SWMM calculates the change in depth per unit of time with the formula below which is based on the conservation of mass in each subcatchment:

$$\frac{\partial d_s}{\partial t} = i - e - f - q \tag{2.13}$$

where, i is the rainfall or snowmelt rate (mm/s), e is for evaporation rate (mm/s), f is for infiltration to the sub-soil rate (mm/s), and q is the runoff rate (mm/s). All the parameters are per unit area.

For a subcatchment with a width of "W" a slope of "s" and a height (depression storage) of "d_s" SWMM uses Manning's equation for obtaining the volumetric flow rate:

$$Q = \frac{1}{n} s^{\frac{1}{2}} A_x R_x^{\frac{2}{3}} \tag{2.14}$$

where, Q is the volumetric flow rate (m^3/s), n is the surface roughness coefficient, s is the average slope of the subcatchment, A_x is the area across the subcatchment's width (m^2), R_x is the hydraulic radius associated with the area (m).

For the flow routing in the conduits, SWMM uses conservation of mass and momentum equations generally known as "Saint Venant Equations". In this study among the different flow routing options available such as steady flow routing, Kinematic flow routing, and dynamic flow routing, the dynamic flow routing method was selected. This method provides the most real and accurate results related to the other options since it applies the complete one-dimensional Saint Venant Equation which consists of continuity and momentum equations in conduits and nodes. Although run time increases by selecting this method, it is possible to model the pressurized flow and calculate the backwater effect in the conduits and nodes which frequently occurs in large drainage networks with low invert elevation variation.

- Momentum equation:

$$\frac{\partial Q}{\partial t} = gA\frac{\partial H}{\partial x} + gAS_f + \frac{\partial(\frac{Q^2}{A})}{\partial x} \tag{2.15}$$

- Continuity equation:

$$H_{t+1} = H_t + \frac{\sum_{t}^{\Delta t} Q}{A_{st}} \tag{2.16}$$

In fully pressurized flow in a circular pipe instead of Manning equation Hazen-Williams or Darcy-Weisbach formulas are used in SWMM. In this study, the Hazen-Williams formula was selected:

$$h_f = 10.7(\frac{Q}{C})^{1.852} \times \frac{L}{d^{4.87}} \tag{2.17}$$

where, h_f is friction head loss (m), Q is the discharge rate of the pipe (m^3/s), C is Hazen-Williams coefficient, L is pipe length (m), and d is the pipe diameter (m).

For the infiltration, the Modified Green-Ampt Method was selected in this study. This method is the modified version of the original Green-Ampt Method and is based on not depleting the moisture deficit of the top surface layer of the soil during initial times of low-intensity rainfall. More accurate results are obtained in this method especially when storms with long initial periods occur with intensities below the soil's saturated hydraulic conductivity. The integrated Green-Ampt Method formula:

$$F = K_s + \psi_s\theta_d \ln(1 + \frac{F}{\psi_s\theta_d}) \tag{2.18}$$

where, F is the cumulative infiltration (mm), K_s is the saturated hydraulic conductivity (mm/hr), ψ_s is the capillary suction head along the wetting front (mm), and θ_d is the initial moisture deficit.

Another important component of SWMM is the LID module. This module is responsible for designing and incorporating the different LID units in the developed hydrologic model. In general LID units are a combination of vertical layers such as pavement, soil, storage, and drain (depending on the type of the LID unit). Each layer has its properties which can be defined by the user in accordance with and within the recommended parameter ranges in the SWMM manual. SWMM applies a moisture balance and tracks the amount of moisture moving between the vertical layers of LID units. Some of the main and well-known LID units (types) that are available by default in SWMM are bio-retention cells, rain gardens, green roofs, infiltration trenches, permeable pavement, vegetative swale, rain barrels, etc. However other types of LIDs that are designed based on the general concept of LID practices such as cisterns and drywells can be designed by modifying one of the available and default LID units in the SWMM.

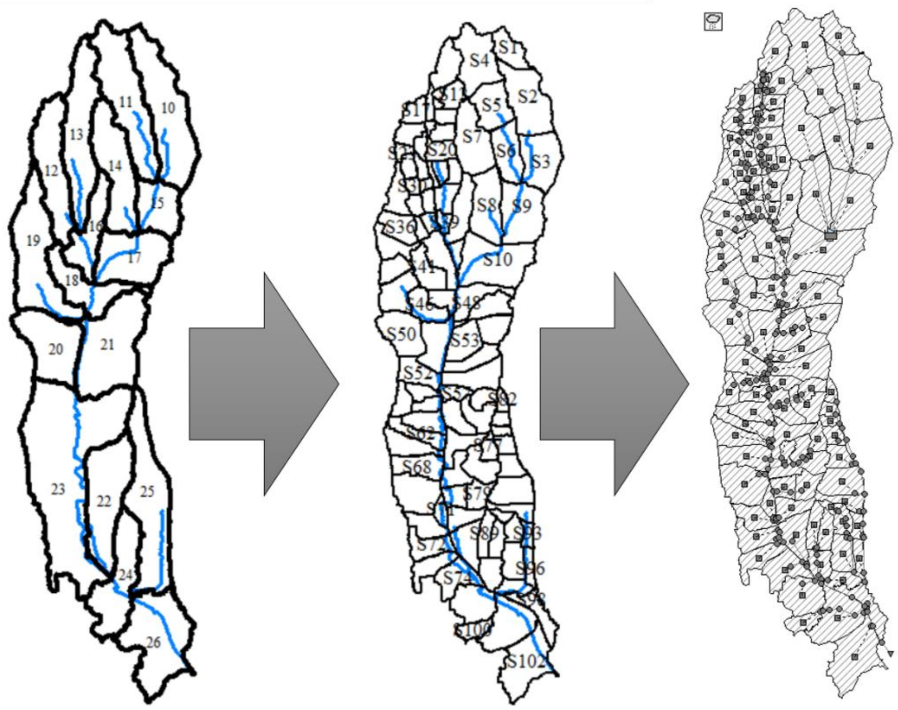

Figure 2.11 : Subcatchment delineation in SWMM.

For defining the number and borders of the subcatchments in the hydrologic model, first, the entire watershed was divided into smaller sub-watersheds using QGIS and based on the DEM. At the end of this process, the watershed was divided into 17 sub-watersheds. Later, based on the land cover, slope, and location of the drainage water inlet points, previously created sub-watersheds were divided into 102 sub-catchments.

Finally, the 102 subcatchments were modeled in SWMM and detailed geospatial information related to each subcatchment such as slope, %imperviousness, depression storage, % zero imperviousness, subcatchment outlet, etc. were added to the SWMM model.

In the next step, information regarding the nodes and conduits was extracted from the autocad file of the infrastructure and then entered into the model. This information includes but is not limited to the elevation of the invert, depth of the nodes, cross-section shape, diameter (depth for open channels), length, roughness of the conduits, etc. In total 219 nodes, 220 conduits, one reservoir, and one outfall were included in the model.

For the meteorological data, 13 randomly selected rainfall events from 2012 to 2019 were combined in consecutive order to create a single time series and then entered into the model along with the corresponding temperature time series. In this process, specific events with a corresponding water depth measurement in the channel were selected.

In this study, most of the watershed is covered with industrial and residential areas with a high density and concentration. Additionally, the traffic speed on the main roads is relatively high compared to the other areas in the city, and parking areas are significantly limited. Due to this, it is tried to benefit from those decentralized stormwater management units that occupy relatively less space. Another reason that plays a key role in the type selection process is the climate assessments. As explained in the next chapters of this thesis, temperature and precipitation both follow an increasing trend in Istanbul. Therefore, it is crucial to benefit from decentralized stormwater management systems that can effectively play a dual role of being a runoff control and a water harvesting device simultaneously. Considering the fact that residential and industrial areas are abundant in the Ayamama watershed and also because of the trend analysis results, three types of LIDs such as rain barrels, cisterns, and drywells were determined to be implemented in this study. To simplify language these units are denoted as RB, CI, and DW respectively in this thesis.

Dimensions, materials, and shapes of the RB, CI, and DW units designed to be implemented in this study are presented in Table 2.3. This table also determines the pre-defined rule that is used for calculating the maximum number of RB, CI, and DW units in each subcatchment based on the residential and industrial areas.

Figure 2.12 : A sample Rain barrel (RB) unit schematic used in this study.

Rain barrels (RB), which are small-scale systems typically installed at individual properties, capture rainwater from rooftops for reuse. Their primary benefit lies in reducing immediate runoff while providing an alternative water source for non-potable uses such as irrigation or outdoor washing. In a watershed facing increasing precipitation trends, widespread adoption of RB units can collectively prevent localized flooding during smaller storm events. Moreover, by using stored water during warmer periods, these systems can alleviate stress on water supply systems, which may become strained as temperature increases leading to higher water demand.

In SWMM an individual and pre-defined template exists inside the LID module for defining the details of RB units, specifying their dimensions such as height and other characteristics such as availability of a drain valve or the quantitative value of flow coefficient. Figure 2.12 shows a sample RB unit that has been designed and used in the SWMM model of the study area.

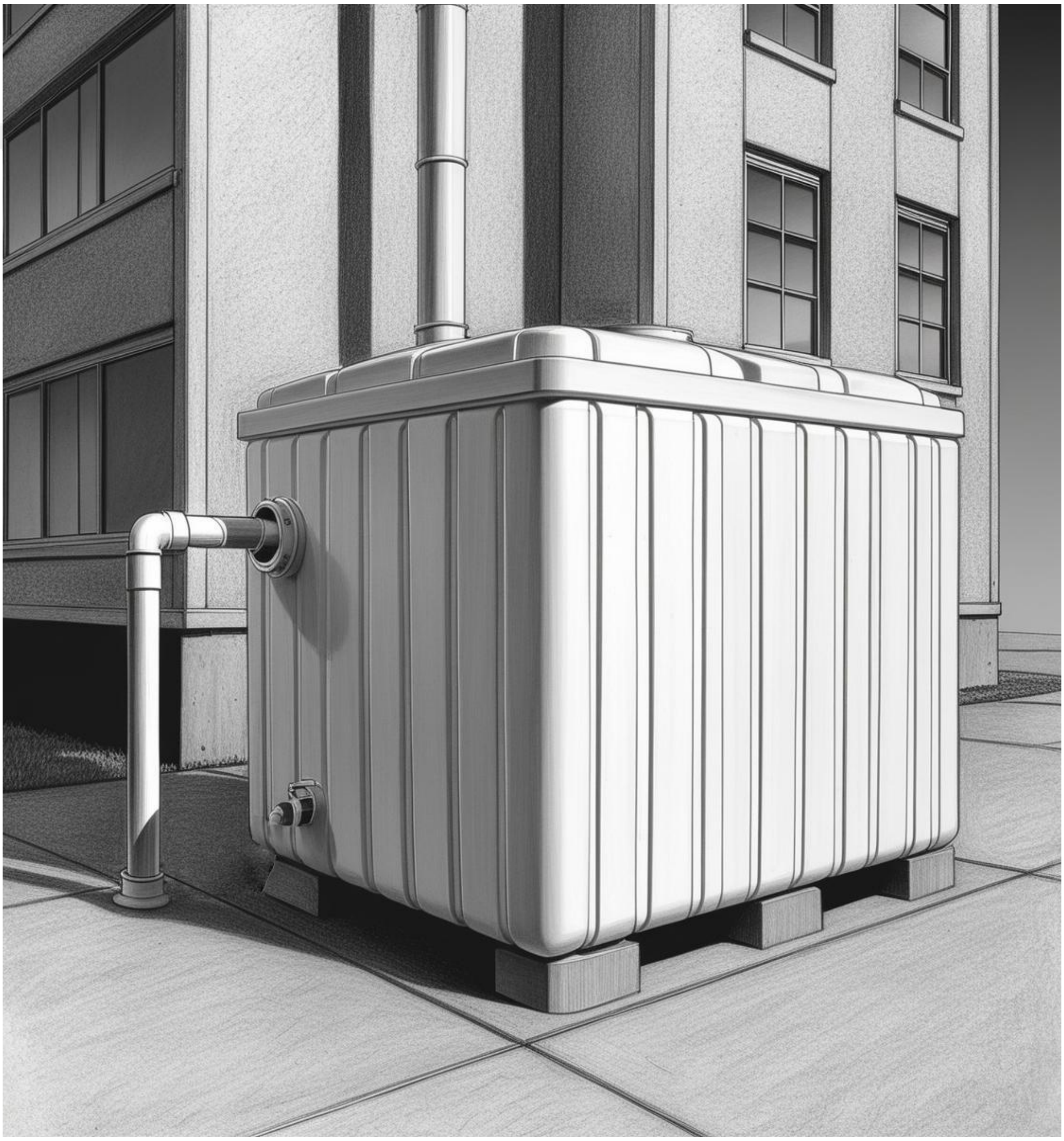

Figure 2.13 : A sample Cistern (CI) unit schematic used in this study.

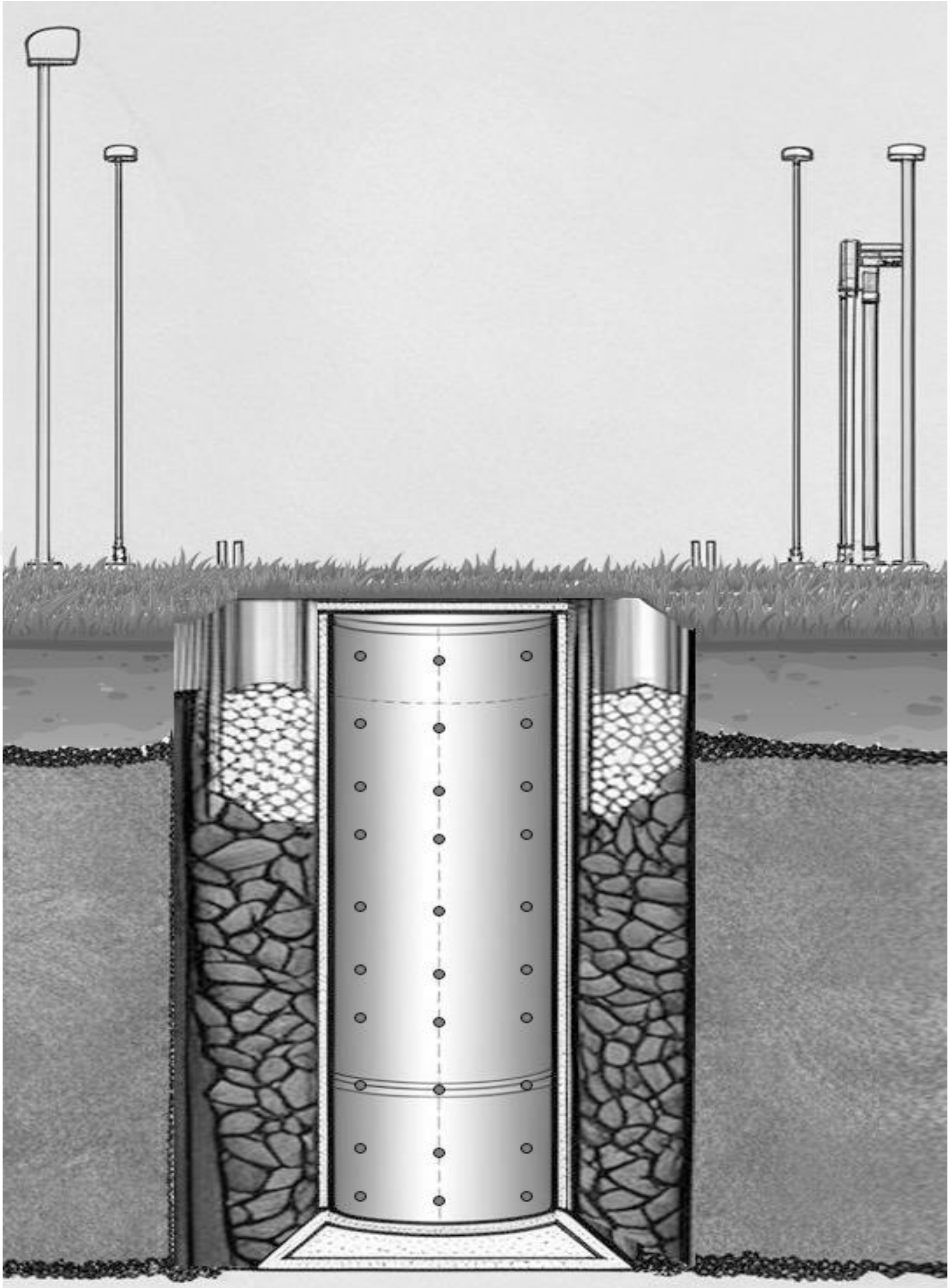

Figure 2.14 : A sample Drywell (DW) unit schematic used in this study.

Cisterns are another type of decentralized stormwater management unit and their working principle is very similar to rain barrels however compared to the RB units they are generally larger storage systems and are designed to hold greater volumes of rainwater and are especially effective in areas experiencing prolonged or heavy rainfall. Their ability to retain significant amounts of water mitigates peak stormwater flow into drainage systems, reducing the likelihood of infrastructure failure during extreme events. Cisterns also serve as a reliable source of water during drier periods, providing a sustainable solution to address the dual challenges of water scarcity and excess. In the context of rising temperatures such as is the case in Istanbul, cisterns contribute to climate adaptation by buffering seasonal variations in water availability. Figure 2.13 shows a sample CI unit next to an industrial building that has been designed and used in the SWMM model of the study area.

Table 2.3 : Rain barrel (RB), cistern (CI), and drywell (DW) dimensions, structure, and implementation details

	Rain barrel (RB)	Cistern (CI)	Drywell (DW)
Base area	1 m^2	2X4 m^2	1 m^2
Height/Depth	1.5 m	2.2 m	6 m
Structure	Cylindrical plastic barrel with drain valve	Cubic plastic reservoir with drain valve	Gravel filled well
Implementation area	Residential	Industrial	Residential and Industrial
Maximum number per area	1/100 m^2	1/1000 m^2	1/500 m^2

Drywells (DW), which are also known as soakaways or infiltration devices, offer a complementary solution by focusing on infiltration rather than storage. These underground structures are designed to collect and infiltrate stormwater, replenishing groundwater aquifers and reducing surface runoff. In watersheds prone to flooding, DWs are instrumental in managing excess rainfall, especially during high-intensity storms. Additionally, increased infiltration through DWs enhances the resilience of groundwater resources against long-term temperature increases, which often lead to heightened evapotranspiration rates. Figure 2.14 shows a sample DW unit in the yard of an industrial building that has been designed and used in the SWMM model of the study area.

It is noteworthy to mention that, in SWMM there is no separate or individual pre-defined template for determining the details of CI or DW units. However, by adjusting the characteristics and details of pre-defined units such as rain barrels or infiltration trenches which is the case in this study, it is possible to design CI and DW units in SWMM respectively.

2.3.6 Sensitivity analysis and model auto-calibration by OSTRICH

One of the most popular methods for parameter sensitivity analysis of SWMM models or generally any physically-based hydrologic model is a manual sensitivity analysis, which involves changing the value of a single parameter by a specific amount (in this study ± 50%) at a time and comparing the percent change in the water depth in the main channel. This was done to identify the most important parameters before the start of the auto-calibration process in this study. Only the characteristics that were computed without absolute confidence were included in the sensitivity analysis; parameters that were measured or defined with good accuracy, such as the slope and dimensions of pipelines and channels, were excluded from the sensitivity analysis.

In total, 12 parameters, including width, % impervious, N-impervious, slope, Ds-impervious, Ds-pervious, % zero-imperviousness, and N-pervious, which are associated with the subcatchments' runoff in SWMM, and conductivity, and initial deficit, suction head, which are associated with the infiltration process in SWMM, and conduit roughness associated with the flow routing in SWMM, were selected for performing the sensitivity analysis. Based on the results of the sensitivity analysis, the sensitive parameters were selected to be calibrated by OSTRICH. The obtained results are explained in detail in the results chapter of the thesis.

Calibration and validation are two indispensable parts of any physically-based model. Without precise calibration and validation, the accuracy and reliability of the obtained results are compromised, potentially leading to flawed interpretations and suboptimal decision-making. Calibration adjusts model parameters to ensure alignment with observed data, while validation tests the model's performance against independent datasets to confirm its predictive capabilities. Together, these processes establish confidence in the model's applicability and ensure it can produce results that accurately represent real-world conditions under various scenarios.

Optimization Software Tool for Research Involving Computational Heuristics (OSTRICH) is a model-independent multi-algorithm calibration and optimization tool that provides a range of options for search algorithms such as Dynamically

Dimensioned Search (DDS) (Tolson & Shoemaker, 2007), Genetic Algorithms (Holland, 1992), Particle Swarm Optimization (Poli et al., 2007), and Powell's Algorithm (Powell, 1976). This tool may be used for the optimization of a set of design variables according to a user-specified objective or cost function, or it can be used to carry out the calibration process of model parameters using different weights based on a non-linear least-squares approach (Matott, 2017). This tool can be freely accessed through (URL-1).

OSTRICH has been utilized in several research projects, mainly in the fields of water resources management (Ghodsi et al., 2023; Matott & Rabideau, 2008; Matott et al., 2006; Shahed Behrouz et al., 2023), groundwater remediation, and environmental modeling systems on a regional scale (Haghnegahdar et al., 2014; Johnston et al., 2011). The technical structure of OSTRICH is similar to that of other independent tools such as Parameter Estimation and Uncertainty Analysis (PEST) (Doherty, 1994) or other similar tools that are developed based on R or Python programming languages. However, the availability of practical tools that can be integrated with OSTRICH, such as SWMMtoolbox (https://pypi.org/project/swmmtoolbox/), for carrying out post-processing operations, along with its capability of running in parallel and also single/multi-objective calibration and optimization, makes it advantageous in comparison to other tools (Behrouz et al., 2023).

OSTRICH accesses the necessary instructions for calibrating the pre-determined parameters of the SWMM model through a model configuration file and a template file. The configuration file contains essential instructions for executing the calibration and optimization processes, such as the optimization algorithm, model executable, objective function, model template files corresponding to the input files, name, initial, lower, and upper boundaries of the parameters to be calibrated, and observation values along with corresponding simulated values. The template file is a text file identical to the model input file, except that instead of the values of the parameters, a unique identifier is assigned.

In this study, the configuration file of the OSTRICH was prepared by creating a text file with a .txt extension including essential details for operating OSTRICH integrated with the developed SWMM model. For instance, the model executable file was set to be a batch file with a .bat extension to consecutively repeat several operations such as 1- running the developed SWMM model based on the initial parameter values; 2- running the

SWMMtoolbox to extract the water depth at the subjected node in the main channel (J139 in the SWMM model) which is used for calibration; 3- running the previously created Python code for calculating the NSE value for the comparison of simulated and observed water depths at the subjected node in the main channel (Node J139 in the SWMM model) and saving the result in the directory with .dat extension.

Further to creating and defining the model executable file, in the configuration file the objective function was set to General Purpose Constrained Optimization Platform (GCOP); the “File Pairs” were set to be paired files of the SWMM model input (.inp) and template file (.tpl); the search algorithm was set to DDS; the parameters and their initial value, upper and lower boundaries were specified; a perturbation value of 0.2 and a maximum iteration number of 500 were also specified. In the model template file with a .tpl extention only the parameteres to be calibrated were specified with a name for each instead of their initial values. Figure 2.15 shows a flowchart that OSTRICH follows in the auto-calibration of the SWMM model.

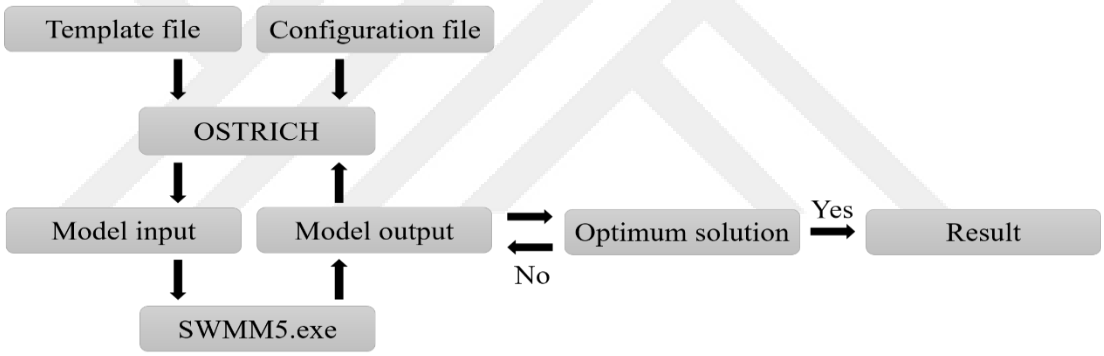

Figure 2.15 : Flowchart of SWMM auto-calibration by OSTRICH. (Behrouz et al., 2020).

2.3.7 Developing the implementation strategy based on a survey from experts and AHP

The quantity and placement of LID units can also have a big impact on the hydrologic model results in major urbanized watersheds. As a result, the implementation plan must be realistically established by taking into account the parameters that affect the performance and selection of LID units, while also being based on site specifications. In this study, a hybrid GIS-MCDA method was used to identify the number and position of each unit within the study area. First, the maximum number of RB, CI, and DW units that could be potentially implemented in each subcatchment was determined based on the residential and industrial areas in each subcatchment by using the QGIS program and defining a rule of 1 RB per 100 m^2 of residential area, 1 CI per 1000 m^2 of industrial area, and 1 DW per 500 m^2 of combined residential and industrial area as per Table 2.3. Similar considerations and assumptions were also made in relevant literature about the implementation of RB, CI, and DW units (Aad et al., 2010; Ghodsi et al., 2023; Russo et al., 2022).

Thereafter, a Multi-Criteria Decision Analysis (MCDA) approach based on the Analytic Hierarchy Process (AHP), was employed to incorporate expert knowledge in implementing the RB, CI, and DW units throughout the study area and also for restraining the number of RB, CI, and DW in each subcatchment up to a logical limit. A survey was conducted with 10 participating experts from academia and the private sector through a questionnaire. Three pairwise comparison matrices with a 1–9 Likert scale, where 1 represents the equal importance degree of two criteria against each other and 9 represents an extremely high importance degree, were created for comparing the criteria influencing the location of RB, CI, and DW units within the study area. Three criteria were selected for RB and CI implementations, and eight criteria were selected for DW. Influencing criteria were selected based on SWMM model output, the most common criteria in the literature for the implementation of RB, CI, and DW, and also the availability of data for the criteria.

A brief description of the influencing criteria for each of the LID types is provided below:

- Total subcatchment runoff (SWMM model output)

After developing and calibrating the hydrologic model of the study area, the total runoff from each subcatchment under the Ayamama flooding event in September 2009 was calculated in m^3 and included in the list of criteria influencing the implementation location of RB, CI, and DW. Physical characteristics of each subcatchment, such as area, slope, the width of the subcatchment, land cover type, and Manning's roughness coefficients, were all included in calculating the runoff by SWMM and therefore excluded from the criteria list.

- Residential area in subcatchment

Residential areas, because of their small rooftop area and the availability of nearby spaces like yards or parking spots, are favorable for RB and DW implementations (Locatelli et al., 2017; Steffen et al., 2013); therefore, residential areas in each subcatchment were calculated in QGIS in m^2 and added to the criteria list of RB and DW units.

- Industrial area in subcatchment

Industrial areas generally have large rooftop areas and also nearby spaces like yards, parking lots, or open warehouses that are favorable for CI and DW implementations (Ghodsi et al., 2021); therefore, industrial areas in each subcatchment were calculated similar to residential areas in m^2 and added to the criteria list of CI and DW units.

- Main stormwater drainage capacity (Length x Cross section area)

This decision criterion demonstrates the capacity of the conveyance system in each subcatchment. The quantitative value of this criterion in m^3 was calculated by multiplying the length and cross section area of the main drainage network that exists in each subcatchment. Subcatchments with sporadic and poor drainage systems receive a higher priority in the implementation of RB, CI, and DW units.

- Subcatchment slope

Although the subcatchment slope was taken into consideration in calculating the subcatchment runoff by SWMM (the first criterion), it is necessary to consider the slope as a decision-making criterion separately for implementing DW units since it affects the movement of surface water, the infiltration process, and the overall performance of the DW units. For instance, based on the literature, to increase the infiltration ratio of DW units and avoid clogging by the suspended sediments conveyed in the stormwater, flat locations are more convenient, and as the slope increases, the infiltration drops drastically (Chowdhury et al., 2010; Chowdhury & Paul, 2021; Mohamed Mouhoumed et al., 2023).

- Distance to seawater

Distance to the sea water is also one of the important criteria in the decision-making process for locating DW units. Due to the saltwater intrusion, it’s important to place DWs far from the sea. Saltwater intrusion is the movement of saline water into freshwater aquifers, which can lead to groundwater quality degradation, including drinking water sources, and other adverse consequences (Hussain et al., 2019).

- Distance to main roads

Main transportation roads and highways are known as major surface water pollution sources. There are three main roads within the study area with the names E80, E5, and O-7 (Figure 2.6). Similar to distance to seawater, distance to the main roads is not an issue in the implementation of RB and CI units. However, it's essential to consider a buffer zone between the main roads and the implementation sites of DW units to avoid contamination by different chemicals such as sodium chloride (i.e., salt), which is used for defrosting in the winter season, and heavy metals (Snodgrass et al., 2017; von Gunten et al., 2020). Therefore, as much as the distance between DW implementation locations and main roads increases, the chance of groundwater contamination through DW infiltrations will decrease.

- Subcatchment sub-soil type

The permeability of the sub-soil at a depth of 6 m and lower, which is beneath the base level of the DW units in this study, is another important decision-making criterion in the implementation process. Implementing DW units in subcatchments with impermeable sub-soils decreases their performance in infiltrating the drained water. In order to create a quantitative comparison scale, values of 3, 2, and 1 were assigned, respectively, to the permeable, semi-permeable, and impermeable sub-soil layers. Based on the available data (Demiroglu, 2019), the sub-soil of the study area falls into the permeable and impermeable categories, and the semi-permeable soil layer is not evident in the study area. Therefore, only assigned quantitative values of 3 and 1 were used based on the sub-soil type in calculating the suitability score and rank.

To examine the reliability of the obtained weights from the survey, the consistency ratio was calculated as per the equations below for each response. For responses with a Consistency Ratio (CR) greater than 0.1, the survey was repeated until achieving a consistency ratio lower than or close to 0.1 (Saaty et al., 2001; Stefanidis & Stathis, 2013).

Consistency Ratio (CR):

$$CR = \frac{Consistency\ Index}{RI} \tag{2.19}$$

where RI is the Random Index as demonstrated in Table 2.

$$Concictency\ Index = \frac{\lambda_{\max} - n}{n-1} \tag{2.20}$$

where, $\lambda_{\max}$ is the sum of products between the sum of columns of the pairwise comparison matrix and the relative weights, and n is the size of the pairwise comparison matrix.

Table 2.4 : The Random Index for different size matrices (Triantaphyllou & Mann, 1995).

n	1	2	3	4	5	6	7	8	9
RI	0.00	0.00	0.58	0.9	1.12	1.24	1.32	1.41	1.45

Hereby, the total number of allowed RB, CI, and DW units in each subcatchment is obtained by multiplying the maximum number of each unit by the suitability rank of that specific subcatchment, which is defined based on the cumulative average of weights for each LID type. Figure 2.16, demonstrates the main framework of the study, including the auto-calibration of the SWMM model and the development of the implementing strategy for RB, CI, and DW units.

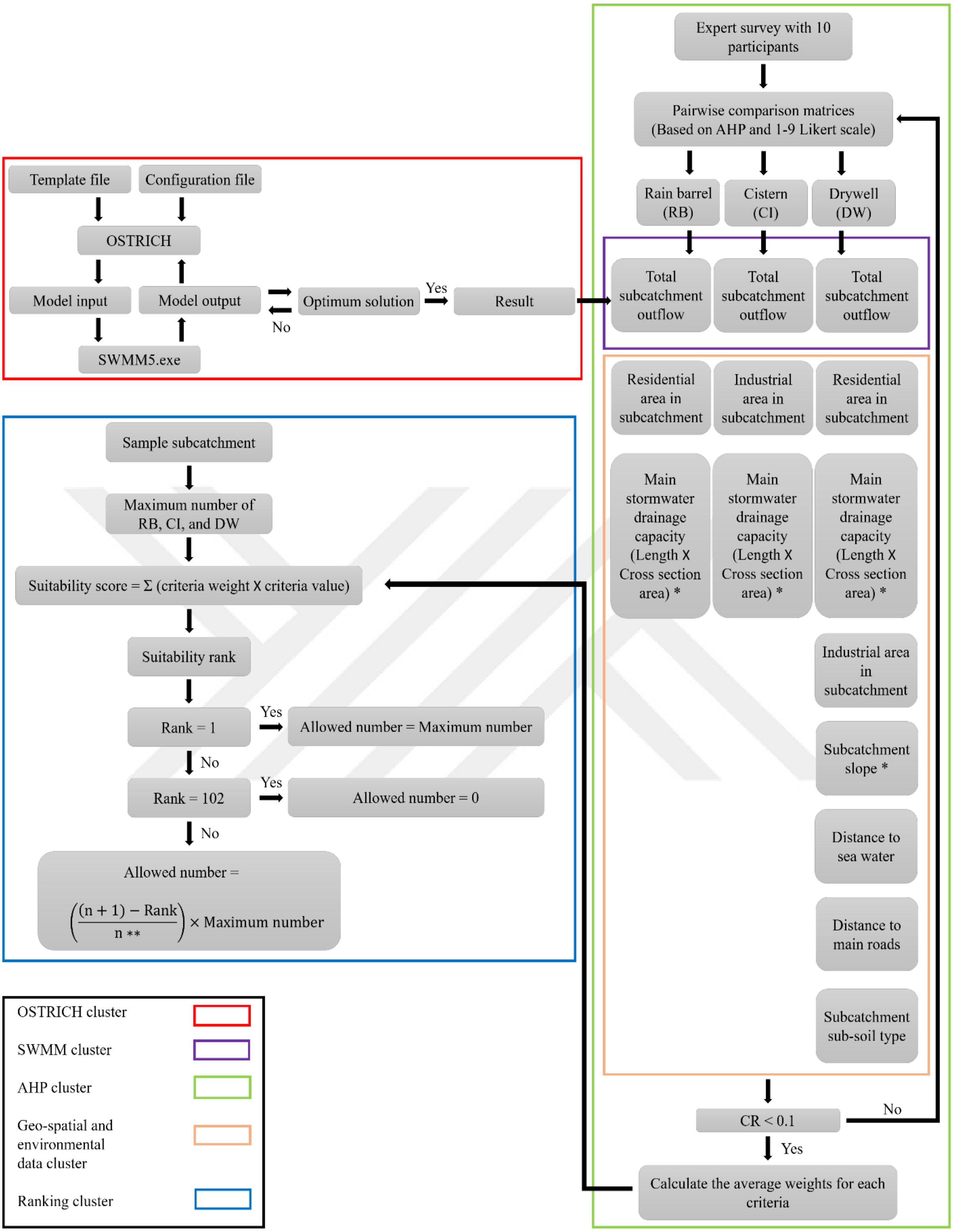

Figure 2.16 : Main framework of the study and consisting clusters.

* Criteria with inverse relation

** Total number of subcatchments = 102

3. RESULTS AND DISCUSSION

3.1 Climate Analysis

To preserve data originality and avoid the use of tempered data, pre-whitening was not applied to the time series (Bayazit & Önöz, 2007; Sang et al., 2014). Before trend analysis of precipitation and temperature, the homogeneity of the time series was tested by the Pettitt test. Temperature time series from the ground-based meteorological station and also MERRA-2 were found to be non-homogenous, with a matching possible change year of 1997, despite having different temporal ranges of 1960–2019 for the ground-based meteorological stations and 1980–2019 for the MERRA-2. The observed non-homogeneity of the temperature over the study area is considered a sign of tangible climatic change. Similar findings were reported in the long-term analysis of temperature change points in the region (Aksu, 2021; Hadi & Tombul, 2018). Precipitation time series determined to be homogenous based on the Pettitt test for the ground-based meteorological station and also IMERG data. However, in contrast to the temperature, the possible change year in the precipitation time series demonstrated variation for the ground-based meteorological station and also IMERG data due to the shorter data duration of IMERG and was found to be 1995 and 2014, respectively.

In addition to the studies conducted on the validity of MERRA-2 and IMERG data over Türkiye (Aksu et al., 2023; Hasan Karaman & Akyürek, 2023; Tulger Kara & Elbir, 2024), the precipitation and temperature time series of MERRA-2 and IMERG were tested against the ground-based meteorological station in this study. A strong fit was found between the temperature data of the ground-based meteorological station and MERRA-2 for the overlapping period of 1980 to 2019 based on the coefficient of determination (R^2) equal to 0.99, as shown in Figure 3.1 (a).

While, for the precipitation, the obtained R^2 value was lower in comparison to the temperature. The R^2 value for precipitation data, as shown in Figure 3.1 (b) obtained to be equal to 0.74, indicating a good agreement rate between the ground-based meteorological station records and IMERG data.

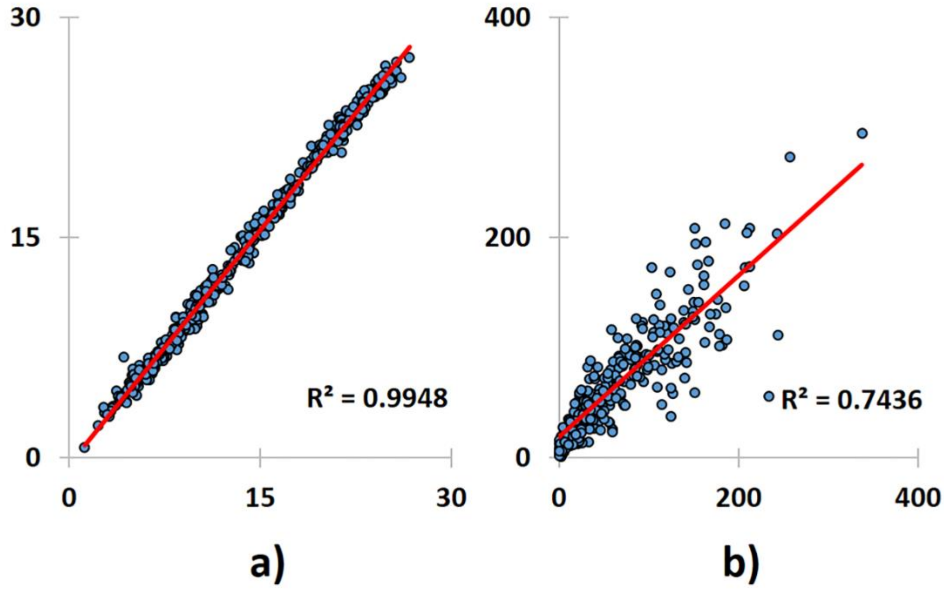

Figure 3.1 : The R^2 values of ground-based meteorological station data versus MERRA-2 temperature data: (a) and IMERG precipitation data: (b).

3.1.1 Temperature analysis

The temperature trend of Istanbul was analyzed on a seasonal and annual basis by using long-term records from a local ground-based meteorological station. Seasons in this study were defined as December, January, and February as winter; March, April, and May as spring; June, July, and August as summer; and September, October, and November as fall. Sen's slope estimator was used along with the MK test at two-tailed significance levels of α = 0.1 and α = 0.05. The results were then compared with a visual interpretation using the single-duration ITA method.

Table 3.1 : Values of P for the Pettitt test, Z for the Mann-Kendall test, β for the Sen's slope, and D for the single-duration ITA method for the temperature trends based on the ground-based meteorological station records.

Winter			Spring			Summer			Fall			Annual			
Z	β	D	Z	β	D	Z	β	D	Z	β	D	P	Z	β	D
2.12*	0.01	0.39	3.25*	0.03	0.80	5.98*	0.04	0.66	2.09*	0.01	0.38	<0.0001 (Ha)*	3.82*	0.02	0.59

* Statically significant at the α=0.05 level

In temperature trend assessments, seasonal and annual time series from the ground-based meteorological station showed an increasing tendency based on the obtained positive values for Z, β, and D, as shown in Table 3.1. The observed increasing trends were considered significant based on the MK test at the $\alpha = 0.05$ level both on an annual basis and all of the seasons with no exception.

The calculated summer and spring Z values were greater than the fall and winter Z values, revealing that the summer and spring had a greater spike in temperature than the fall and winter seasons. Figure 3.2 shows the time series plot of the temperature data obtained from the local ground-based meteorological station for the winter through fall seasons and also on an annual basis.

A distinctive upward trend was found in seasonal analysis based on the single-duration ITA method. The majority of the trends were found to be monotonic upward trends, although there were some non-monotonic and downward sub-trends in the seasonal temperature like low temperatures in the winter season. In the spring season analysis, while the mid values were mainly located between the +10% and +5% bands, most of the higher values demonstrated a greater increase by locating higher than the +10% band, and lower values demonstrated an increase in the +5% band.

In the summer season, a more homogenous increasing pattern was observed in low, mid, and higher values based on data points located between the +10% and +5% bands. Due to having the longest distance between data points and the 1:1 trendless line, in comparison to the other seasons, it can be concluded that the temperature rise in the summer season has been more severe, with a higher contribution to the annual temperature rise.

In the fall season, similar to the other seasons, an increasing trend exists in the data obtained from the ground-based meteorological station. However, data points in the fall season are closer to the 1:1 trendless line in comparison to the other seasons, indicating that the magnitude of the increase is comparatively less.

Similar to the seasonal analysis, a monotonic increasing trend was found in the annual analysis with greater magnitude (between +5% and +10% bands) in the higher values and lower magnitude (between trendless line and +5% band) in the lower values as per demonstrated in Figure 3.2.

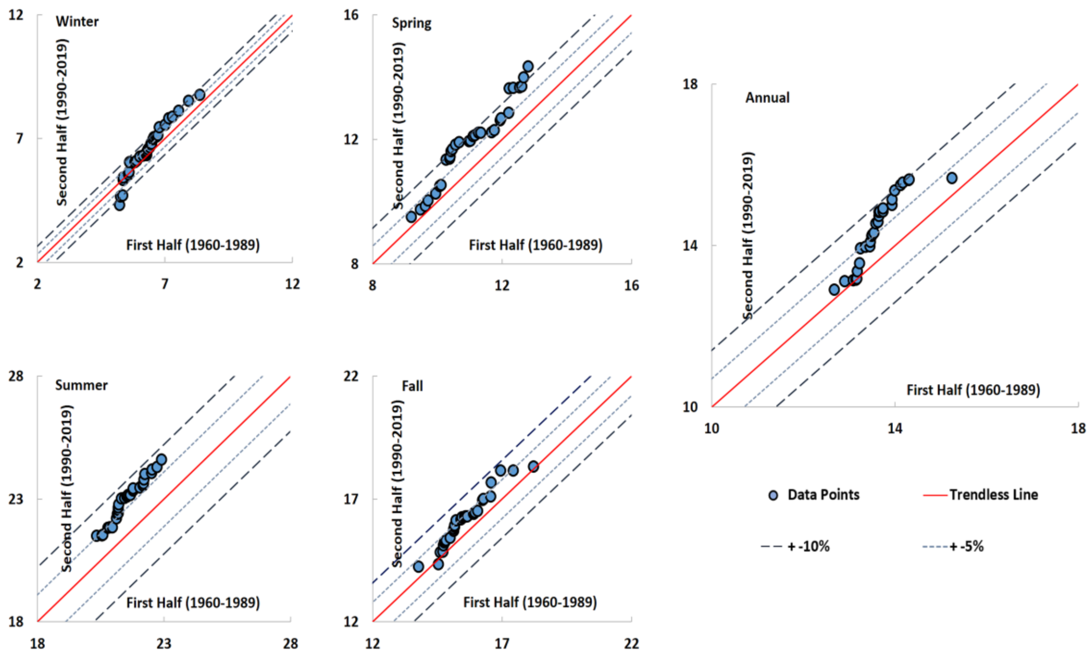

Figure 3.2 : Seasonal and annual temperature trend analysis based on ground-based meteorological station data using single-duration ITA method.

In the 20-year interval analysis of the temperature trend, time series from the ground-based meteorologic station and within the temporal interval of 1960 to 1979 were selected as the referral interval, and time series of the successive 20-year intervals from both the ground-based meteorologic station and MERRA-2 were compared with the selected referral interval.

The trend indicator values (D) were calculated for the referral interval and successive intervals from the ground-based meteorologic station and MERRA-2, as shown in Table 3.2. According to the obtained D values, the general trend of the temperature in the 1980-1999 interval was decreasing in comparison to the referral interval (1960-1979), and the highest reduction trend was observed in the winter season. For the same interval (1980-1999), the time series obtained from MERRA-2 demonstrated inconsistent results in comparison to the ground-based station data for the spring and fall seasons and also on an annual basis. In the summer and winter analysis of the 1980-1999 interval, although the direction of the trend was increasing and decreasing, respectively, the magnitude of the trend was higher in the MERRA-2 time series in comparison to the data from the ground-based station.

Table 3.2 : D values of the multi-duration ITA method for the temperature trends based on the ground-based meteorological station records and MERRA-2. (Blue: decreasing trend; red: increasing trend).

Successive 20-Years	Referral Interval (1960-1979)				
	Winter	Spring	Summer	Fall	Annual
1980-1999	-0.46944	-0.15165	0.090675	-0.29659	-0.1353
1980-1999 MERRA-2	-0.78142	0.396595	0.60501	0.076517	0.248736
2000-2019	0.583414	1.041707	0.798989	0.36707	0.698844
2000-2019 MERRA-2	0.209509	1.384788	1.235227	0.714389	0.995934

Compared to the time series for the 1980-1999 interval, the time series for the 2000-2019 interval both from the ground-based station and MERRA-2 demonstrated increasing behavior against the referral interval of 1960-1979 in all seasons and also on an annual basis.

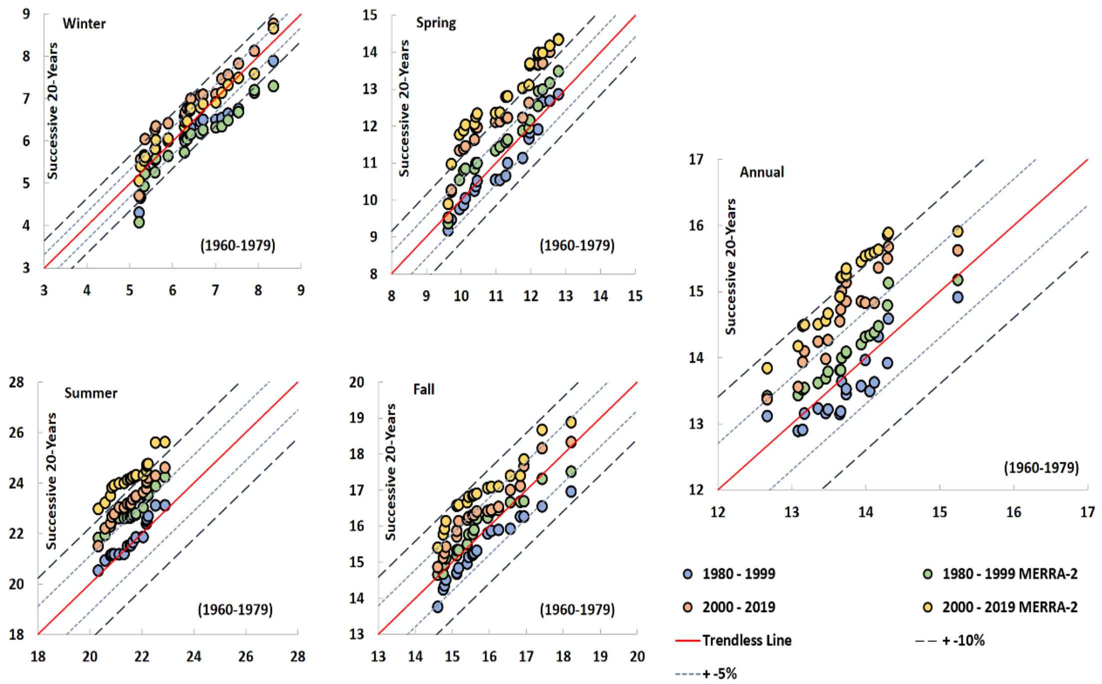

Figure 3.3 : Seasonal and annual temperature trend analysis based on the ground-based meteorological station data and MERRA-2 data in overlapping 20-year intervals using the multi-duration ITA method.

In general, for the decreasing trends in the 1980-1999 interval, an increasing trend was observed in the corresponding time series in the 2000-2019 interval, and for those time series with an increasing trend in 1980-1999, an increasing trend with a higher magnitude was detected for the corresponding time series in the 2000-2019 interval.

3.1.2 Precipitation analysis

Daily total precipitation records from the ground-based meteorological station were used in seasonal and annual precipitation trend analysis. Unlike the temperature, detected trends were not completely parallel to each other in single-duration precipitation analysis on a seasonal and annual basis. The results of the MK test, Sen's slope estimator, and single-duration ITA method are presented in Table 3.3.

According to the MK and Sen's slope evaluation outcomes, a non-significant decreasing trend was detected in the winter and spring seasons due to the negative Z and β values. In the summer season, a significant increase was detected at the α=0.1 level based on the MK test, which complied with Sen's slope estimator and single-duration ITA method. In the fall season and on an annual basis analysis, a significant increasing trend at the α = 0.05 level was detected congruously by all three methods used.

Table 3.3 : Values of P for the Pettitt test, Z for the Mann-Kendall test, β for the Sen's slope, and D for the single-duration ITA method for the precipitation trends based on the ground-based meteorological station records.

Winter			Spring			Summer			Fall			Annual			
Z	β	D	Z	β	D	Z	β	D	Z	β	D	P	Z	β	D
-0.10	-0.09	-0.24	-0.20	-0.06	0.13	1.66*	0.63	1.87	2.29**	1.59	1.80	0.207 (H0)**	2.18**	2.82	0.66

** Statically significant at the α=0.05 level
* Statistically significant at the α=0.1 level

In the precipitation time series plot of the winter season as per Figure 3.4, with the exception of some of the low and high values, the majority of data points are located lower than the 1:1 trendless line, indicating a decreasing. The spring season time series plot demonstrated a non-monotonic decreasing trend mainly dominated by high values, with low values following an increasing trend. Visual inspection of the precipitation trends through the single-duration ITA method revealed an increasing trend in summer and fall seasons parallel to the MK test and Sen's slope results. In the annual analysis, except for some of the low-value data points, the majority of data points are located in the upper triangle and higher than the +5% band, indicating a significant increasing trend similar to the summer and fall seasons.

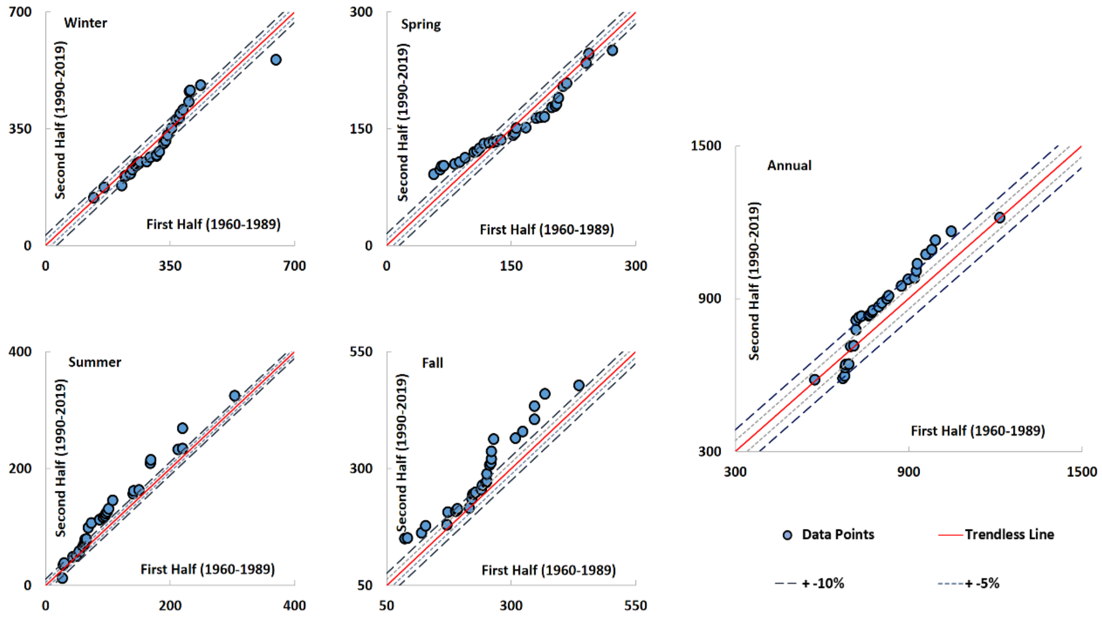

Figure 3.4 : Seasonal and annual precipitation trend analysis based on ground-based meteorological station using single-duration ITA method.

In 20-year interval analysis of the precipitation trend, similar to the temperature analysis, the1960-1979 interval was selected as the referral interval and trend indicator (D) values for the successive intervals of 1980-1999 and 2000-2019 from ground-based station data and IMERG, were calculated and presented in Table 3.4. According to the obtained D values, seasonal analysis of the precipitation trend in 1980-1999 revealed an evident decreasing trend in the winter season, opposing the general increasing trend in the spring, summer, and fall seasons.

Table 3.4 : D values of the multi-duration ITA method for the precipitation trends based on the ground-based meteorological station records and IMERG. (Blue: decreasing trend; red: increasing trend).

Successive 20-Years	Referral Interval (1960-1979)				
	Winter	Spring	Summer	Fall	Annual
1980-1999	-0.74188	0.147413	3.039543	0.852959	0.349987
2000-2019	0.726464	-0.63488	2.156117	3.457385	1.415065
2000-2019 IMERG	0.801404	2.102662	1.547286	0.899049	1.173827

In the same interval, summer season precipitation exhibited the highest increasing trend, followed by the fall season. On an annual basis, with a D value equal to 0.35, a slight increasing trend was observed in the 1980-1999 interval in comparison to the referral interval of 1960-1979.

In the visual inspection of the precipitation trend as depicted in Figure 3.5, in the winter season the majority of the data points belonging to the 1980-1999 interval are located in the lower triangle, indicating a monotonic decreasing trend. For the same interval, the spring season followed a non-monotonic increasing trend with a decreasing low-values sub-trend and an increasing high-values sub-trend.

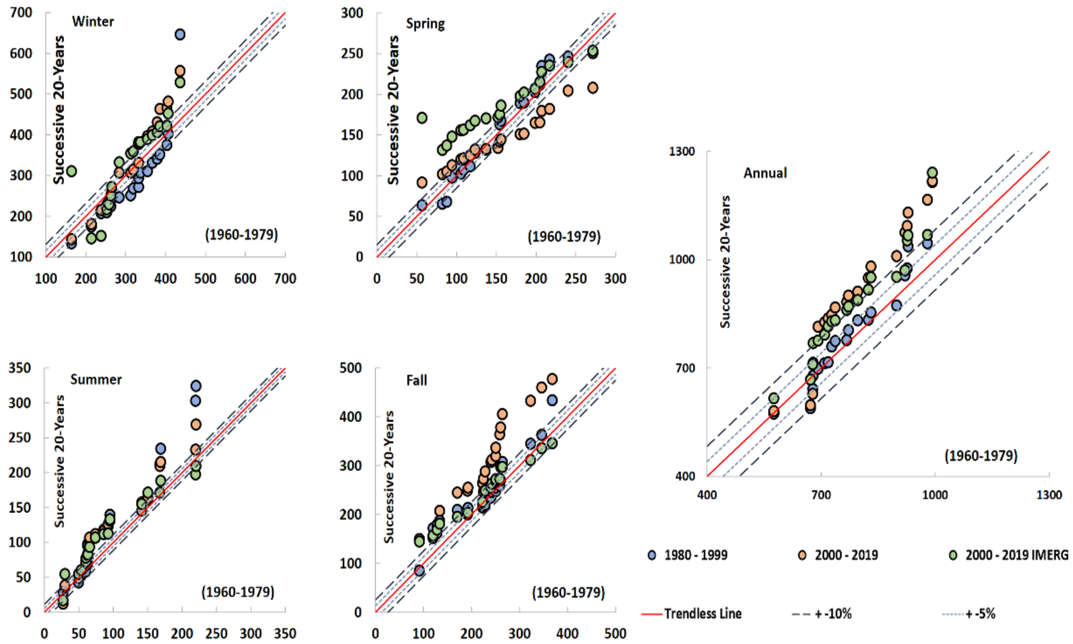

Figure 3.5 : Seasonal and annual precipitation trend analysis based on the ground-based meteorological station and IMERG data in overlapping 20-year intervals using the multi-duration ITA method.

The summer season demonstrated a rather monotonic increasing trend with distinct positive rates in higher values. The fall season and annual analysis of the same interval (1980-1999) demonstrated a slightly increasing trend with major data points sporadically varying between the 1:1 line and the +10% band.

In the 2000-2019 interval, major contradictory trends were observed in comparison to the previous and referral intervals and also between the ground-based meteorologic station data and IMERG time series. For instance, in 2000-2019, the winter season demonstrated an increasing trend which was confirmed both by the ground-based station and IMERG data. The direction and magnitude of the trend for the spring season in 2000-2019 were contradictory in time series from the ground-based station and IMERG data. While the IMERG time series demonstrated a distinctive increasing trend, data from the ground-based station exhibited a decreasing trend with a D value equal to -0.63.

This discrepancy presumably originates from the spatio-temporal variation of the precipitation over Istanbul in the spring season. In the summer season, along with a substantial increasing trend, a notable consistency was found between the time series from the ground-based station and IMERG in the direction and magnitude of the trend. The highest increase in the precipitation trend in the 2000-2019 interval was observed in the fall season based on the ground-based data with the D value equal to 3.45. The upward direction of the trend in this interval was also confirmed by the IMERG data. However, in the high values, despite the existence of a significant increasing trend in time series from the ground-based station, a reduction was noticed based on the IMERG time series (Figure 3.5). In the annual analysis, a pronounced increasing trend was observed for the 2000-2019 interval from the ground-based station time series, which complied with the IMERG time series both in cases of direction and magnitude.

3.2 Model Development

3.2.1 Sensitivity analysis, calibration, and validation

Before starting the calibration and validation of the model, a manual sensitivity analysis was carried out to find the most sensitive parameters from the ones that were not measured or defined with good accuracy. In total, 12 parameters, including width, % impervious, N-impervious, slope, Ds-impervious, Ds-pervious, % zero-imperviousness, and N-pervious, which are associated with the subcatchments' runoff in SWMM, and conductivity, initial deficit, suction head, which are associated with the infiltration process in SWMM, and conduit roughness associated with the flow routing in SWMM, were selected for performing the sensitivity analysis. Comparing the percent change in water depth in the channel calculated by the SWMM model after changing the value of the aforementioned parameters by ±50% at a time demonstrated that the developed model is not tangibly sensitive to the N-pervious and % zero-imperviousness. The rest of the parameters demonstrated a percent change in water depth in the channel greater than 0.25% and were included in the calibration process in comply with the similar studies in the literature (Shahed Behrouz et al., 2020). % impervious, conduit roughness and subcatchment width demonstrated the first three highest change rates in the channel water depth, with 33.65%, 5.99%, and 3.38%, respectively.

Table 3.5 below shows the corresponding percent change in water depth at the measuring point in the main channel for each parameter.

Table 3.5 : SWMM model sensitivity to ±50% change in the parameters.

Parameter			% Change in the water depth	Rank
Conduit	Soil	Subcatchment		
		% Impervious	33.65	1
Conduit roughness			5.99	2
		Width	3.38	3
		N-impervious	2.88	4
		Slope	2.84	5
	Conductivity		0.68	6
		Ds-impervious	0.43	7
	Initial deficit		0.38	8
	Suction head		0.36	9
		Ds-pervious	0.25	10
		% Zero-imperviousness	0.14	11
		N-pervious	0.08	12

The sensitive parameters were then entered into the OSTRICH configuration file to be calibrated within the range provided in the SWMM manual. Based on the algorithm type, perturbation value, and maximum number of iterations that are defined in the configuration file, OSTRICH builds new parameters to comply with the structure of the template file and runs the SWMM model to obtain and compare the model results with the observed values. This cycle is followed consecutively by OSTRICH until reaching the maximum number of iterations or satisfying the objective function with a value defined by the user.

13 rainfall events with different durations and random occurrences within the span of 2012 to 2019 and the corresponding water depth records in the channel were combined

in consecutive order for performing the calibration and validation processes. The total length of observed rainfall and water depth data covers 58 hours and 54 minutes, with a resolution of one pair of data points per minute. 56.6% of the observations corresponding to 33 hours and 19 minutes were used for the calibration process, and the remaining 43.4% corresponding to 25 hours and 35 minutes were used for conducting the validation process.

The DDS algorithm, which is a heuristic (global search) algorithm for single objective calibration and optimization (Tolson & Shoemaker, 2007) was selected as the search algorithm. Heuristic algorithms perform better at avoiding getting trapped in local minima; however, they may require more time and a larger number of model runs in comparison to the deterministic (local search) algorithms. For comparing the simulated and measured water depth in the main channel and at node J139, in the model calibration process, Nash-Sutcliffe Efficiency (NSE) (Nash & Sutcliffe, 1970) was used.

$$NSE = 1 - \frac{\sum_{i=1}^{n}(O_i - P_i)^2}{\sum_{i=1}^{n}(O_i - \bar{O})^2} \tag{3.1}$$

where, O_i stands for the observed water depth in the channel, P_i stands for the simulated water depth, $\bar{O}$ represents the observed values' average, and n is the total number of samples.

Initial assessment of the simulated and observed water depth for this rainfall time series revealed an NSE value of 0.63, which was within the satisfactory range of $0.5 < NSE \leq 0.65$, according to (N. Moriasi et al., 2007). To increase the accuracy of the model results within a logical range of computational system effort and time, the sensitive parameters of the developed SWMM model were calibrated against the measured water depth data by OSTRICH up to 500 iterations with a perturbation value of 0.2. It is noteworthy to mention that, instead of calibrating the sensitive parameters that were calculated specifically for each subcatchment, such as % impervious, width, slope, and N-impervious, individually, which imposes a significantly great amount of computational effort and time on the system performing the calibration process, the average of these parameters was calibrated, and the percent change in the initial average value was applied to the individual parameters in each subcatchment. By employing this method, the initial NSE value of 0.63 was increased to 0.77, which indicates a very good agreement between observed and simulated water depth (N. Moriasi et al., 2007).

Table 3.6 : Initial, range, and calibrated values of SWMM model parameters.

Parameter	Initial	Low	High	Calibrated
% Impervious*	88.67	- 20%$_{\text{Initial Value}}$ **	100 **	- 18%$_{\text{Initial}}$
Width*	552.64	- 20%$_{\text{Initial Value}}$ **	+ 20%$_{\text{Initial Value}}$ **	- 8%$_{\text{Initial Value}}$
Slope*	9.77	- 10%$_{\text{Initial Value}}$ **	+ 10%$_{\text{Initial Value}}$ **	- 2%$_{\text{Inital Value}}$
N-impervious*	0.037	0.011***	0.06***	+ 54%$_{\text{Initial}}$
Ds-impervious	2.54$_{\text{mm}}$	1.27$_{\text{mm}}$***	2.54$_{\text{mm}}$***	1.3
Suction head	320	49***	320***	109.34
Conductivity	1.016	0.254***	120.4***	37.55
Initial deficit	0.43	0***	0.501***	0.4
Conduit roughness	Natural 0.1	0.03***	0.4***	0.167
	Concrete 0.01	0.01***	0.02***	0.0166

* Average value
** User-defined range
*** Suggested range in SWMM (Rossman, 2010).

To test the validity of the calibrated model, a rainfall time series consisting of six events that were randomly selected between the years 2012 and 2019 in consecutive order was created. Consequently, a time series with a duration of 25 hours and 35 minutes was simulated in the calibrated SWMM model, and the resulting water depths in the channel were compared with the corresponding observed water depths. Validation analysis resulted in an NSE value of 0.67, which is within the range denoted as good agreement in the literature (Figure 3.6) (N. Moriasi et al., 2007).

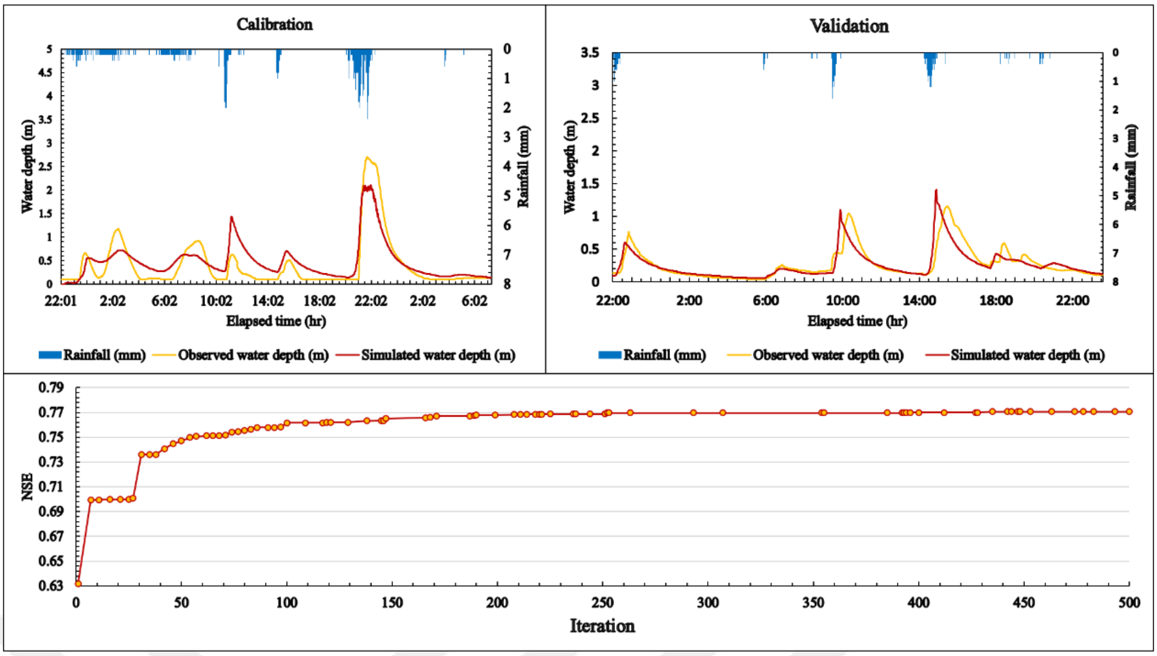

Figure 3.6 : Observed and simulated water depths in the channel for calibration, validation, and improvement of the NSE value during the calibration process by OSTRICH.

3.2.2 Developing the implementation strategy based on a survey from experts and AHP:

After achieving acceptable and accurate results in the model calibration and validation, an implementation strategy was developed based on a survey through experts and the MCDA method for implementing RB, CI, and DW units in the study area.

In this step, a questionnaire survey was prepared based on AHP and distributed to 10 randomly selected experts in the field of urban flood control, urban planning, hydrology, and environment protection.

Each questionnaire survey sheet was designed to include three pairwise comparison matrices, one for each type of LIDs (RB, CI, DW). In each questionnaire sheet along with the pairwise comparison matrices, the required information about criteria or influencing factors, clear instructions about how to fill out the matrices, and an example were provided to avoid ambiguity and confusion among participants.

In the survey, the participants were asked to fill out the pairwise comparison matrices by indicating the degree of importance that they believe exists between two decision-making criteria or factors. The corresponding value of each importance level is demonstrated in Table 3.7.

Table 3.7 : Corresponding value of importance levels.

Preference Expressions	Corresponding Value
Equally important	1
Intermediate	2
Slightly more important	3
Intermediate	4
Moderately more important	5
Intermediate	6
Strongly more important	7
Intermediate	8
Extremely more important	9

A sample pairwise comparison matrix consists of n columns and n rows which are identical in case of content and order. The diagonal elements are equal to 1 since the importance degree of any criteria compared to itself is equal to 1. The lower triangle is redundant since it will be the reflection of the upper triangle. The element a_{ij} is the expert's response to the importance level of criteria i compared to j. Therefore, the reciprocal element (a_{ji}) which is the expert's response to the importance level of criteria j to i is calculated automatically as $1/a_{ij}$. Figures 3.7 and 3.8 show the pairwise comparison matrices used for evaluating the decision-making criteria of RB and CI, and DW units.

Factors	**Total Subcatchment Runoff (SWMM model output)**	**% Residential Area in Subcatchment**	**%Industrial Area in Subcatchment**	**Main Stormwater Drainage Network (Length X Diameter)**
Total Subcatchment Runoff (SWMM model output)	1.0	-----	-----	-----
% Residential Area in Subcatchment		1.0	-----	-----
%Industrial Area in Subcatchment			1.0	-----
Main Stormwater Drainage Network (Length X Diameter)				1.0

Figure 3.7 : Pairwise comparison matrix used for RB and CI implementation.

As it is obvious in Figure 3.8, in comparison to RB, and CI units, the number of influencing criteria in DW implementation is more. This is mainly because of the higher number of environmental and geospatial criteria involved in DW implementation compared to RB, and CI units.

Factors	Total Subcatchment Runoff (SWMM model output)	Subcatchment Slope	Distance to Sea Water	% Residential Area in Subcatchment	%Industrial Area in Subcatchment	Distance to Main Roads	Main Stormwater Drainage Network (Length X Diameter)	Subcatchment Soil Type
Total Subcatchment Runoff (SWMM model output)	1.0	-----	-----	-----	-----	-----	-----	-----
Subcatchment Slope		1.0	-----	-----	-----	-----	-----	-----
Distance to Sea Water			1.0	-----	-----	-----	-----	-----
% Residential Area in Subcatchment				1.0	-----	-----	-----	-----
%Industrial Area in Subcatchment					1.0	-----	-----	-----
Distance to Main Roads						1.0	-----	-----
Main Stormwater Drainage Network (Length X Diameter)							1.0	-----
Subcatchment Soil Type								1.0

Figure 3.8 : Pairwise comparison matrix used for DW implementation.

After collecting the experts' responses to the survey, each pairwise comparison matrix was tested for the level of consistency ratio (CR) based on the equation (2.19).

The consistency ratio (CR), indicates how much the provided responses are logical and reasonable based on the participant's judgment. While a low CR indicates the robustness of the derived weights and enhances confidence in the decision-making process, a high CR could indicate issues such as overlapping or contradictory priorities, bias or misunderstanding during judgment, or complexity or subjectivity in the criteria being compared.

Therefore, for the responses with a consistency rate of higher than 0.1, the participant expert was asked to revise the given response until a consistency rate lower or equal to 0.1 is achieved. The profile of the attended experts and the final consistency rate of their correspondence to each pairwise comparison matrix are demonstrated in Table 3.8.

Table 3.8 : Profile of the attended experts and consistency rate results of the responses.

	Position	Experience (Year)	CR		
			RB	CI	DW
E1	Professor	+10	0.05	0.06	0.04
E2	Professor	+10	0.02	0.05	0.1
E3	Private sector	+10	0	0.09	0.06
E4	Professor	+5	0.02	0.05	0.02
E5	Professor	+5	0	0.1	0.1
E6	Professor	+10	0.02	0.02	0.07
E7	Researcher	+8	0.07	0.01	0.04
E8	Private sector	+6	0.07	0.07	0.1
E9	Private sector	+7	0.05	0.09	0.02
E10	Private sector	+6	0.06	0.1	0.04

The average of suggested criteria weights by the experts was obtained at the end of the AHP process to determine the weight of each criterion involved in the decision-making process of LID implementations.

As demonstrated in Table 3.9, total subcatchment runoff (SWMM model output) was found to have the highest criteria weight among other criteria for the implementation of RB, CI, and DW units. This criterion was followed by % residential area and % industrial area in the subcatchments, respectively, for the RB and CI implementations, and subcatchment sub-soil type for the DW implementation. Conversely, the main stormwater drainage network capacity in RB and CI implementation and distance to main roads in DW implementation were found to attain the least criteria weight among others. The main stormwater drainage network density and distance from main roads, along with the hydraulic conductivity of the sub-soil, which is equivalent to the subcatchment sub-soil type criterion in this study, were also assigned similar weights (importance level) in detecting suitable locations for DW implementations by (Mohamed Mouhoumed et al., 2023). Distance to the seawater attained an average weight of 0.107 and ranked third among other criteria in the AHP process, which considering the location of the watershed in the vicinity of the Marmara Sea plays a significant role in limiting the number of DW implemented in the southern subcatchments of the study area.

Table 3.9 : Average of the suggested weights by experts for RB, CI, and DW implementations.

Criteria	Average weight		
	Rain	Cistern	Drywell
Total Subcatchment Runoff (SWMM model output)	0.636	0.607	0.284
% Residential Area in Subcatchment	0.241	-	0.073
% Industrial Area in Subcatchment	-	0.272	0.06
Main Stormwater Drainage Network Capacity (Length x Diameter)	0.122	0.119	0.071
Subcatchment Slope	-	-	0.09
Distance to Sea Water	-	-	0.107
Distance to Main Roads	-	-	0.057
Subcatchment Sub-Soil Type	-	-	0.255

After calculating the average weights of the involved criteria based on the survey results, the maximum number of the RB, CI, and DW units that potentially could be implemented in each subcatchment was calculated. This step was carried out based on a pre-defined rule of 1 RB unit per 100 m^2 of residential area, 1 CI unit per 1000 m^2 of industrial area, and 1 DW unit per 500 m^2 of combined residential and industrial area as explained in section 2.3.7. For this purpose, the area occupied by residential and industrial buildings in each subcatchment was determined by the QGIS program and based on a high-resolution land cover map that was prepared earlier in this study as demonstrated in Figure 2.7.

The maximum number of the LIDs in each subcatchment determines the highest number of the RB, CI, and DW units that can be installed in each subcatchment if the subcatchment can fully satisfy the suitability. It's the suitability score that determines how much of the maximum number of LIDs can be implemented in each subcatchment. As visually explained in the schematic framework of the study in Figure

2.16, calculating the suitability score of the subcatchments is necessary in order to determine how many RB, CI, or DW units can be actually implemented in each subcatchment. Therefore, the suitability score of each subcatchment was calculated as below:

$$\text{Suitability score} = \sum(\text{criteria weight} \times \text{criteria value}) \tag{3.2}$$

Once the suitability score was calculated, subcatchments were descendingly ordered according to their suitability scores for calculating the allowed number of the RB, CI, and DW units.

For the subcatchments possessing the highest and lowest ranks the allowed number of RB, CI, and DW units was set to be equal to the maximum number and zero respectively. For instance, the subcatchment with the highest suitability score for RB implementation was assigned the top rank (#1) and subsequently allocated the maximum number of RBs within that subcatchment. Conversely, the subcatchment with the lowest suitability score for RB implementation was assigned the lowest rank, and consequently, no RBs were implemented in that specific subcatchment. This process was repeated for the subcatchments with the highest and lowest ranks for CI, and DW as well.

For the subcatchments with a suitability rank between 1 and 102 which is the total number of subcatchments, the allowed number of RB, CI, and DW units to be implemented in each subcatchment was calculated as below:

$$\text{Allowed number} = \left(\frac{(n+1) - \text{ Rank}}{n}\right) \times \text{ Maximum number} \tag{3.3}$$

where n resembles the total number of subcatchments in the SWMM model.

As a result of this operation, the maximum number of RB, CI, and DW units in this study was constrained based on expert knowledge to achieve practical and realistic results in stormwater runoff reduction. Furthermore, the RB, CI, and DW units were implemented in the most suitable subcatchments so that they could effectively contribute to the runoff reduction process. Moreover, through this process, a thorough assessment was conducted to ensure that potential negative environmental consequences associated with the implementation of DW units were effectively eliminated or minimized.

In general, this implementation strategy which is based on expert knowledge incorporation, underscores the commitment to sustainable and environmentally responsible project execution, prevents or reduces adverse impacts on the surrounding ecosystems, and assists long-term ecological balance while meeting infrastructure development goals. Table 3,10 shows specific residential and industrial areas, the maximum number of LID types, and the allowed number of LID types for sample subcatchments. The full list of subcatchments is available in Appendix A.

Table 3.10 : Specific residential and industrial areas, suitability rank, Maximum and allowed number of RB, CI, and DW units for sample subcatchments. (A Full list is available in the Appendix A.)

	Residential (m^2)	Industrial (m^2)	Max RB	RB Rank	Allowed RB	Max CI	CI Rank	Allowed CI	Max DW	DW Rank	Allowed DW
S1	749000	0	7490	11	6756	0	31	0	1498	2	1483
.											
.											
S29	0	663000	0	39	0	663	18	553	1326	20	1079
.											
.											
S50	681200	628800	6812	4	6612	629	3	616	2620	48	1413
.											
.											
102	38240	0	382	1	382	0	1	0	77	101	1

Figures 3.9 to 3.11 demonstrate the maximum and implemented numbers of RB, CI, and DW units in the study area.

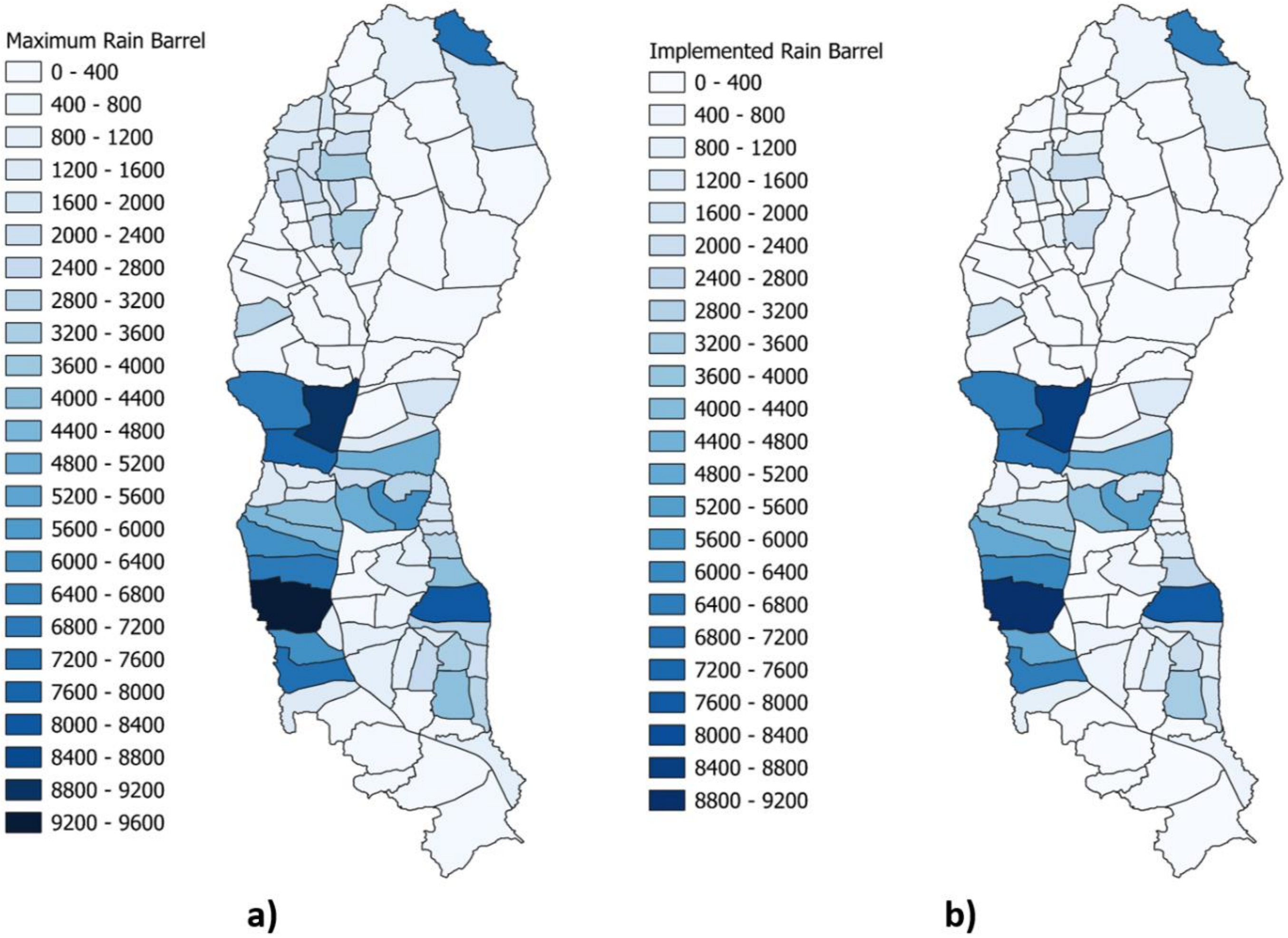

Figure 3.9 : Maximum versus the implemented number of RB units in each subcatchment.

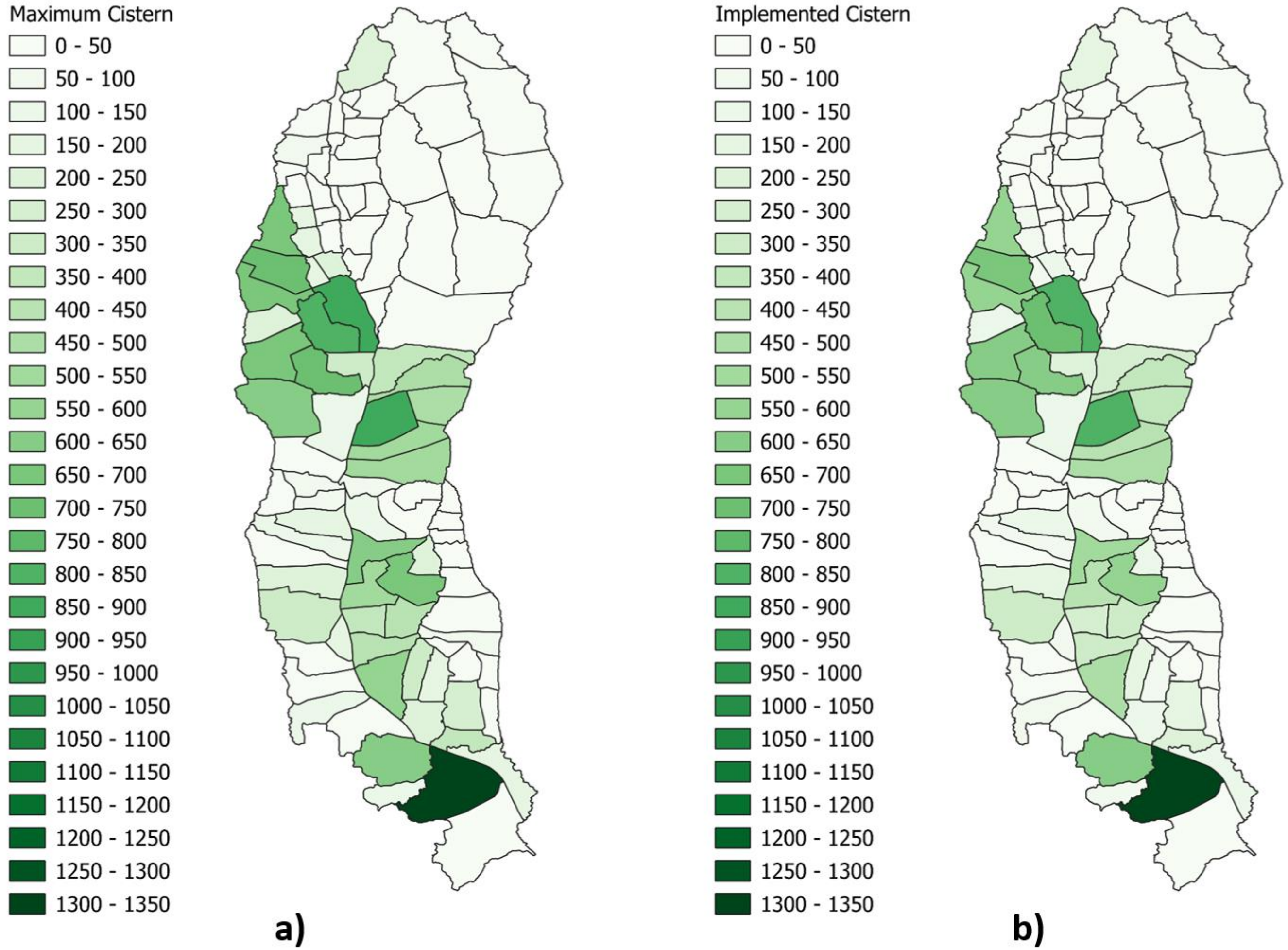

Figure 3.10 : Maximum versus the implemented number of CI units in each subcatchment.

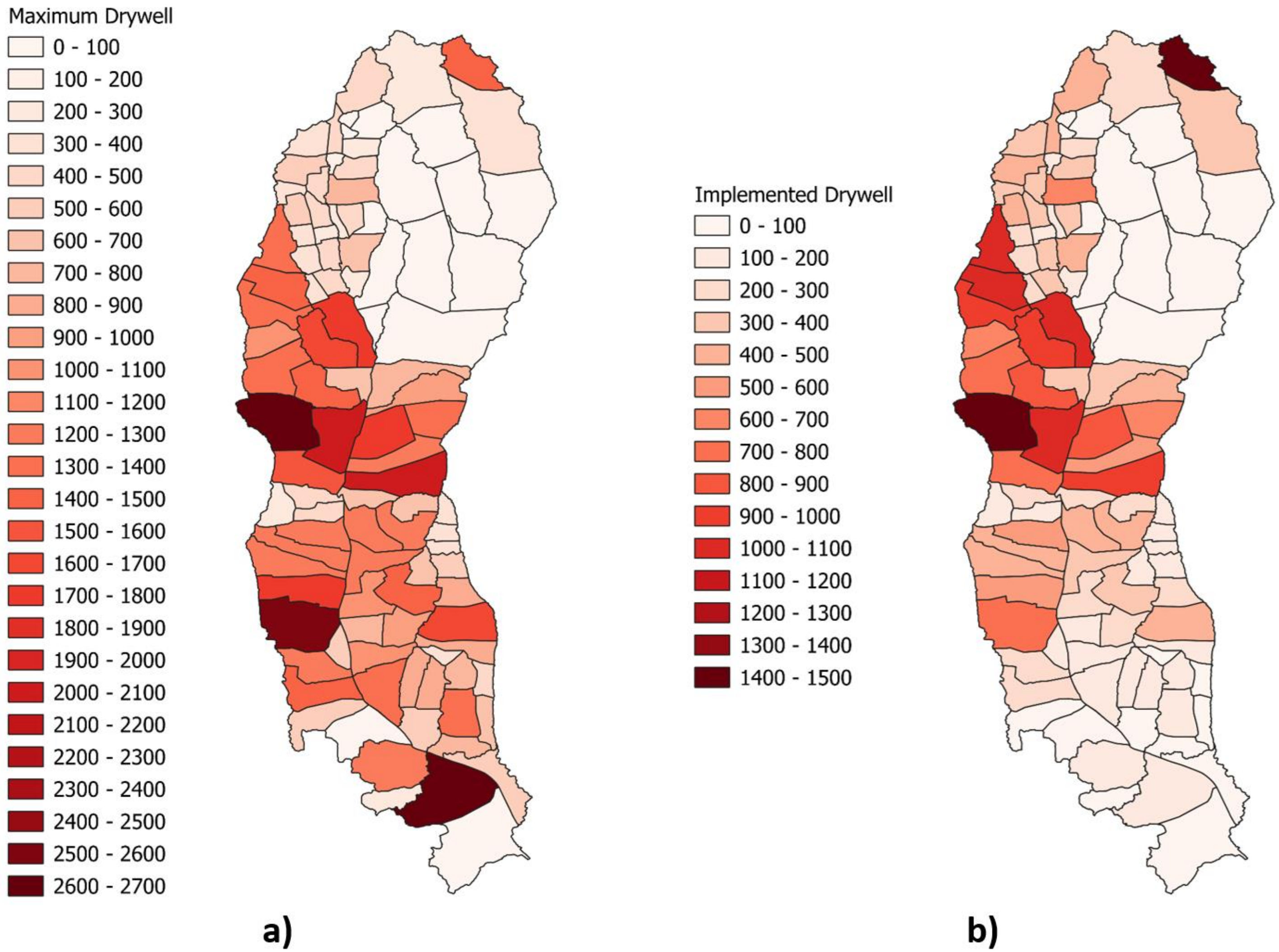

Figure 3.11 : Maximum versus the implemented number of DW units in each subcatchment.

Explicit variation exists in the implementation locations of the aforementioned decentralized stormwater management unit types, which indicates the profound influence of site characteristics reflected by the survey conducted in accordance with the AHP. For instance, in Figure 3.9, to 3.11, the majority of the northeastern parts of the study area are occupied with pale colors, which points to a lower number of implemented RB, CI, and DW units. These areas are mostly covered with wooded and vegetated areas, and the lack of large or small rooftops chiefly limits the allowed number of LID units.

Additionally, based on Figures 3.9 to 3.11, what is common to all of the LID types is the concentration of LID units in the central subcatchments of the study area. This is mainly because of the abundance of residential and industrial areas in the central parts of the study area. On the other hand, as presented in Figure, 2.8 (a) the slope variation of the central parts of the Ayamama watershed is relatively less and rather flat compared to the northern parts. This triggers inundations and floods in the central parts and can negatively affect a large proportion of the residents and industrial sections active in this location. Therefore, it is of utmost importance to benefit from decentralized stormwater management units in this location since centralized drainage systems, including underground pipelines or superficial channels, may experience malfunctions due to the existing gentle slope.

By comparing the map of subcatchments' suitability for RB and CI implementation, the existence of a complementary pattern is obvious in the central toward mid-southern parts of the study area. This pattern originates from the fact that a major proportion of the central and southern subcatchments are occupied by only residential and industrial areas. For instance, major industrial regions known as İkitelli OSB and Güneşli textile industry and Oto Pazarı, Kuyumcukent, etc. are located in this part of the study area and the vicinity or opposite of these areas large residential areas exist within a distinctive border. This arrangement creates a complementary pattern in the suitable subcatchments for RB, and CI implementations in the central and mid-southern parts of the study area.

About the subcatchments suitable for DW implementations, what is tangible from Figure 3.11 is that the lack of residential and industrial areas and distance to the seawater, along with the permeability of the sub-soil, profoundly control the number of DW units that are allowed to be implemented in the northern and southern subcatchments. In general, northern subcatchments are not relatively suitable for DW implementations because of marginal residential and industrial buildings, high slope, and most importantly dominant impermeable sub-soil. Southern subcatchments are also not fully suitable because of the close distance to the sea which triggers saltwater intrusion. Considering the overall influencing criteria and their associated weights obtained from the AHP survey, it can be concluded that central, western, and minor parts in the north and east of the Ayamama watershed are suitable for DW implementations.

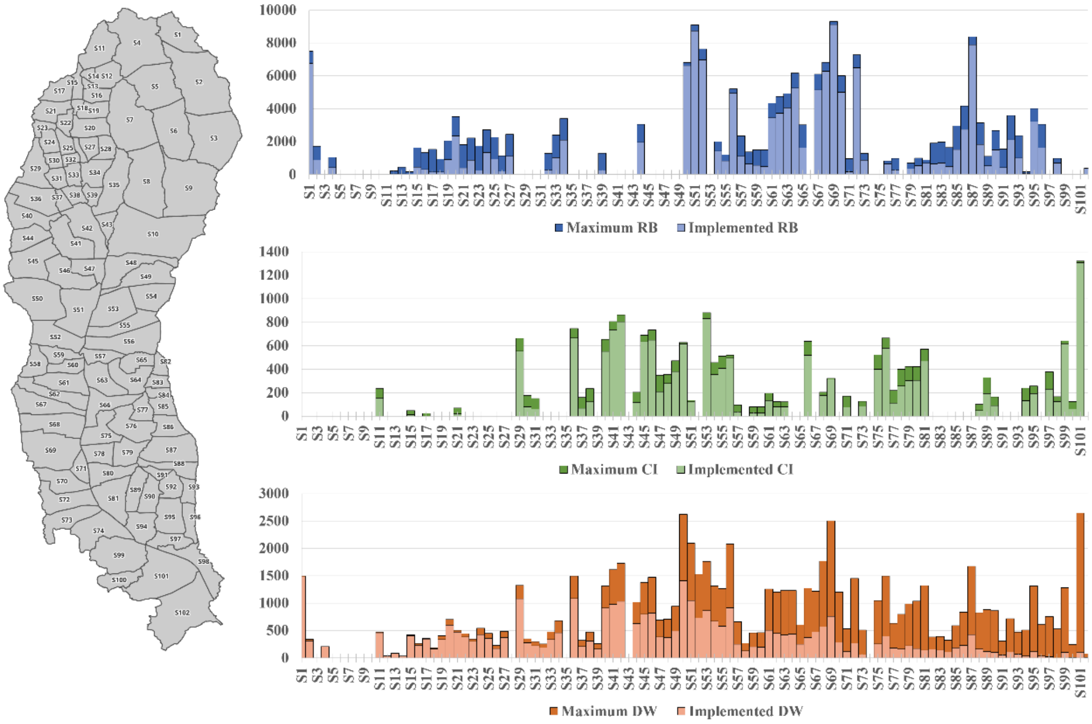

Figure 3.12 : Histogram of maximum versus the implemented number of RB, CI, and DW units in the study area subcatchments.

3.2.3 Hydrologic responses of the developed SWMM model

To assess the impacts of implemented RB, CI, and DW units on the hydrologic response of the study area, the developed and calibrated SWMM model was tested against five designed storm events with a duration of 2 hours and return periods of 2, 5, 10, 25, and 50 years, as well as the flooding event of September 2009.

For the designed storm events, Frequency, Duration, and Intensity (IDF) curves were used to create five storm event hyetograph according to the Chicago storm profile (Keifer & Chu, 1957).

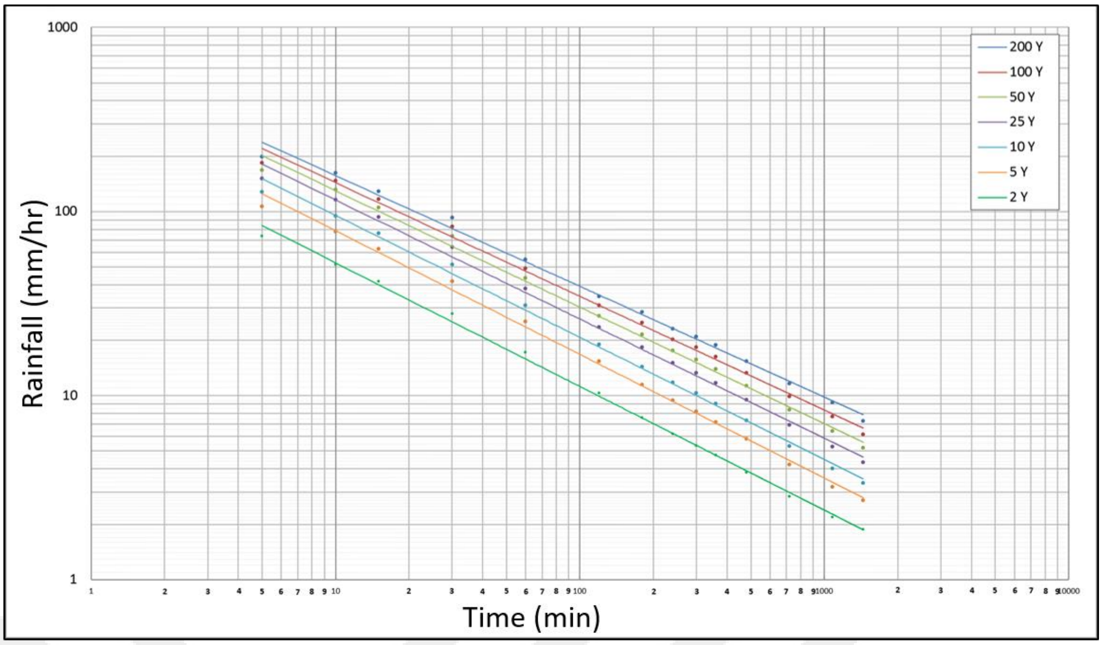

Figure 3.13 : Precipitation Frequency, Duration, and Intensity (IDF) curves used for storm design.

The created storm hyetographs, with the duration of 2 hours and return intervals of T=2, 5, 10, 25, and 50 years were simulated in the hydrologic model of the study area before and also after RB, CI, and DW implementations.

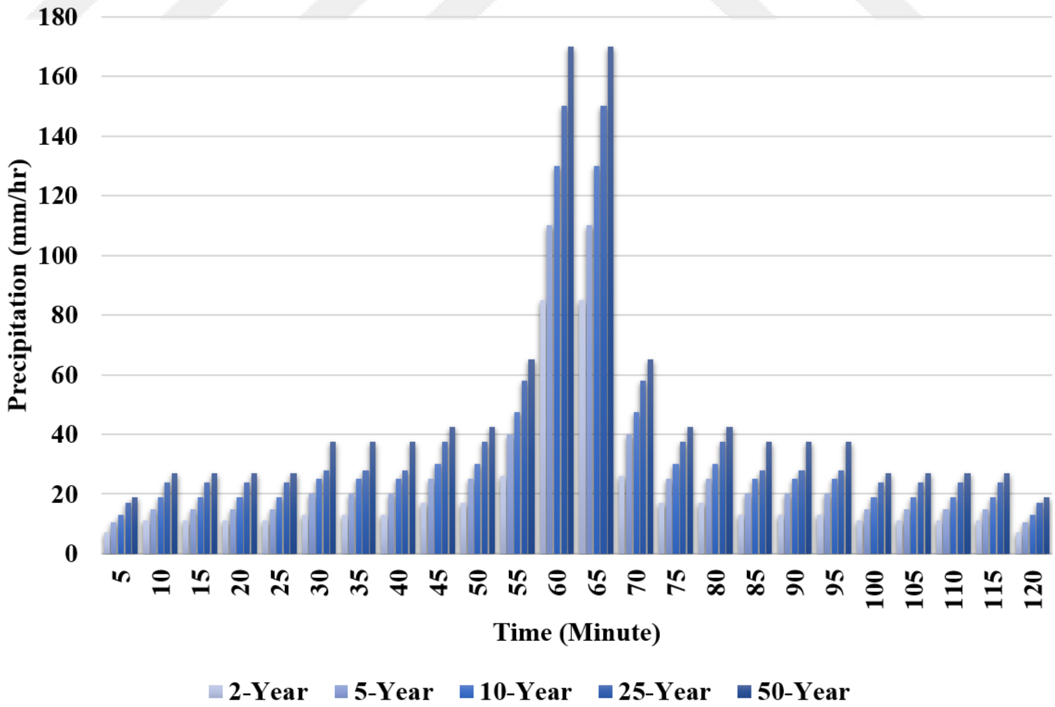

Figure 3.14 : Designed storm hyetographs with various return intervals according to the Chicago storm profile (Keifer & Chu, 1957).

Later the variation in different indicators of the hydrologic response of the watershed, including peak runoff, total runoff volume, and time to peak, in the base SWMM model (without RB, CI, and DW units) and the SWMM model of the study area after RB, CI, and DW implementations were assessed under the aforementioned storm events.

A significant reduction in peak runoff was observed following the implementation of RB, CI, and DW units in the base SWMM model of the study area under all designed storm events. As per Table 3.11, for the designed storm events with the return periods of T = 2, 5, 10, 25, and 50, peak runoff was obtained as 328.72, 506.7, 740.9, 954.2, and 1175 (m^3/s) respectively, which, after implementing RB, CI, and DW units, reduced to 177.6, 196.5, 292.5, 318.8, and 277.65 (m^3/s) respectively, equivalent to reduction rates of 54.03%, 38.78%, 39.48%, 33.41%, and 23.63%.

This reduction highlights the effectiveness of decentralized stormwater management units or LID practices in mitigating stormwater runoff by enhancing infiltration, storage, and delay mechanisms, which collectively reduce the volume and intensity of surface runoff during storm events. The results demonstrated that the amount of peak runoff reduction was inversely proportional to the return period of the storm event. Specifically, storm events with shorter return periods, which are typically less intense and occur more frequently, showed a greater percentage reduction in peak runoff. Conversely, as the return period and intensity of the storm event increased, the ratio of runoff reduction decreased, indicating the reduced capacity of the implemented systems to offset the impacts of more severe storms.

For instance, the most notable reduction in peak runoff was observed under the storm event with a return period of T = 2 years, where the percentage reduction reached 54.03%, equivalent to 177.6 (m^3/s). This considerable decrease underscores the efficiency of the combined application of RB, CI, and DW systems in managing stormwater during frequent, less intense rainfall events. In comparison, the reduction percentages of the peak runoff in storm events with return periods of T = 5, 10, 25, and 50 years were recorded as 38.78%, 39.18%, 33.41%, and 23.63%, equivalent to 196.5, 292.5, 318.8, and 277.65 (m^3/s), respectively. These results illustrate that although the amount of peak runoff reduced by the implemented RB, CI, and DW units is higher in the storm events with longer return periods because of their higher amount of precipitation, the percent reduction is diminishing as the intensity and magnitude of storm events increase.

This trend can be attributed to the design limitations of the aforementioned units. For instance, in high-intensity storms associated with longer return periods, the rapid accumulation of runoff from the surfaces of rooftops may exceed the storage of RB, and CI units and infiltration capacity of DW units, leading to an overall lower percentage reduction in peak runoff. However, even in these cases, the implementation of decentralized stormwater management units provides a meaningful reduction in peak flows considering the reduced amount of runoff in (m^3/s) which contributes to reduced risks of flooding.

Overall, the findings based on the peak runoff reduction, underscore the critical role of implemented units as a part of decentralized stormwater management systems in urban runoff mitigation. Implemented RB, CI, and DW units are particularly effective in addressing frequent storm events with shorter return periods, where they can significantly alleviate the pressure on conventional drainage systems and promote sustainable water resource management. Although their efficiency diminishes for more severe storm events, their contribution remains valuable, demonstrating their potential as an integral component of integrated stormwater management strategies.

Figure 3.15 shows the hydrologic response of the SWMM model of the study area before (without RB, CI, and DW) and after (with RB, CI, and DW) implementations under different designed storm events.

Total runoff volume also was assessed after implementing RB, CI, and DW units in the study area under the aforementioned storm events. Similar to the peak runoff, significant reductions were also observed in total runoff based on the hydrograph results. However, in comparison to the peak runoff reduction, the total runoff volume reduction rate demonstrated variation in a lower range and an inverse relation to the return period of the storm event. For instance, according to Table 3.11, for the storm event with a 2-year return period, the runoff volume reduction was obtained as $412.5X10^3$ (m^3), equivalent to 27.43%, while this amount for the storm events with T = 5, 10, 25, and 50-year was obtained as $416.7X10^3$, $419.2X10^3$, $421.7X10^3$, and $424.1X10^3$ (m^3) respectively, equivalent to 19.45%, 15.85%, 13.23%, and 11.17% of the total runoff volume without RB, CI, and DW implementations.

Another critical indicator of the variation in the hydrologic response of the study area after the implementation of RB, CI, and DW units is the change in the time it takes to reach the peak of the runoff hydrograph. This parameter, often referred to as the time-to-peak, is essential for understanding how much time is available for completing the evacuation process. In this study, this indicator is used to test the influence of implemented units in extending the time to the peak of the runoff hydrograph.

The results from the SWMM simulations revealed significant alterations in the time-to-peak for different design storm events, showcasing the effectiveness of the implemented RB, CI, and DW units in delaying stormwater runoff and attenuating peak flows.

For the designed storm event with a 2-year return period (T = 2), the time to peak increased substantially by 55 minutes compared to the base condition. This considerable delay demonstrates the ability of RB, CI, and DW units to temporarily store and slow down runoff, thereby providing an extended response time. The increased time to peak in this scenario is particularly beneficial for reducing immediate downstream flooding risks, allowing stormwater to be released at a more manageable rate and providing critical time for drainage systems to cope with inflows.

However, as the return period of the designed storm event increased, the delay in time to peak progressively decreased. For the storm events with return periods of T = 5, 10, and 25 years, the respective increases in time-to-peak were recorded as 25, 15, and 10 minutes. This trend indicates a declining influence of RB, CI, and DWs on delaying peak runoff as storm intensity and magnitude grow. The reduced delay is primarily due to the limitations of these systems in handling larger runoff volumes generated by higher-intensity storms. Under these conditions, the storage and infiltration capacities of these units may reach the upper threshold more quickly, reducing their ability to further delay runoff.

For the most extreme storm event analyzed, with a return period of T = 50 years, the time-to-peak remained unchanged at 70 minutes, identical to the base condition of the study area. This result suggests that under such high-magnitude storm conditions, the hydrologic response of the study area is dominated by the storm's intensity and duration, with minimal influence from the implemented LID measures. The inability of the implemented units to affect the time to peak in this scenario highlights the challenges of relying solely on decentralized storm management systems for mitigating runoff during rare and extreme storm events.

In general, based on the observed results, the variation in time-to-peak after implementation reflects the dynamic interaction between storm characteristics and the performance of the decentralized stormwater management systems. The substantial delays observed for smaller storm events emphasize the importance of incorporating RB, CI, and DW units into urban planning to manage frequent rainfall effectively. However, for extreme storms, these systems may require supplementary measures, such as detention basins, retention ponds, stormwater wetlands or enhanced drainage networks, to mitigate their limitations. As demonstrated in figures 3.9, 3.10, and 3.11, some of the subcatchments located in the northern parts of the study area are not fully suitable for RB, CI, and DW implementations because of a lack of residential or industrial areas and an abundance of vegetated and wooded areas. These areas can be a convenient location for implementing other types of LIDs, such as retention ponds or stormwater wetlands, instead of RB, CI, and DW units to assist mitigation of stormwater in extreme events.

The hydrologic response of the watershed under designed storm events in the base case and after implementing RB, CI, and DW units are demonstrated in Figure 3.15.

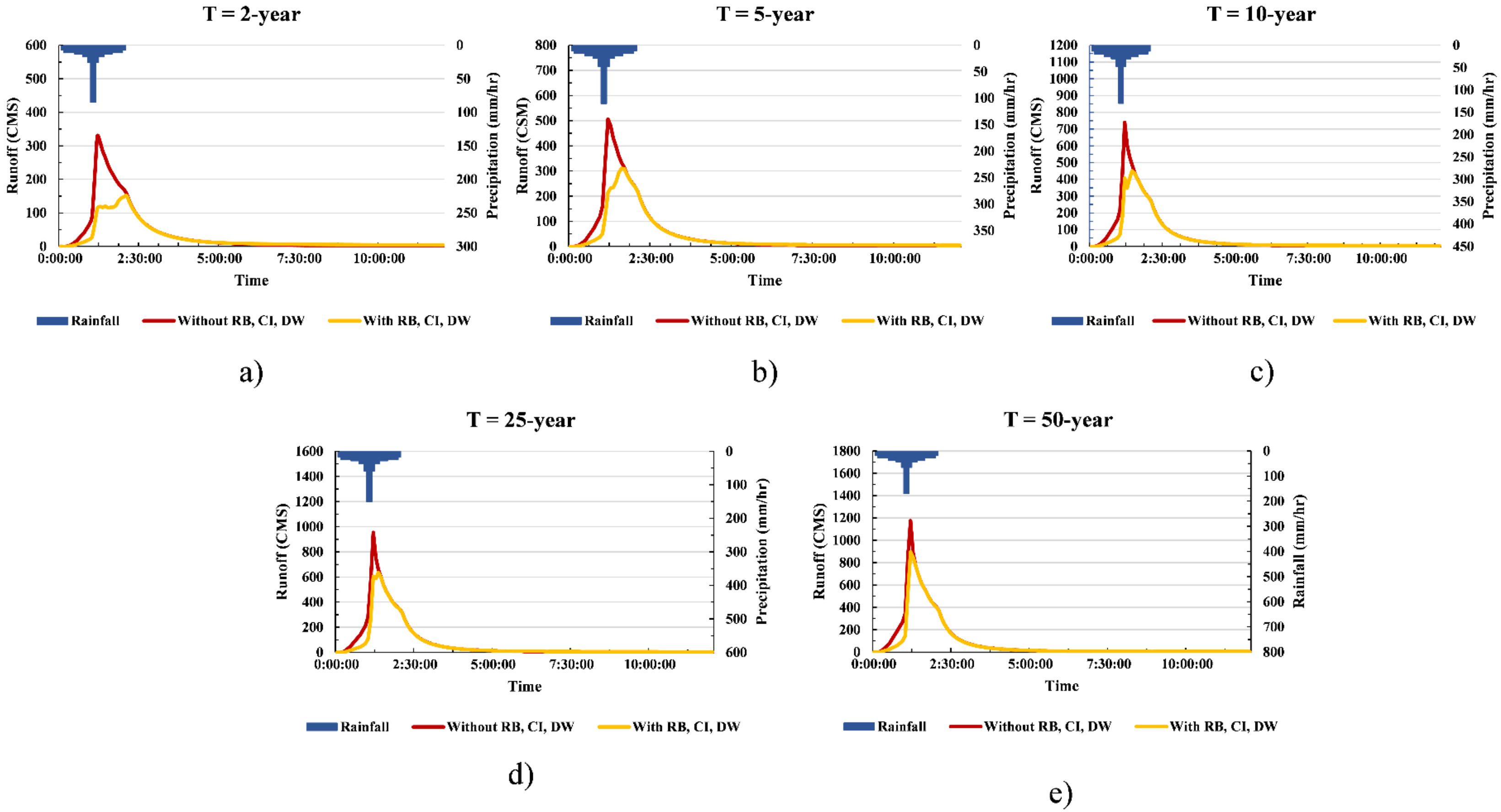

Figure 3.15 : Hydrographs of the study area before and after implementing RB, CI, and DW units under designed storm events with a duration of 2 hours and a) T = 2-year, b) T = 5-year, c) T = 10-year, d) T = 25-year, and e) T = 50-year return periods.

Table 3.10 demonstrates the variation in indicators of the hydrologic response of the watershed in the base condition and after RB, CI, and DW implementations under designed storm events.

Table 3.11 : Variation in indicators of hydrologic response of the watershed in the base condition (without RB, CI, and DW) and after RB, CI, and DW implementations under designed storm events.

		T = Return period (Year)				
		2	5	10	25	50
Peak runoff (CMS)	Base Condition	328.72	506.7	740.9	954.2	1175
	With RB, CI, DW	-54.03%	-38.78%	-39.48%	-33.41%	-23.63%
Total runoff volume (m^3)	Base Condition	$1504X10^3$	$2142.5X10^3$	$2645.1X10^3$	$3187.8X10^3$	$3797.3X10^3$
	With RB, CI, DW	-27.43%	-19.45%	-15.85%	-13.23%	-11.17%
Time to runoff peak (Min)	Base Condition	70				
	With RB, CI, DW	+55	+25	+15	+10	+0

In addition to the synthetically designed storm events with a duration of 2 hours and return intervals of 2 to 50 years, the flooding event of September 2009 was also simulated in the SWMM model of the study area to evaluate the performance of implemented RB, CI, and DW units in runoff reduction under a flooding event that was actually experienced.

The accumulated rainfall amount associated with this flooding event was entered into the model in millimeters with 1-minute time steps, and the resulting runoff was compared with the SWMM model runoff after implementing RB, CI, and DW units in the model.

The rainfall time series of this event consists of continuous and intermittent precipitations with varying intensity and duration over 43 hours. Despite the remarkable reductions that were observed after implementing RB, CI, and DW units in the study area under designed storm events with a duration of 2 hours, reductions in the peak runoff and runoff volume and improvements in the time to peak duration were not as tangible under the September 2009 flooding event scenario.

In total, the hydrograph of the SWMM model under this flooding event consists of 4 local peaks and 1 global peak over the threshold of 50 CMS. In the first local peak (Figure 3.16, point A), with a value of 261.88 (m^3/s), the peak runoff reduction was observed to be equal to 169 (m^3/s) equivalent to 64.57%, with no delay in time to peak runoff. In the second local peak (Figure 3.16, Point B), with a value of 63.44 (m^3/s), a reduction equal to 8.25 (m^3/s) equivalent to 13%, was observed along with a 2-minute delay in time to peak. In the third local peak (Figure 3.16, point C), with a value of 189.61 (m^3/s), no change was observed in the peak runoff value or its time to peak. Likewise, at the global runoff peak point (Figure 3.16, point D), with a value of 781.3 (m^3/s), no change was detected in the peak runoff value or occurring time. At the fourth local peak runoff point (Figure 3.16, point E), with a value of 84.76 (m^3/s), a 16.45% runoff reduction was observed in the peak runoff value with no change to the occurring time. Considering the entire period of the flooding event, only a 3.82% reduction was observed in the total runoff volume.

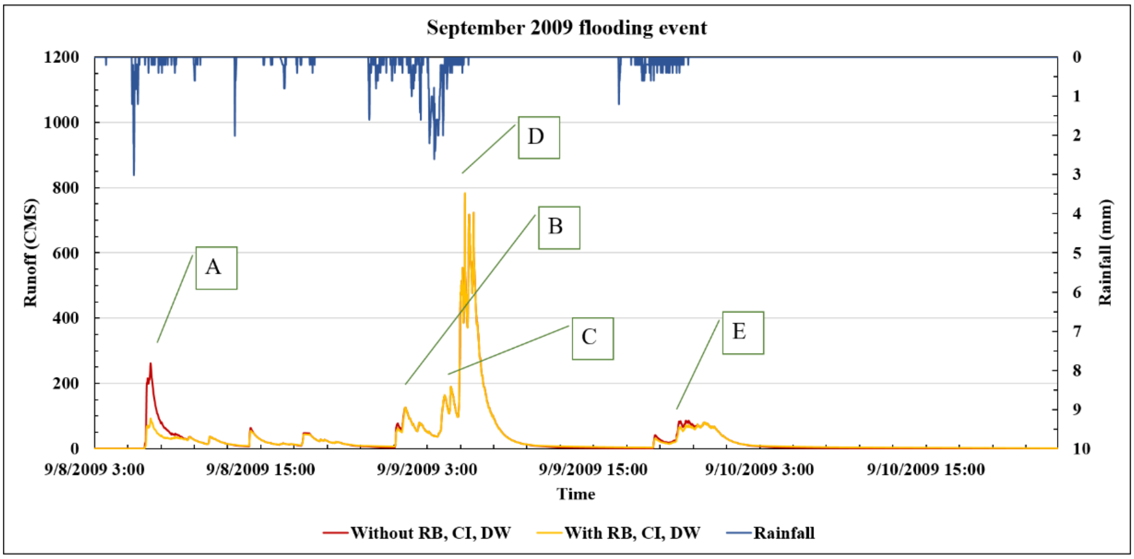

Figure 3.16 : Hydrologic response of the study area before and after implementing RB, CI, and DW units in the SWMM model under the flooding event of September 2009.

The findings suggest that the effectiveness of the implemented RB, CI, and DW units in runoff reduction in the case of storm events with long durations, such as the flooding event of September 2009, is not as great as it is during storm events that last shorter, even if they have higher intensities. In the circumstances that the storm event continues steadily or intermittently with short breaks for long hours, RB, CI, and DW units can effectively reduce the peak runoff within the first hours of flooding; however, because of the limited reservoir capacity of the RB and CI units and saturation of the DW units, their runoff reduction performance decreases drastically until a point that they become quite ineffective in runoff reduction. Owing to the infiltration process that occurs continuously in DW units, a portion of the runoff reduction process is restored, as is apparent in Figure 3.16 for point E; however, for retrieving the initial performance of the implemented RB, CI, and DW units, consecutive dry days are required to allow consumption of the water accumulated in the RB and CI units and also infiltration of the water to sub-soil through DW units.

Table 3.12 : Variation in indicators of hydrologic response of the watershed in the base condition (without RB, CI, and DW) and after RB, CI, and DW implementations under the flooding event of September 2009.

		Point A	Point B	Point C	Point D	Point E
Peak runoff (CMS)	Base Condition	261.88	63.44	189.61	781.37	84.76
	With RB, CI, DW	-64.57%	-13%	0%	0%	-16.45%
Time	Base Condition	9/8/2009 7:03	9/8/2009 14:15	9/9/2009 4:43	9/9/2009 5:44	9/9/2009 21:42
	With RB, CI, DW	9/8/2009 7:03	9/8/2009 14:17	9/9/2009 4:43	9/9/2009 5:44	9/9/2009 21:42
Total runoff volume (m^3)	Base Condition	$7953.9X10^3$				
	With RB, CI, DW	-3.82%				

Further to the assessment of the hydrologic response of the watershed under different designed and real-case storm scenarios, the impact of implemented units was also assessed in a long temporal interval to determine the amount of water captured by RB, and CI units that can be used for meeting various needs such as irrigation of small yards, outdoor washing needs, etc. In this step, annual precipitation and temperature data from the year 2018 were used in the previously developed model of the study area with RB, CI, and DW applications. The year 2018 was selected as a sample temporal interval.

The simulated results reveal that the implemented LID units can significantly and vividly reduce the peak runoff expected in various rainfall events in a sample year. As demonstrated in Figure 3.17, a substantial amount of reduction is apparent in peak runoff in various events during one year. Specifically, in events with sudden occurrences and without near predecessor rainfall events the amount of reduction is higher and more obvious based on the hydrograph presented in Figure 3.17. This is most likely related to the completion of the capacity of the implemented RB, and CR units and the gradual infiltration process in DW units. Overall the peak runoff reduction rate in various rainfall events during one year can range up to 30%. The runoff volume reduction however demonstrated a negligible rate of 1%.

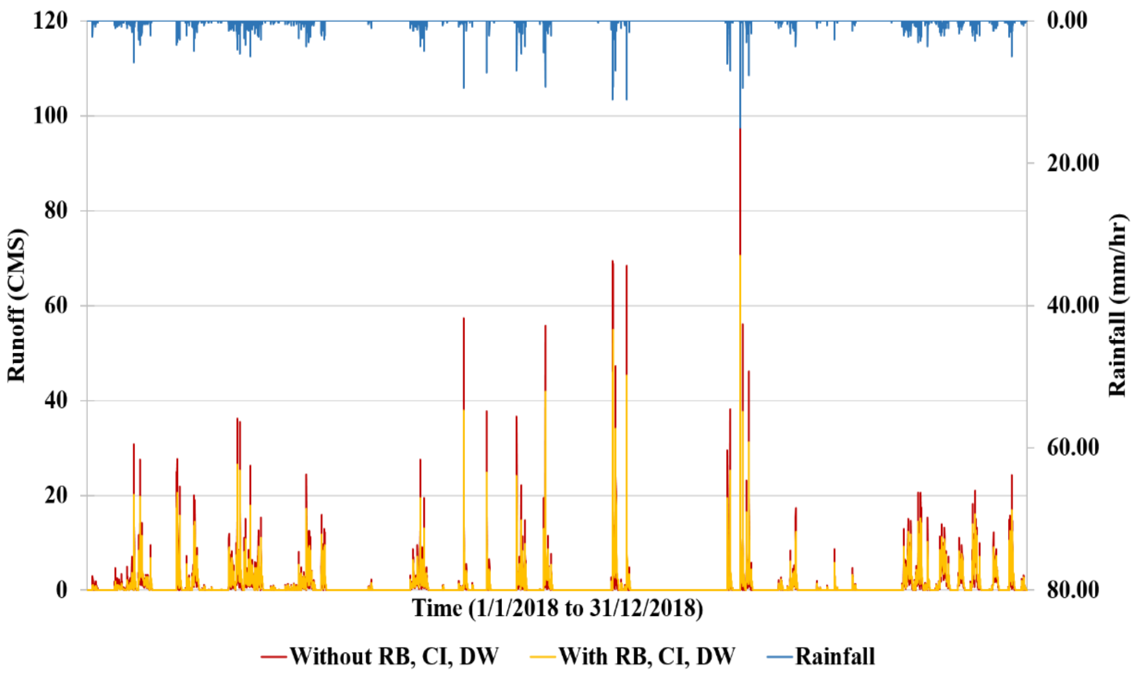

Figure 3.17 : Hydrologic response of the study area before and after implementing RB, CI, and DW units in the SWMM model in annual inspection (year 2018).

The findings indicate that implemented decentralized stormwater management units are more beneficial in single, short but intense storm events rather than mild but long and extensive rainfall events in runoff control. However, LID units have also the potential to serve as a mechanism for water harvesting.

In the long-term inspection of the developed model with and without RB, CI, and DW units, the water harvesting capabilities of the aforementioned units were confirmed in a year-long simulation.

SWMM enables the user to add a drain valve and define a drainage rate for different LID units. In this study, an assumption was made about the drainage of RB and CR units such as complete depletion of the water accumulated in each RB unit in 45 days and complete depletion of the accumulated water in each CI unit every 6 months. The drained water is assumed to be consumed for irrigation and outdoor washing needs. Based on the assumptions made, the amount of water captured, accumulated, and drained by RB, and CI units in the study area in a sample year was calculated.

Results revealed that in a sample year (2018), RB units implemented in the study area provided 11.5 million m^3 of water for outdoor uses, and CI units provided 560.3 thousand m^3 of water for various industrial uses. Thereby, in total more than 12 million m^3 of rainwater is entered into the consumption cycle instead of being released into the Marmara Sea. Further to this amount, implemented DW units in the study area also enrich the groundwater resources which can be used as an auxiliary source for meeting some of the irrigation water needs.

Comparing the volume of water harvested by the RB, and CI units with the reservoir capacity of the dams in Istanbul which are providing the required water for the population living in Istanbul, unvails substantial proportions as per Figure 3.18. Based on the obtained results the amount of water captured by RB, and CI units in a year-long period is about 5% of the Ömerli dam and 7.5% of the Terkos dam which are two of the biggest dams in Istanbul.

This amount of water is important for a city like Istanbul, which experiences water scarcity because of its high population and consumption rate, especially in the summer season. The implementation of decentralized stormwater systems like RB, CI, and DW units not only will assist in urban runoff mitigation in a significant amount but also will assist in addressing the available water challenge caused by climate change and population growth.

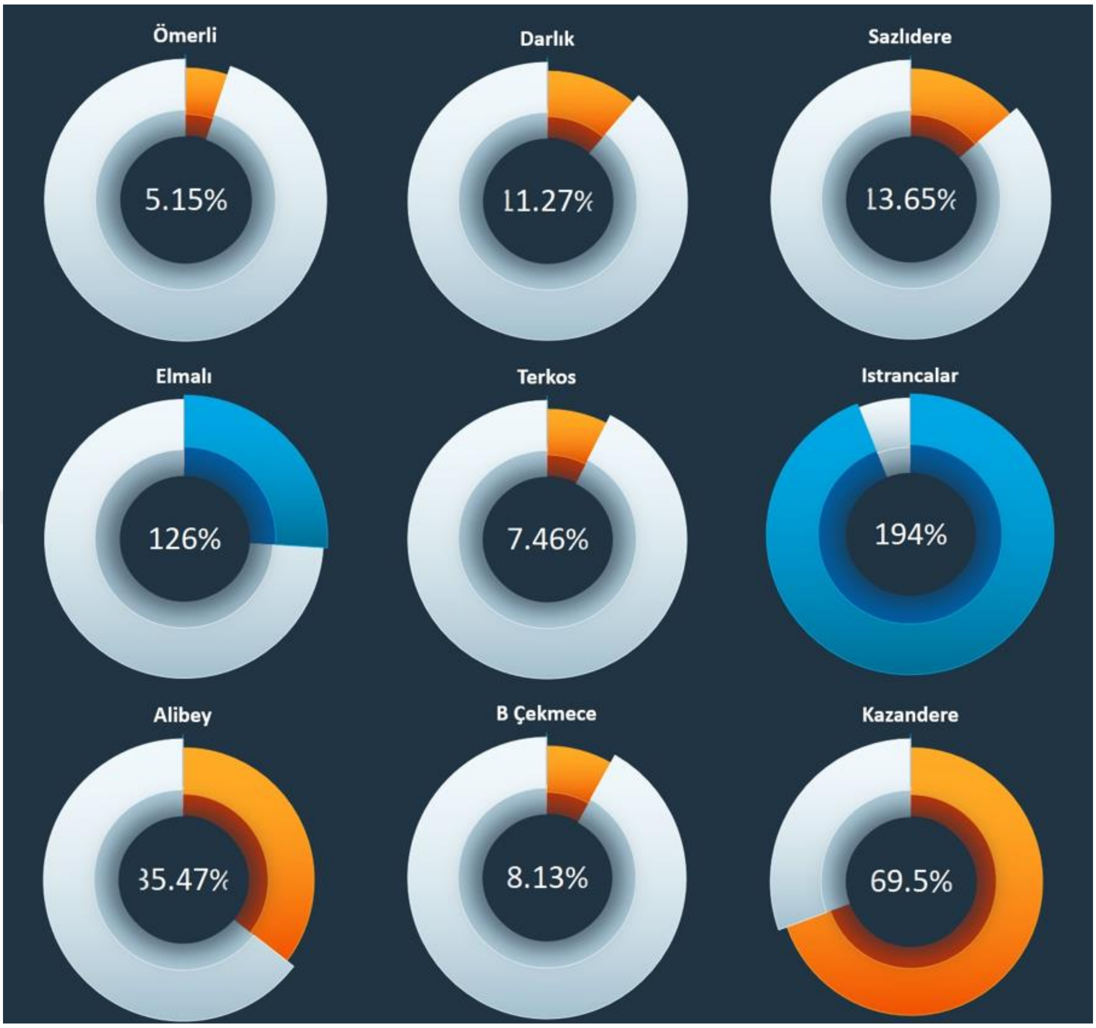

Figure 3.18 : Ratio of the water harvested by RB, and CI units to the capacity of various dams in Istanbul in m^3.

4. CONCLUSIONS

In this study, a comprehensive assessment of decentralized stormwater systems was carried out in a flood-prone and large urbanized watershed in Istanbul. The main focus of this study was to evaluate the impacts of these systems on urban runoff mitigation under climate change conditions and based on the physical characteristics of the watershed. Climate assessments and model development constitute the two main phases of this study.

In the climate assessment, the precipitation and temperature trends of Istanbul were analyzed by using data from a ground-based meteorologic station, MERRA-2 temperature reanalysis, and IMERG precipitation estimations. Moreover, three different non-parametric analysis methods including the MK test, Sen's slope estimator, and the ITA method were employed to determine the magnitude and direction of the trends. The obtained results unveiled major increasing trends in temperature and precipitation although minor decreasing trends were also observed in the precipitation trend.

To elaborate in detail, in the single-duration trend analysis of temperature, seasonal and annual temperature records from the ground-based meteorological station showed significant upward trends, which were congruously confirmed by the MK test, Sen's slope estimator, and ITA methods. The summer season showed the strongest tendency toward rising temperatures, followed by the spring, fall, and winter seasons.

Despite the pronounced increasing trends in single-duration analysis of temperature, decreasing trends were detected in multi-duration analysis by the ITA method on a seasonal and annual basis. In comparison to the referral interval of 1960-1979, seasonal and annual temperature followed a decreasing trend in 1980-1999 except during the summer season. For this interval, only the winter and summer seasons' trend directions were affirmative in data from the ground-based station and MERRA-2. A distinctive increasing trend was observed in the 2000-2019 interval simultaneously based on data from ground-based station records and MERRA-2.

Compared to the temperature, the single-duration analysis of precipitation resulted in less consistent trends. Significant increasing trends were observed in the fall and summer seasons as well as yearly, along with insignificant decreasing trends in the winter and spring seasons. The direction of the trend was reversed in the MK test and Sen’s slope versus the ITA method in the spring season; nevertheless, the trend's magnitude was not significant.

Multi-duration analysis of the precipitation trend revealed that the insignificant decreasing trends that were observed in winter and spring seasons in the single-duration analysis include significant decreasing and increasing trends in the 1980-1999 and 2000-2019 intervals.

Results of the multi-duration trend analysis were consistent in the winter, summer, and partially fall seasons, as well as yearly analysis based on the ground-based station records and IMERG estimations. However, IMERG estimations in the spring season and high values in the fall season demonstrated conflicting results against time series from ground-based station records.

Because of its graphical effectiveness, the multi-duration ITA approach was determined to be advantageous compared to Sen's slope and the MK test for spotting sub-trends in low, medium, or high-value groups of temperature or precipitation. This feature is substantially important in trend analysis of hydrometeorological variables in short intervals or drought-flood frequency studies, especially in highly populated megacities.

Based on the results obtained in the climate assessment, it was decided to use Rain Barrel (RB), Cistern (CI), and Drywell (DW) units in the model development phase as components of the decentralized stormwater system. This was mainly because of the substantial retention and infiltration capabilities of the aforementioned units making them well-suited to address the rising temperature and precipitation challenges in Istanbul.

In general, decentralized stormwater management systems have demonstrated promising results in mitigating stormwater in urbanized watersheds over time. However, among various types of these systems, rain barrels (RB), cisterns (CI), and especially drywells (DW) have been less attended comparatively. A robust framework for the design, implementation, and simulation of these systems can provide realistic and accurate results in urban runoff mitigation studies as well as assist in the development of sustainable and resilient cities.

Therefore, in the model development phase, a framework was developed to integrate various processes that incorporate the design, implementation, and simulation of RB, CI, and DW units in a highly urbanized and flood-prone watershed and provide an accurate perception of the performance of these units in urban runoff reduction. Initially, a physically-based hydrologic-hydraulic model of the Ayamama watershed was developed using SWMM and various geospatial and meteorological data. An auto-calibration process was employed by integrating the SWMM model of the study area and OSTRICH. The most sensitive parameters were tuned up to a certain iteration threshold to increase the goodness of fit between simulated and measured water depth in the main channel for several rainfall events.

Later, the runoff volume in each subcatchment was obtained by the calibrated and validated SWMM model for the flooding event of September 2009 and was used in conjunction with other influential criteria for specifying the suitability of subcatchments for the implementation of RB, CI, and DW units. For this purpose, a survey was conducted by 10 experts to determine the weights of each decision criterion through the AHP process. The average of the assigned weights for each criterion was multiplied by the quantitative values of the criteria to calculate the suitability score of each subcatchment for RB, CI, and DW implementations. Subsequently, subcatchments were ranked based on their suitability scores. This process led to establishing a logical limit to the maximum number of RB, CI, and DW units within each subcatchment and determining the allowed number of RB, CI, and DW units to be implemented.

By calibrating the developed SWMM model and comparing the hydrologic response of the watershed after implementations with the base condition under five designed storm events with a duration of 2 hours and return periods of T = 2, 5, 10, 25, and 50-year, as well as the flooding event of September 2009, and a year-long simulation based on the data from the year 2018, significant conclusions were reached as below:

• Regardless of the large size of the study area and the high number of model components and parameters, OSTRICH demonstrated a notable capability in integrating with and auto-calibration the developed SWMM model in this study, which further affirms the achievements of this new calibration-optimization tool in previously conducted trials and studies.

• Among various decision-making criteria, the total subcatchment runoff amount (SWMM model output) was assigned the highest weights by the experts contributing to the survey for RB, CI, and DW implementations. This indicates the determinant role of the initial SWMM model run in detecting precedent subcatchments for LID implementations. Along with this criterion, the permeability of the sub-soil and distance to the seawater due to attaining higher weights play a significant role in detecting the most suitable subcatchments for DW implementations.

• Benefiting from expert knowledge through AHP significantly assisted in specifying a threshold for restricting the number of RB, CI, and DW units within a logical and practical limit. By employing this method, the initially defined maximum number of RB, CI, and DW units that could be potentially implemented in the study area based on the availability of space was reduced by 30.4%, 20%, and 57.2%, respectively, considering the influencing geospatial, hydrological, and environmental criteria. Therefore, an assurance was achieved that all of the RB, CI, and DW units (with a total number of, respectively, 136312, 15917, and 33788) that are allowed to be implemented in the study area are capable of accomplishing the expected task of runoff reduction and are in compliance with the site specifications.

• Significant improvements in the hydrologic response of the watershed were observed under five designed storm events as a result of implementing RB, CI, and DW units in the study. For the storm events with a 2-hour duration and a return interval of T = 2, 5, 10, 25, and 50-year, respectively, 54.03%, 38.78%, 39.48%, 33.41%, and 23.63% reductions were observed in peak runoff, and respectively, 27.43%, 19.45%, 15.85%, 13.23%, and 11.17% reductions were observed in runoff volume. Furthermore, after RB, CI, and DW implementation, the time to peak of the obtained hydrographs for the aforementioned storm events increased by 55, 25, 15, and 10 minutes for the storms with T = 2, 5, 10, and 25 and remained unchanged for the storm with T = 50-year.

• Despite the remarkable performance of implemented RB, CI, and DW units in runoff reduction under storm events with a 2-hour duration, obtained results revealed that in the circumstances of continuous or intermittent storm events with a long duration, such as the flooding event of September 2009, the performance of the implemented units drops significantly over time. This reduction in mitigating runoff peak and volume is mainly due to the limited capacity of RB and CI units and saturation of the DW units, which are retrieved over time through infiltration and consumption of the accumulated water in RB and CI units.

• In a year-long simulation based on the meteorological data from the year 2018, implemented RB, and CI units demonstrated that a substantial amount of water can be captured and entered into the consumption cycle in household and industrial units. RB, and CI units implemented in the SWMM model of the Ayamama watershed can capture more than 12 million m^3 of rainwater which is equivalent to 5.15% of the Ömerli and 7.46% of the Terkos dams which are two of the biggest dams in Istanbul. This can significantly assist in addressing the water challenge in Istanbul city which suffers from extensive consumption due to population growth and climate change.

It is noteworthy to mention that the current study has certain limitations, including the type and scope of decentralized stormwater management units or LID practices considered and the potential for greater diversity in their implementation. While the framework developed focuses on rain barrels (RB), cisterns (CI), and drywells (DW) due to their substantial retention and infiltration capacities, the inclusion of additional LID practices, such as permeable pavements, green roofs, stormwater wetlands, vegetated filter strips, or other similar systems, could provide a more holistic approach to stormwater mitigation. This would enhance the robustness of the results by addressing a wider range of urban conditions and hydrological responses. Future research could extend the framework to integrate these additional practices, thereby improving adaptability and effectiveness. Furthermore, the challenges associated with scaling up the implementation of RB, CI, and DW units across varied urban settings and their associated cost and maintenance implications were not deeply analyzed in this study. Addressing these challenges through interdisciplinary approaches could lead to more effective and sustainable stormwater management solutions.The findings of this study can guide urban planners and decision-makers in developing mitigation strategies based on climate conditions and through decentralized stormwater management systems, especially in areas with limited groundwater resources or space for large-scale systems. Future research can direct the concentration on evaluating the impact of climate change on LID performance or optimizing implementation strategies under competing objectives, such as budget constraints, to advance sustainable urban water management.

REFERENCES

Aad, M. P. A., Suidan, M. T., & Shuster, W. D. (2010). Modeling Techniques of Best Management Practices: Rain Barrels and Rain Gardens Using EPA SWMM-5. *Journal of Hydrologic Engineering*, 15(6), 434-443. https://doi.org/doi:10.1061/(ASCE)HE.1943-5584.0000136

Adshead, D., Paszkowski, A., Gall, S. S., Peard, A. M., Adnan, M. S. G., Verschuur, J., & Hall, J. W. (2024). Climate threats to coastal infrastructure and sustainable development outcomes. *Nature Climate Change*, *14*(4), 344-352. https://doi.org/10.1038/s41558-024-01950-2

Agbo, E. P., Nkajoe, U., & Edet, C. O. (2023). Comparison of Mann–Kendall and Şen's innovative trend method for climatic parameters over Nigeria's climatic zones. *Climate Dynamics*, *60*(11), 3385-3401. https://doi.org/10.1007/s00382-022-06521-9

Ahammed, F., Hewa, G. A., & Argue, J. R. (2012). Applying multi-criteria decision analysis to select WSUD and LID technologies. *Water Supply*, *12*(6), 844-853. https://doi.org/10.2166/ws.2012.060

Ahiablame, L. M., Engel, B. A., & Chaubey, I. (2013). Effectiveness of low impact development practices in two urbanized watersheds: Retrofitting with rain barrel/cistern and porous pavement. *Journal of environmental management*, *119*, 151-161. https://doi.org/https://doi.org/10.1016/j.jenvman.2013.01.019

Aksu, H. (2021). Nonstationary analysis of the extreme temperatures in Turkey. *Dynamics of Atmospheres and Oceans*, *95*, 101238. https://doi.org/https://doi.org/10.1016/j.dynatmoce.2021.101238

Aksu, H., & Şen, K. (2021). İstanbul İçin Standart Süreli Gözlenen En Büyük Yağışların Eğilimleri [Trend Analysis of Observed Standart Duration Maximum Precipitation for Istanbul]. *Teknik Dergi*, *32*(1), 10495-10514. https://doi.org/10.18400/tekderg.647558

Aksu, H., Taflan, G. Y., Yaldiz, S. G., & Akgül, M. A. (2023). Evaluation of IMERG for GPM satellite-based precipitation products for extreme precipitation indices over Turkiye. *Atmospheric Research*, *291*, 106826. https://doi.org/https://doi.org/10.1016/j.atmosres.2023.106826

Alamdari, N., Sample, D. J., Liu, J., & Ross, A. (2018). Assessing climate change impacts on the reliability of rainwater harvesting systems. *Resources, Conservation and Recycling*, *132*, 178-189. https://doi.org/https://doi.org/10.1016/j.resconrec.2017.12.013

Alves, A., Gersonius, B., Sanchez, A., Vojinovic, Z., & Kapelan, Z. (2018). Multi-criteria Approach for Selection of Green and Grey Infrastructure to Reduce Flood Risk and Increase CO-benefits. *Water Resources Management*, *32*(7), 2505-2522. https://doi.org/10.1007/s11269-018-1943-3

Andualem, T. G., Hewa, G. A., Boland, J., Peters, S., & Myers, B. R. (2024). Multi-Method Comparative Analysis of Hydroclimatic Trends and Variability in Dry Creek Catchment, South Australia. *Earth Systems and Environment*. https://doi.org/10.1007/s41748-024-00401-4

Ashraf, M. S., Ahmad, I., Khan, N. M., Zhang, F., Bilal, A., & Guo, J. (2021). Streamflow Variations in Monthly, Seasonal, Annual and Extreme Values Using Mann-Kendall, Spearmen's Rho and Innovative Trend Analysis. *Water Resources Management*, *35*(1), 243-261. https://doi.org/10.1007/s11269-020-02723-0

Ay, M., & Kisi, O. (2015). Investigation of trend analysis of monthly total precipitation by an innovative method. *Theoretical and Applied Climatology*, *120*(3), 617-629. https://doi.org/10.1007/s00704-014-1198-8

Azari, B., & Tabesh, M. (2022). Urban storm water drainage system optimization using a sustainability index and LID/BMPs. *Sustainable Cities and Society*, *76*, 103500. https://doi.org/https://doi.org/10.1016/j.scs.2021.103500

Bąk, J., & Barjenbruch, M. (2022). Benefits, Inconveniences, and Facilities of the Application of Rain Gardens in Urban Spaces from the Perspective of Climate Change—A Review. *Water*, *14*(7), 1153. https://www.mdpi.com/2073-4441/14/7/1153

Bayazit, M., & Önöz, B. (2007). To prewhiten or not to prewhiten in trend analysis? *Hydrological Sciences Journal*, *52*(4), 611-624.

Behrouz, M. S., Sample, D. J., & Yazdi, M. N. (2023). Robustness of storm water management model parameter sets for dry and wet hydroclimatic conditions. *Journal of Cleaner Production*, *411*, 137328.

Behrouz, M. S., Zhu, Z., Matott, L. S., & Rabideau, A. J. (2020). A new tool for automatic calibration of the Storm Water Management Model (SWMM). *Journal of Hydrology*, *581*, 124436.

Benabdelouahab, T., Gadouali, F., Boudhar, A., Lebrini, Y., Hadria, R., & Salhi, A. (2020). Analysis and trends of rainfall amounts and extreme events in the Western Mediterranean region. *Theoretical and Applied Climatology*, *141*(1), 309-320. https://doi.org/10.1007/s00704-020-03205-4

Boroomandnia, A., Bozorg-Haddad, O., Bahrami, M., Goharian, E., Singh, V. P., & Loáiciga, H. A. (2021). Optimizing urban stormwater control strategies and assessing aquifer recharge through drywells in an urban watershed. *Hydrogeology Journal*, *29*(4), 1379-1398. https://doi.org/10.1007/s10040-021-02316-0

Botturi, A., Ozbayram, E. G., Tondera, K., Gilbert, N. I., Rouault, P., Caradot, N., Gutierrez, O., Daneshgar, S., Frison, N., Akyol, Ç., Foglia, A., Eusebi, A. L., & Fatone, F. (2021). Combined sewer overflows: A critical review on best practice and innovative solutions to mitigate impacts on environment and human health. *Critical Reviews in Environmental Science and Technology*, *51*(15), 1585-1618. https://doi.org/10.1080/10643389.2020.1757957

Burian Steven, J., & Edwards Findlay, G. (2012). Historical Perspectives of Urban Drainage. In *Global Solutions for Urban Drainage* (pp. 1-16). https://doi.org/doi:10.1061/40644(2002)28410.1061/40644(2002)284

Busso, M., Chauvin, J. P., & Herrera L, N. (2021). Rural-urban migration at high urbanization levels. *Regional Science and Urban Economics*, *91*, 103658. https://doi.org/https://doi.org/10.1016/j.regsciurbeco.2021.103658

Butler, D., Ward, S., Sweetapple, C., Astaraie-Imani, M., Diao, K., Farmani, R., & Fu, G. (2017). Reliable, resilient and sustainable water management: the Safe & SuRe approach. *Global Challenges*, *1*(1), 63-77. https://doi.org/https://doi.org/10.1002/gch2.1010

Caloiero, T., Coscarelli, R., & Ferrari, E. (2018). Application of the Innovative Trend Analysis Method for the Trend Analysis of Rainfall Anomalies in Southern Italy. *Water Resources Management*, *32*(15), 4971-4983. https://doi.org/10.1007/s11269-018-2117-z

Chaudhary, M. T., & Piracha, A. (2021). Natural Disasters—Origins, Impacts, Management. *Encyclopedia*, *1*(4), 1101-1131. https://www.mdpi.com/2673-8392/1/4/84

Chen, W., Wang, W., Huang, G., Wang, Z., Lai, C., & Yang, Z. (2021). The capacity of grey infrastructure in urban flood management: A comprehensive analysis of grey infrastructure and the green-grey approach. *International Journal of Disaster Risk Reduction*, *54*, 102045. https://doi.org/https://doi.org/10.1016/j.ijdrr.2021.102045

Chikhi, F., Li, C., Ji, Q., & Zhou, X. (2023). Review of Sponge City implementation in China: performance and policy. *Water Science and Technology*, *88*(10), 2499-2520. https://doi.org/10.2166/wst.2023.312

Chowdhury, A., Jha, M. K., & Chowdary, V. M. (2010). Delineation of groundwater recharge zones and identification of artificial recharge sites in West Medinipur district, West Bengal, using RS, GIS and MCDM techniques. *Environmental Earth Sciences*, *59*(6), 1209-1222. https://doi.org/10.1007/s12665-009-0110-9

Chowdhury, M., & Paul, P. K. (2021). Identification of suitable sites for rainwater harvesting using fuzzy AHP and fuzzy gamma operator: a case study. *Arabian Journal of Geosciences*, *14*(7), 585. https://doi.org/10.1007/s12517-021-06607-4

***Copernicus Europe's Eye on Earth and Land Monitoring Service*.** (2020). https://land.copernicus.eu/en/products/corine-land-cover/clc2018

D'Ambrosio, R., Longobardi, A., & Schmalz, B. (2023). SuDS as a climate change adaptation strategy: Scenario-based analysis for an urban catchment in northern Italy. *Urban Climate*, *51*, 101596. https://doi.org/https://doi.org/10.1016/j.uclim.2023.101596

Dannenberg, A. L., Frumkin, H., Hess, J. J., & Ebi, K. L. (2019). Managed retreat as a strategy for climate change adaptation in small communities: public health implications. *Climatic Change*, *153*(1), 1-14. https://doi.org/10.1007/s10584-019-02382-0

Das, J., Mandal, T., Rahman, A. T. M. S., & Saha, P. (2021). Spatio-temporal characterization of rainfall in Bangladesh: an innovative trend and discrete wavelet transformation approaches. *Theoretical and Applied Climatology*, *143*(3), 1557-1579. https://doi.org/10.1007/s00704-020-03508-6

Demiroglu, M. (2019). Groundwater budget rationale, time, and regional flow: a case study in Istanbul, Turkey. *Environmental Earth Sciences*, *78*(24), 682. https://doi.org/10.1007/s12665-019-8713-2

Dietz, M. E. (2007). Low Impact Development Practices: A Review of Current Research and Recommendations for Future Directions. *Water, Air, and Soil Pollution*, *186*(1), 351-363. https://doi.org/10.1007/s11270-007-9484-z

Doherty, J. (1994). PEST: a unique computer program for model-independent parameter optimisation. In *Water Down Under 94: Groundwater/Surface Hydrology Common Interest Papers; Preprints of Papers* (pp. 551-554). Institution of Engineers, Australia Barton, ACT.

DSI. (2013). *Su Dünyası*. 122, 60-63. https://cdniys.tarimorman.gov.tr/api/File/GetGaleriFile/425/DosyaGaleri/1010/122.pdf

Edwards, E. C., Nelson, C., Harter, T., Bowles, C., Li, X., Lock, B., Fogg, G. E., & Washburn, B. S. (2022). Potential effects on groundwater quality associated with infiltrating stormwater through dry wells for aquifer recharge. *Journal of Contaminant Hydrology*, *246*, 103964. https://doi.org/https://doi.org/10.1016/j.jconhyd.2022.103964

Ekmekcioğlu, Ö., Koc, K., & Özger, M. (2021). District based flood risk assessment in Istanbul using fuzzy analytical hierarchy process. Stochastic *Environmental Research and Risk Assessment*, 35(3), 617-637. https://doi.org/10.1007/s00477-020-01924-8

Forgione, E. R., Felton, G. K., Aydilek, A. H., & Davis, A. P. (2024). Hydrologic Performance of Vegetated Compost Blankets for Highway Stormwater Management. *Journal of Sustainable Water in the Built Environment*, 10(3), 04024002. https://doi.org/doi:10.1061/JSWBAY.SWENG-537

Gao, J., Liang, J., Lu, Y., Zhou, R., & Lu, X. (2023). Automatic SWMM Parameter Calibration Method Based on the Differential Evolution and Bayesian Optimization Algorithm. *Water*, *15*(20), 3582. https://www.mdpi.com/2073-4441/15/20/3582

Garcia, M. V. d. S., Moruzzi, R. B., & Behzadian, K. (2023). Assessment of sustainable drainage strategies in urban water systems using urban water metabolism and multi-criteria decision analyses. *Water Science and Technology*, *88*(11), 2809-2825. https://doi.org/10.2166/wst.2023.377

Gelaro, R., McCarty, W., Suárez, M. J., Todling, R., Molod, A., Takacs, L., Randles, C. A., Darmenov, A., Bosilovich, M. G., Reichle, R., Wargan, K., Coy, L., Cullather, R., Draper, C., Akella, S., Buchard, V., Conaty, A., da Silva, A. M., Gu, W., . . . Zhao, B. (2017). The Modern-Era Retrospective Analysis for Research and Applications, Version 2 (MERRA-2). *Journal of Climate*, *30*(14), 5419-5454. https://doi.org/https://doi.org/10.1175/JCLI-D-16-0758.1

Ghodsi, S. H., Zahmatkesh, Z., Goharian, E., Kerachian, R., & Zhu, Z. (2020). Optimal design of low impact development practices in response to climate change. *Journal of Hydrology*, *580*, 124266. https://doi.org/https://doi.org/10.1016/j.jhydrol.2019.124266

Ghodsi, S. H., Zhu, Z., Gheith, H., Rabideau, A. J., Torres, M. N., & Meindl, K. (2021). Modeling the Effectiveness of Rain Barrels, Cisterns, and Downspout Disconnections for Reducing Combined Sewer Overflows in a City-Scale Watershed. *Water Resources Management*, *35*(9), 2895-2908. https://doi.org/10.1007/s11269-021-02875-7

Ghodsi, S. H., Zhu, Z., Matott, L. S., Rabideau, A. J., & Torres, M. N. (2023). Optimal siting of rainwater harvesting systems for reducing combined sewer overflows at city scale. *Water Research*, *230*, 119533. https://doi.org/https://doi.org/10.1016/j.watres.2022.119533

Gogate, N. G., Kalbar, P. P., & Raval, P. M. (2017). Assessment of stormwater management options in urban contexts using Multiple Attribute Decision-Making. *Journal of Cleaner Production*, *142*, 2046-2059. https://doi.org/https://doi.org/10.1016/j.jclepro.2016.11.079

Gosset, A., Ferro, Y., & Durrieu, C. (2016). Methods for evaluating the pollution impact of urban wet weather discharges on biocenosis: A review. *Water Research*, *89*, 330-354. https://doi.org/https://doi.org/10.1016/j.watres.2015.11.020

Güçlü, Y. S. (2018). Multiple Şen-innovative trend analyses and partial Mann-Kendall test. *Journal of Hydrology*, *566*, 685-704.

Gülbaz, S., Kazezyılmaz-Alhan, C. M., Bahçeçi, A., & Boyraz, U. (2019). Flood modeling of Ayamama river watershed in Istanbul, Turkey. *Journal of Hydrologic Engineering*, *24*(1), 05018026.

Gulshad, K., Szydłowski, M., Yaseen, A., & Aslam, R. W. (2024). A comparative analysis of methods and tools for low impact development (LID) site selection. *Journal of environmental management*, *354*, 120212. https://doi.org/https://doi.org/10.1016/j.jenvman.2024.120212

Gupta, P., Verma, S., Bhatla, R., Chandel, A. S., Singh, J., & Payra, S. (2020). Validation of Surface Temperature Derived From MERRA-2 Reanalysis Against IMD Gridded Data Set Over India. *Earth and Space Science*, *7*(1), e2019EA000910. https://doi.org/https://doi.org/10.1029/2019EA000910

Hadi, S. J., & Tombul, M. (2018). Long-term spatiotemporal trend analysis of precipitation and temperature over Turkey. *Meteorological Applications*, *25*(3), 445-455. https://doi.org/https://doi.org/10.1002/met.1712

Haghnegahdar, A., Tolson, B. A., Davison, B., Seglenieks, F. R., Klyszejko, E., Soulis, E. D., Fortin, V., & Matott, L. S. (2014). Calibrating Environment Canada's MESH Modelling System over the Great Lakes Basin. *Atmosphere-Ocean*, *52*(4), 281-293. https://doi.org/10.1080/07055900.2014.939131

Hanley, P. A., Livesley, S. J., Fletcher, T. D., Grey, V., & Szota, C. (2024). Stormwater retention performance of tree integrated infiltration trenches designed for suburban streetscapes. *Science of The Total Environment*, *954*, 176634. https://doi.org/https://doi.org/10.1016/j.scitotenv.2024.176634

Hasan Karaman, Ç., & Akyürek, Z. (2023). Evaluation of near-surface air temperature reanalysis datasets and downscaling with machine learning based Random Forest method for complex terrain of Turkey. *Advances in Space Research*, *71*(12), 5256-5281. https://doi.org/https://doi.org/10.1016/j.asr.2023.02.006

Hesarkazzazi, S., Bakhshipour, A. E., Hajibabaei, M., Dittmer, U., Haghighi, A., & Sitzenfrei, R. (2022). Battle of centralized and decentralized urban stormwater networks: From redundancy perspective. *Water Research*, *222*, 118910. https://doi.org/https://doi.org/10.1016/j.watres.2022.118910

Hino, M., Field, C. B., & Mach, K. J. (2017). Managed retreat as a response to natural hazard risk. *Nature Climate Change*, *7*(5), 364-370. https://doi.org/10.1038/nclimate3252

Holland, J. H. (1992). Genetic Algorithms. *Scientific American*, *267*(1), 66-73. http://www.jstor.org/stable/24939139

Hou, A. Y., Kakar, R. K., Neeck, S., Azarbarzin, A. A., Kummerow, C. D., Kojima, M., Oki, R., Nakamura, K., & Iguchi, T. (2014). The global precipitation measurement mission. *Bulletin of the American Meteorological Society*, *95*(5), 701-722.

Huffman, G. J., Bolvin, D. T., Braithwaite, D., Hsu, K.-L., Joyce, R. J., Kidd, C., Nelkin, E. J., Sorooshian, S., Stocker, E. F., Tan, J., Wolff, D. B., & Xie, P. (2020). Integrated Multi-satellite Retrievals for the Global Precipitation Measurement (GPM) Mission (IMERG). In V. Levizzani, C. Kidd, D. B. Kirschbaum, C. D. Kummerow, K. Nakamura, & F. J. Turk (Eds.), *Satellite Precipitation Measurement: Volume 1* (pp. 343-353). Springer International Publishing. https://doi.org/10.1007/978-3-030-24568-9_19

Huffman, G. J., E.F. Stocker, D.T. Bolvin, E.J. Nelkin, & Tan, J. (2023). GPM IMERG Final Precipitation L3 1 day 0.1 degree x 0.1 degree V07, Edited by Andrey Savtchenko, Greenbelt, MD, Goddard Earth Sciences Data and Information Services Center (GES DISC), Accessed: [Data Access Date], 10.5067/GPM/IMERGDF/DAY/07

Hussain, M. S., Abd-Elhamid, H. F., Javadi, A. A., & Sherif, M. M. (2019). Management of Seawater Intrusion in Coastal Aquifers: A Review. *Water*, *11*(12), 2467. https://www.mdpi.com/2073-4441/11/12/2467

Jaagus, J. (2006). Climatic changes in Estonia during the second half of the 20th century in relationship with changes in large-scale atmospheric circulation. *Theoretical and Applied Climatology*, *83*(1), 77-88. https://doi.org/10.1007/s00704-005-0161-0

Johnston, J. M., McGarvey, D. J., Barber, M. C., Laniak, G., Babendreier, J., Parmar, R., Wolfe, K., Kraemer, S. R., Cyterski, M., Knightes, C., Rashleigh, B., Suarez, L., & Ambrose, R. (2011). An integrated modeling framework for performing environmental assessments: Application to ecosystem services in the Albemarle-Pamlico basins (NC and VA, USA). *Ecological Modelling*, *222*(14), 2471-2484. https://doi.org/https://doi.org/10.1016/j.ecolmodel.2011.03.036

Kabenge, I., Ouma, G., Aboagye, D., & Banadda, N. (2018). Performance of a constructed wetland as an upstream intervention for stormwater runoff quality management. *Environmental Science and Pollution Research*, 25(36), 36765-36774. https://doi.org/10.1007/s11356-018-3580-z

Kasprzyk, M., Szpakowski, W., Poznańska, E., Boogaard, F. C., Bobkowska, K., & Gajewska, M. (2022). Technical solutions and benefits of introducing rain gardens – Gdańsk case study. *Science of The Total Environment*, 835, 155487. https://doi.org/https://doi.org/10.1016/j.scitotenv.2022.155487

Kaykhosravi, S., Abogadil, K., Khan, U. T., & Jadidi, M. A. (2019). The Low-Impact Development Demand Index: A New Approach to Identifying Locations for LID. *Water*, *11*(11), 2341. https://www.mdpi.com/2073-4441/11/11/2341

Kaykhosravi, S., Khan, U. T., & Jadidi, M. A. (2022). A simplified geospatial model to rank LID solutions for urban runoff management. *Science of The Total Environment*, *831*, 154937. https://doi.org/https://doi.org/10.1016/j.scitotenv.2022.154937

Keeley, M., Koburger, A., Dolowitz, D. P., Medearis, D., Nickel, D., & Shuster, W. (2013). Perspectives on the Use of Green Infrastructure for Stormwater Management in Cleveland and Milwaukee. *Environmental Management*, *51*(6), 1093-1108. https://doi.org/10.1007/s00267-013-0032-x

Keifer, C. J., & Chu, H. H. (1957). Synthetic storm pattern for drainage design. *Journal of the hydraulics division*, *83*(4), 1332-1331-1332-1325.

Kendall, M. G. (1938). A new measure of rank correlation. *Biometrika*, *30*(1-2), 81-93.

Kendall, M. G. (1938). A New Measure of Rank Correlation. *Biometrika*, *30*(1/2), 81-93. https://doi.org/10.2307/2332226

Kömüşcü, A. Ü., & Aksoy, M. (2023). Long-term spatio-temporal trends and periodicities in monthly and seasonal precipitation in Turkey. *Theoretical and Applied Climatology*, *151*(3), 1623-1649. https://doi.org/10.1007/s00704-022-04349-1

Lee, H., Calvin, K., Dasgupta, D., Krinner, G., Mukherji, A., Thorne, P., Trisos, C., Romero, J., Aldunce, P., & Barrett, K. (2023). *Climate change 2023: synthesis report. Contribution of working groups I, II and III to the sixth assessment report of the intergovernmental panel on climate change*. The Australian National University.

Li, J., Deng, C., Li, Y., Li, Y., & Song, J. (2017). Comprehensive Benefit Evaluation System for Low-Impact Development of Urban Stormwater Management Measures. *Water Resources Management*, *31*(15), 4745-4758. https://doi.org/10.1007/s11269-017-1776-5

Lin, J., Uchiyama, S., Bhattacharya, Y., & Nakamura, H. (2023). Efficacy of rain barrels and rain gardens to reduce urban pluvial flooding in densely built-up residential areas: a case study on Miyahara-Cho in Saitama City, Japan. *City and Built Environment*, *1*(1), 19. https://doi.org/10.1007/s44213-023-00024-x

Liu, T., Lawluvy, Y., Shi, Y., & Yap, P.-S. (2021). Low Impact Development (LID) Practices: A Review on Recent Developments, Challenges and Prospects. *Water, Air, & Soil Pollution*, *232*(9), 344. https://doi.org/10.1007/s11270-021-05262-5

Liu, Y., Cibin, R., Bralts, V. F., Chaubey, I., Bowling, L. C., & Engel, B. A. (2016). Optimal selection and placement of BMPs and LID practices with a rainfall-runoff model. *Environmental Modelling & Software*, *80*, 281-296. https://doi.org/https://doi.org/10.1016/j.envsoft.2016.03.005

Liu, Z. (2016). Comparison of Integrated Multisatellite Retrievals for GPM (IMERG) and TRMM Multisatellite Precipitation Analysis (TMPA) monthly precipitation products: Initial results [Article]. *Journal of Hydrometeorology*, *17*(3), 777-790. https://doi.org/10.1175/JHM-D-15-0068.1

Locatelli, L., Mark, O., Mikkelsen, P. S., Arnbjerg-Nielsen, K., Deletic, A., Roldin, M., & Binning, P. J. (2017). Hydrologic impact of urbanization with extensive stormwater infiltration. *Journal of Hydrology*, *544*, 524-537. https://doi.org/https://doi.org/10.1016/j.jhydrol.2016.11.030

Malaviya, P., & Singh, A. (2012). Constructed Wetlands for Management of Urban Stormwater Runoff. *Critical Reviews in Environmental Science and Technology*, 42(20), 2153-2214. https://doi.org/10.1080/10643389.2011.574107

Malczewski, J., & Rinner, C. (2015). *Multicriteria decision analysis in geographic information science* (Vol. 1). Springer.

Mann, H. B. (1945). Nonparametric tests against trend. *Econometrica: Journal of the econometric society*, 245-259.

Matott, L. S. (2017). OSTRICH–An Optimization Software Toolkit for Research Involving Computational Heuristics Documentation and User's Guide Version 17.12. 19, Department of Civil, Structural, and Environmental Engineering, State University of New York at Buffalo, Buffalo, NY. *University at Buffalo Center for Computational Research*, *1*, 79.

Matott, L. S., & Rabideau, A. J. (2008). Calibration of complex subsurface reaction models using a surrogate-model approach. *Advances in Water Resources*, *31*(12), 1697-1707. https://doi.org/https://doi.org/10.1016/j.advwatres.2008.08.006

Matott, L. S., Rabideau, A. J., & Craig, J. R. (2006). Pump-and-treat optimization using analytic element method flow models. *Advances in Water Resources*, *29*(5), 760-775. https://doi.org/https://doi.org/10.1016/j.advwatres.2005.07.009

Mersin, D., Tayfur, G., Vaheddoost, B., & Safari, M. J. S. (2022). Historical Trends Associated with Annual Temperature and Precipitation in Aegean Turkey, Where Are We Heading? *Sustainability*, *14*(20), 13380. https://www.mdpi.com/2071-1050/14/20/13380

Modarres, R., & da Silva, V. d. P. R. (2007). Rainfall trends in arid and semi-arid regions of Iran. *Journal of arid environments*, *70*(2), 344-355.

Mohamed Mouhoumed, R., Ekmekcioğlu, Ö., & Özger, M. (2023). A hybrid MCDA approach for delineating sites suitable for artificial groundwater recharge using drywells. *Journal of Hydrology*, *620*, 129387. https://doi.org/https://doi.org/10.1016/j.jhydrol.2023.129387

Mohorji, A. M., Şen, Z., & Almazroui, M. (2017). Trend Analyses Revision and Global Monthly Temperature Innovative Multi-Duration Analysis. *Earth Systems and Environment*, *1*(1), 9. https://doi.org/10.1007/s41748-017-0014-x

Molod, A., Takacs, L., Suarez, M., & Bacmeister, J. (2015). Development of the GEOS-5 atmospheric general circulation model: evolution from MERRA to MERRA2. *Geosci. Model Dev.*, *8*(5), 1339-1356. https://doi.org/10.5194/gmd-8-1339-2015

Morris, R. L., Konlechner, T. M., Ghisalberti, M., & Swearer, Stephen E. (2018). From grey to green: Efficacy of eco-engineering solutions for nature-based coastal defence. *Global Change Biology*, *24*(5), 1827-1842. https://doi.org/https://doi.org/10.1111/gcb.14063

Motovalibashi Naeini, A., Tabesh, M., & Soltaninia, S. (2024). Modeling the effect of land use change to design a suitable low impact development (LID) system to control surface water pollutants. *Science of The Total Environment*, *932*, 172756. https://doi.org/https://doi.org/10.1016/j.scitotenv.2024.172756

N. Moriasi, D., G. Arnold, J., W. Van Liew, M., L. Bingner, R., D. Harmel, R., & L. Veith, T. (2007). Model Evaluation Guidelines for Systematic Quantification of Accuracy in Watershed Simulations. *Transactions of the ASABE*, *50*(3), 885-900. https://doi.org/https://doi.org/10.13031/2013.23153

Nash, J. E., & Sutcliffe, J. V. (1970). River flow forecasting through conceptual models part I—A discussion of principles. *Journal of Hydrology*, *10*(3), 282-290.

Nguyen, P., Ombadi, M., Sorooshian, S., Hsu, K., AghaKouchak, A., Braithwaite, D., Ashouri, H., & Thorstensen, A. R. (2018). The PERSIANN family of global satellite precipitation data: a review and evaluation of products. *Hydrol. Earth Syst. Sci.*, *22*(11), 5801-5816. https://doi.org/10.5194/hess-22-5801-2018

Nicholls, R. J., Marinova, N., Lowe, J. A., Brown, S., Vellinga, P., De Gusmao, D., Hinkel, J., & Tol, R. S. (2011). Sea-level rise and its possible impacts given a 'beyond 4 C world'in the twenty-first century. *Philosophical transactions of the Royal Society A: mathematical, physical and engineering sciences*, *369*(1934), 161-181.

Nigussie, T. A., & Altunkaynak, A. (2016). Assessing the hydrological response of Ayamama watershed from urbanization predicted under various landuse policy scenarios. *Water Resources Management*, *30*, 3427-3441.

Partal, T., & Kahya, E. (2006). Trend analysis in Turkish precipitation data. *Hydrological Processes: An International Journal*, *20*(9), 2011-2026.

Perin, R., Trigatti, M., Nicolini, M., Campolo, M., & Goi, D. (2020). Automated calibration of the EPA-SWMM model for a small suburban catchment using PEST: a case study. *Environmental Monitoring and Assessment*, *192*, 1-17.

Pettitt, A. N. (1979). A non-parametric approach to the change-point problem. *Journal of the Royal Statistical Society: Series C (Applied Statistics)*, *28*(2), 126-135.

Poli, R., Kennedy, J., & Blackwell, T. (2007). Particle swarm optimization: An overview. *Swarm intelligence*, *1*, 33-57.

Pour, S. H., Wahab, A. K. A., Shahid, S., & Ismail, Z. B. (2020). Changes in reference evapotranspiration and its driving factors in peninsular Malaysia. *Atmospheric Research*, *246*, 105096. https://doi.org/https://doi.org/10.1016/j.atmosres.2020.105096

Powell, M. J. (1976). Some global convergence properties of a variable metric algorithm for minimization without exact line searches. *Nonlinear programming*, *9*(1), 53-72.

Pradhan, R. K., Markonis, Y., Vargas Godoy, M. R., Villalba-Pradas, A., Andreadis, K. M., Nikolopoulos, E. I., Papalexiou, S. M., Rahim, A., Tapiador, F. J., & Hanel, M. (2022). Review of GPM IMERG performance: A global perspective. *Remote Sensing of Environment*, *268*, 112754. https://doi.org/https://doi.org/10.1016/j.rse.2021.112754

Razavi, S., & Tolson, B. A. (2013). An efficient framework for hydrologic model calibration on long data periods. *Water Resources Research*, *49*(12), 8418-8431. https://doi.org/https://doi.org/10.1002/2012WR013442

Razzaghmanesh, M., & Beecham, S. (2018). A Review of Permeable Pavement Clogging Investigations and Recommended Maintenance Regimes. *Water*, *10*(3), 337. https://www.mdpi.com/2073-4441/10/3/337

Rienecker, M. M., Suarez, M. J., Gelaro, R., Todling, R., Bacmeister, J., Liu, E., Bosilovich, M. G., Schubert, S. D., Takacs, L., Kim, G.-K., Bloom, S., Chen, J., Collins, D., Conaty, A., da Silva, A., Gu, W., Joiner, J., Koster, R. D., Lucchesi, R., . . . Woollen, J. (2011). MERRA: NASA's Modern-Era Retrospective Analysis for Research and Applications. *Journal of Climate*, *24*(14), 3624-3648. https://doi.org/https://doi.org/10.1175/JCLI-D-11-00015.1

Rossman, L. A. (2010). *Storm water management model user's manual, version 5.0*. National Risk Management Research Laboratory, Office of Research and ….

Russo, D., Kurtzman, D., & Nachshon, U. (2022). Hydraulic Issues Concerning Injection of Harvested Rainwater to the Subsurface Through Drywells: Insight From Numerical Simulations of Flow in a Realistic Combined Vadose Zone-Groundwater Flow System. *Water Resources Research*, 58(7), e2021WR031881. https://doi.org/https://doi.org/10.1029/2021WR031881

Rybski, D., & Neumann, J. (2011). A Review on the Pettitt Test Pettitt-test. In J. Kropp & H.-J. Schellnhuber (Eds.), *In Extremis: Disruptive Events and Trends in Climate and Hydrology* (pp. 202-213). Springer Berlin Heidelberg. https://doi.org/10.1007/978-3-642-14863-7_10

Saadat Foomani, M., & Malekmohammadi, B. (2020). Site selection of sustainable urban drainage systems using fuzzy logic and multi-criteria decision-making. *Water and Environment Journal*, *34*(4), 584-599. https://doi.org/https://doi.org/10.1111/wej.12487

Saaty, T. L., Vargas, L. G., Saaty, T. L., & Vargas, L. G. (2001). How to make a decision. *Models, methods, concepts & applications of the analytic hierarchy process*, 1-25.

Sambito, M., Severino, A., Freni, G., & Neduzha, L. (2021). A Systematic Review of the Hydrological, Environmental and Durability Performance of Permeable Pavement Systems. *Sustainability*, *13*(8), 4509. https://www.mdpi.com/2071-1050/13/8/4509

Sam, S., & Özger, M. (2025). A multi-method and multi-duration trend analysis of temperature and precipitation in Istanbul, Turkey, by using meteorological records, MERRA-2 reanalysis, and IMERG estimations. *HydroResearch*, 8, 209-222. https://doi.org/https://doi.org/10.1016/j.hydres.2024.11.005

Samouei, S., & Özger, M. (2020). Evaluating the performance of low impact development practices in urban runoff mitigation through distributed and combined implementation. *Journal of Hydroinformatics*, *22*(6), 1506-1520. https://doi.org/10.2166/hydro.2020.054

Sang, Y.-F., Wang, Z., & Liu, C. (2014). Comparison of the MK test and EMD method for trend identification in hydrological time series. *Journal of Hydrology*, *510*, 293-298.

Sasidharan, S., Bradford, S. A., Šimůnek, J., DeJong, B., & Kraemer, S. R. (2018). Evaluating drywells for stormwater management and enhanced aquifer recharge. *Advances in Water Resources*, *116*, 167-177. https://doi.org/https://doi.org/10.1016/j.advwatres.2018.04.003

Sen, P. K. (1968). Estimates of the Regression Coefficient Based on Kendall's Tau. *Journal of the American Statistical Association*, *63*(324), 1379-1389. https://doi.org/10.1080/01621459.1968.10480934

Şen, Z. (2012). Innovative Trend Analysis Methodology. *Journal of Hydrologic Engineering*, *17*(9), 1042-1046. https://doi.org/10.1061/(ASCE)HE.1943-5584.0000556

Shahed Behrouz, M., Sample, D. J., & Nayeb Yazdi, M. (2023). Robustness of storm water management model parameter sets for dry and wet hydroclimatic conditions. *Journal of Cleaner Production*, *411*, 137328. https://doi.org/https://doi.org/10.1016/j.jclepro.2023.137328

Shokri, M., Kibler, K. M., Hagglund, C., Corrado, A., Wang, D., Beazley, M., & Wanielista, M. (2021). Hydraulic and nutrient removal performance of vegetated filter strips with engineered infiltration media for treatment of roadway runoff. *Journal of environmental management*, 300, 113747. https://doi.org/https://doi.org/10.1016/j.jenvman.2021.113747

Sheikh, V., & Izanloo, R. (2021). Assessment of low impact development stormwater management alternatives in the city of Bojnord, Iran. *Urban Water Journal*, *18*(6), 449-464. https://doi.org/10.1080/1573062X.2021.1893364

Snodgrass, J. W., Moore, J., Lev, S. M., Casey, R. E., Ownby, D. R., Flora, R. F., & Izzo, G. (2017). Influence of Modern Stormwater Management Practices on Transport of Road Salt to Surface Waters. *Environmental Science & Technology*, *51*(8), 4165-4172. https://doi.org/10.1021/acs.est.6b03107

Song, B., & Park, K. (2021). Temperature trend analysis associated with land-cover changes using time-series data (1980–2019) from 38 weather stations in South Korea. *Sustainable Cities and Society*, *65*, 102615. https://doi.org/https://doi.org/10.1016/j.scs.2020.102615

Stefanakis, A. I. (2019). *The Role of Constructed Wetlands as Green Infrastructure for Sustainable Urban Water Management. Sustainability*, 11(24), 6981. https://www.mdpi.com/2071-1050/11/24/6981

Stefanidis, S., & Stathis, D. (2013). Assessment of flood hazard based on natural and anthropogenic factors using analytic hierarchy process (AHP). *Natural hazards, 68*, 569-585.

Steffen, J., Jensen, M., Pomeroy, C. A., & Burian, S. J. (2013). Water supply and stormwater management benefits of residential rainwater harvesting in US cities. *JAWRA Journal of the American Water Resources Association*, *49*(4), 810-824.

Su, J., Wang, M., Zhang, D., Sun, C., Zhao, X., & Razi, M. A. B. M. (2024). A systematic and bibliometric review of bioretention system (BRS) for urban ecosystem regulation services. *Urban Climate*, *55*, 101923. https://doi.org/https://doi.org/10.1016/j.uclim.2024.101923

Tabari, H., Marofi, S., Aeini, A., Talaee, P. H., & Mohammadi, K. (2011). Trend analysis of reference evapotranspiration in the western half of Iran. *Agricultural and Forest Meteorology*, *151*(2), 128-136. https://doi.org/https://doi.org/10.1016/j.agrformet.2010.09.009

Tang, G., Clark, M. P., Papalexiou, S. M., Ma, Z., & Hong, Y. (2020). Have satellite precipitation products improved over last two decades? A comprehensive comparison of GPM IMERG with nine satellite and reanalysis datasets. *Remote Sensing of Environment*, *240*, 111697. https://doi.org/https://doi.org/10.1016/j.rse.2020.111697

Tansar, H., Li, F., Zheng, F., & Duan, H.-F. (2024). A critical review on optimization and implementation of green-grey infrastructures for sustainable urban stormwater management. *AQUA - Water Infrastructure, Ecosystems and Society*, *73*(6), 1135-1150. https://doi.org/10.2166/aqua.2024.310

Thackeray, C. W., Hall, A., Norris, J., & Chen, D. (2022). Constraining the increased frequency of global precipitation extremes under warming. *Nature Climate Change*, *12*(5), 441-448.

Tian, Q., Prange, M., & Merkel, U. (2016). Precipitation and temperature changes in the major Chinese river basins during 1957–2013 and links to sea surface temperature. *Journal of Hydrology*, *536*, 208-221. https://doi.org/https://doi.org/10.1016/j.jhydrol.2016.02.048

Tolson, B. A., & Shoemaker, C. A. (2007). Dynamically dimensioned search algorithm for computationally efficient watershed model calibration. *Water Resources Research*, *43*(1). https://doi.org/https://doi.org/10.1029/2005WR004723

Tosunoglu, F., & Kisi, O. (2017). Trend Analysis of Maximum Hydrologic Drought Variables Using Mann–Kendall and Şen's Innovative Trend Method. *River Research and Applications*, *33*(4), 597-610. https://doi.org/https://doi.org/10.1002/rra.3106

Touhedi, H., Kankal, M., & Yıldız, M. B. (2023). Trend analysis of maximum rainfall series of standard durations in Turkey with innovative methods. *Natural hazards*, *119*(3), 1479-1511. https://doi.org/10.1007/s11069-023-06085-9

Triantaphyllou, E., & Mann, S. H. (1995). Using the analytic hierarchy process for decision making in engineering applications: some challenges. *International journal of industrial engineering: applications and practice*, *2*(1), 35-44.

Tulger Kara, G., & Elbir, T. (2024). Evaluation of ERA5 and MERRA-2 Reanalysis Datasets over the Aegean Region, Türkiye [ERA5 ve MERRA-2 Yeniden Analiz Veri Setlerinin Ege Bölgesi Genelinde Değerlendirilmesi]. *Dokuz Eylül Üniversitesi Mühendislik Fakültesi Fen ve Mühendislik Dergisi*, *26*(76), 9-21. https://doi.org/10.21205/deufmd.2024267602

UN. (2022). *World Population Prospects 2022: Summary of Results.* P. D. United Nations Department of Economic and Social Affairs.

URL-1 <https://www.eng.buffalo.edu/~lsmatott/Ostrich/OstrichMain.html> , date retrieved 15.06.2023.

Von Gunten, K., Konhauser, K. O., & Alessi, D. S. (2020). Potential of asphalt concrete as a source of trace metals. *Environmental Geochemistry and Health*, *42*(2), 397-405. https://doi.org/10.1007/s10653-019-00370-y

Weiss, P. T., Kayhanian, M., Gulliver, J. S., & Khazanovich, L. (2019). Permeable pavement in northern North American urban areas: research review and knowledge gaps. *International Journal of Pavement Engineering*, *20*(2), 143-162. https://doi.org/10.1080/10298436.2017.1279482

Wenger, C. (2015). Better use and management of levees: reducing flood risk in a changing climate. *Environmental Reviews*, *23*(2), 240-255.

Wu, H., & Qian, H. (2017). Innovative trend analysis of annual and seasonal rainfall and extreme values in Shaanxi, China, since the 1950s. *International Journal of Climatology*, *37*(5), 2582-2592. https://doi.org/https://doi.org/10.1002/joc.4866

Xie, Y., Wang, H., Wang, K., Ge, X., & Ying, X. (2024). The Application and Potential of Multi-Objective Optimization Algorithms in Decision-Making for LID Facilities Layout. *Water Resources Management*, *38*(14), 5403-5417. https://doi.org/10.1007/s11269-024-03926-5

Yetik, A. K., Arslan, B., & Şen, B. (2024). Trends and variability in precipitation across Turkey: a multimethod statistical analysis. *Theoretical and Applied Climatology*, *155*(1), 473-488. https://doi.org/10.1007/s00704-023-04645-4

Zahmatkesh, Z., Burian, S. J., Karamouz, M., Tavakol-Davani, H., & Goharian, E. (2015). Low-Impact Development Practices to Mitigate Climate Change Effects on Urban Stormwater Runoff: Case Study of New York City. *Journal of Irrigation and Drainage Engineering*, *141*(1), 04014043. https://doi.org/doi:10.1061/(ASCE)IR.1943-4774.0000770

Zhang, D., Gersberg, R. M., Ng, W. J., & Tan, S. K. (2017). Conventional and decentralized urban stormwater management: A comparison through case studies of Singapore and Berlin, Germany. *Urban Water Journal*, *14*(2), 113-124. https://doi.org/10.1080/1573062X.2015.1076488

Zheng, X., Zou, Y., Lounsbury, A. W., Wang, C., & Wang, R. (2021). Green roofs for stormwater runoff retention: A global quantitative synthesis of the performance. *Resources, Conservation and Recycling*, *170*, 105577. https://doi.org/https://doi.org/10.1016/j.resconrec.2021.105577

Zhuang, Q., Li, M., & Lu, Z. (2023). Assessing runoff control of low impact development in Hong Kong's dense community with reliable SWMM setup and calibration. *Journal of environmental management*, *345*, 118599. https://doi.org/https://doi.org/10.1016/j.jenvman.2023.118599

Zittis, G. (2018). Observed rainfall trends and precipitation uncertainty in the vicinity of the Mediterranean, Middle East and North Africa. *Theoretical and Applied Climatology*, *134*(3), 1207-1230. https://doi.org/10.1007/s00704-017-2333-0

APPENDICES

APPENDIX A: Table.

APPENDIX A : Table.

Table A.1 : Specific residential and industrial areas, suitability rank, Maximum and allowed number of RB, CI, and DW units for subcatchments S1 to S18.

No	Residential Area (m2)	Industrial Area (m2)	Max No of Rain Barrel	Rank for Rain Barrel	Allowed No of Rain Barrel	Max No of Cistern	Rank for Cistern	Allowed No of Cistern	Max No of Drywell	Rank for Drywell	Allowed No of Drywell
S1	749000	0	7490	11	6756	0	31	0	1498	2	1483
S2	171079.8	0	1710.798	50	889	0	49	0	342.1596	10	312
S3	0	0	0	101	0	0	101	0	0	17	0
S4	103781.6	0	1037.816	62	417	0	57	0	207.5632	1	208
S5	0	0	0	66	0	0	59	0	0	12	0
S6	0	0	0	102	0	0	102	0	0	18	0
S7	0	0	0	71	0	0	62	0	0	21	0
S8	0	0	0	100	0	0	100	0	0	35	0
S9	0	0	0	99	0	0	99	0	0	33	0
S10	0	0	0	78	0	0	67	0	0	43	0
S11	0	235252.8	0	42	0	235.2528	35	157	470.5056	3	461
S12	21851.69	0	218.5169	88	32	0	75	0	43.70338	9	40
S13	44302.7	0	443.027	95	35	0	97	0	88.6054	7	83
S14	16693.85	0	166.9385	98	8	0	96	0	33.3877	5	32
S15	162792	48944	1627.92	75	447	48.944	77	12	423.472	6	403
S16	132483.5	0	1324.835	79	312	0	80	0	264.967	14	231
S17	152160.22	25206	1521.6022	93	149	25.206	90	3	354.73244	4	344
S18	93900	0	939	87	147	0	95	0	187.8	11	169

Table A.2 : Specific residential and industrial areas, suitability rank, Maximum and allowed number of RB, CI, and DW units for subcatchments S19 to S39.

No	Residential Area (m^2)	Industrial Area (m^2)	Max No of Rain Barrel	Rank for Rain Barrel	Allowed No of Rain Barrel	Max No of Cistern	Rank for Cistern	Allowed No of Cistern	Max No of Drywell	Rank for Drywell	Allowed No of Drywell
S19	204703.3	0	2047.033	58	903	0	72	0	409.4066	19	337
S20	352073.4	0	3520.734	35	2347	0	52	0	704.1468	16	601
S21	181653.12	71018.64	1816.5312	81	392	71.01864	73	21	505.34352	8	471
S22	221900	0	2219	63	870	0	86	0	443.8	15	383
S23	173200	0	1732	89	238	0	98	0	346.4	13	306
S24	272300	0	2723	53	1335	0	78	0	544.6	23	427
S25	226200	0	2262	61	931	0	85	0	452.4	22	359
S26	114100	0	1141	86	190	0	94	0	228.2	26	172
S27	243600	0	2436	57	1099	0	82	0	487.2	25	373
S28	0	0	0	91	0	0	81	0	0	30	0
S29	0	663000	0	39	0	663	18	553	1326	20	1079
S30	0	176600	0	96	0	176.6	56	81	353.2	24	274
S31	0	150660	0	92	0	150.66	61	62	301.32	28	222
S32	127600	0	1276	83	250	0	93	0	255.2	27	190
S33	239600	0	2396	59	1034	0	83	0	479.2	31	338
S34	339264	0	3392.64	40	2095	0	55	0	678.528	34	459
S35	0	0	0	82	0	0	69	0	0	38	0
S36	0	747000	0	26	0	747	12	666	1494	29	1084
S37	0	161300	0	97	0	161.3	60	68	322.6	37	209
S38	0	235400	0	94	0	235.4	50	122	470.8	36	309
S39	129580	0	1295.8	84	241	0	87	0	259.16	39	163

Table A.3 : Specific residential and industrial areas, suitability rank, Maximum and allowed number of RB, CI, and DW units for subcatchments S40 to S60.

No	Residential Area (m^2)	Industrial Area (m^2)	Max No of Rain Barrel	Rank for Rain Barrel	Allowed No of Rain Barrel	Max No of Cistern	Rank for Cistern	Allowed No of Cistern	Max No of Drywell	Rank for Drywell	Allowed No of Drywell
S40	0	655000	0	37	0	655	17	552	1310	32	912
S41	0	807000	0	20	0	807	10	736	1614	41	981
S42	0	863000	0	15	0	863	8	804	1726	42	1032
S43	0	0	0	90	0	0	79	0	0	45	0
S44	305400	203600	3054	38	1946	203.6	44	118	1018	40	629
S45	0	690000	0	13	0	690	9	636	1380	44	798
S46	0	735000	0	29	0	735	13	649	1470	46	821
S47	0	348664	0	69	0	348.664	42	209	697.328	47	383
S48	0	355340	0	28	0	355.34	23	279	710.68	49	376
S49	0	473154	0	27	0	473.154	21	380	946.308	50	492
S50	681200	628800	6812	4	6612	628.8	3	616	2620	48	1413
S51	910020	135980	9100.2	5	8743	135.98	11	123	2092	52	1046
S52	764000	0	7640	10	6966	0	28	0	1528	54	734
S53	0	882000	0	14	0	882	7	830	1764	53	865
S54	200032	457968	2000.32	31	1412	457.968	24	355	1316	51	671
S55	120270	512730	1202.7	33	825	512.73	22	407	1266	56	583
S56	520000	520000	5200	6	4945	520	6	495	2080	58	918
S57	234158	95642	2341.58	55	1102	95.642	64	37	659.6	64	252
S58	136579.5	0	1365.795	56	629	0	65	0	273.159	55	129
S59	150524	78683	1505.24	65	561	78.683	66	29	458.414	57	207
S60	149548	82404	1495.48	70	484	82.404	68	28	463.904	59	200

Table A.4 : Specific residential and industrial areas, suitability rank, Maximum and allowed number of RB, CI, and DW units for subcatchments S60 to S80.

No	Residential Area (m^2)	Industrial Area (m^2)	Max No of Rain Barrel	Rank for Rain Barrel	Allowed No of Rain Barrel	Max No of Cistern	Rank for Cistern	Allowed No of Cistern	Max No of Drywell	Rank for Drywell	Allowed No of Drywell
S60	149548	82404	1495.48	70	484	82.404	68	28	463.904	59	200
S61	434010	194990	4340.1	22	3447	194.99	33	134	1258	62	506
S62	475580	126420	4755.8	23	3730	126.42	40	78	1204	65	449
S63	492800	123200	4928	19	4058	123.2	38	79	1232	68	423
S64	616000	0	6160	16	5254	0	45	0	1232	67	435
S65	301539	0	3015.39	48	1626	0	70	0	603.078	60	254
S66	0	637000	0	41	0	637	20	518	1274	73	375
S67	609880	0	6098.8	17	5142	0	39	0	1219.76	63	478
S68	681450	203550	6814.5	9	6280	203.55	15	176	1770	70	573
S69	930240	323000	9302.4	3	9120	323	4	314	2506.48	72	762
S70	601000	0	6010	18	5008	0	46	0	1202	79	283
S71	96300	171200	963	85	170	171.2	58	76	535	81	115
S72	727000	0	7270	12	6486	0	34	0	1454	84	271
S73	128250	128250	1282.5	34	868	128.25	36	84	513	90	65
S74	0	0	0	32	0	0	32	0	0	93	0
S75	0	524210	0	45	0	524.21	25	401	1048.42	78	257
S76	82280	665720	822.8	24	637	665.72	14	581	1496	76	396
S77	98208	218592	982.08	77	250	218.592	51	111	633.6	74	180
S78	0	399400	0	74	0	399.4	37	258	798.8	82	164
S79	69202	425098	692.02	52	346	425.098	30	304	988.6	80	223
S80	98800	421200	988	47	542	421.2	29	306	1040	86	173

Table A.5 : Specific residential and industrial areas, suitability rank, Maximum and allowed number of RB, CI, and DW units for subcatchments S81 to S102.

No	Residential Area (m^2)	Industrial Area (m^2)	Max No of Rain Barrel	Rank for Rain Barrel	Allowed No of Rain Barrel	Max No of Cistern	Rank for Cistern	Allowed No of Cistern	Max No of Drywell	Rank for Drywell	Allowed No of Drywell
S81	88550	571550	885.5	25	677	571.55	19	471	1320.2	92	142
S82	191200	0	1912	68	656	0	89	0	382.4	61	157
S83	197400	0	1974	67	697	0	88	0	394.8	66	143
S84	163500	0	1635	72	497	0	91	0	327	69	109
S85	295400	0	2954	51	1506	0	76	0	590.8	71	185
S86	417100	0	4171	36	2740	0	63	0	834.2	75	229
S87	837490	0	8374.9	7	7882	0	16	0	1674.98	77	427
S88	315172	99528	3151.72	44	1823	99.528	54	48	829.4	83	163
S89	110075	330225	1100.75	54	529	330.225	43	194	880.6	89	121
S90	267840	164160	2678.4	46	1497	164.16	48	89	864	91	102
S91	154700	0	1547	76	410	0	92	0	309.4	85	55
S92	358200	0	3582	43	2107	0	71	0	716.4	87	112
S93	236800	0	2368	60	998	0	84	0	473.6	88	70
S94	16320	239360	163.2	64	62	239.36	47	131	511.36	96	35
S95	401380	256620	4013.8	21	3227	256.62	26	194	1316	94	116
S96	305400	0	3054	49	1617	0	74	0	610.8	97	36
S97	0	378000	0	80	0	378	41	230	756	100	22
S98	97720	167520	977.2	30	699	167.52	27	125	530.48	102	0
S99	0	641760	0	8	0	641.76	5	617	1283.52	95	101
S100	0	124527	0	73	0	124.527	53	61	249.054	98	12
S101	0	1321840	0	2	0	1321.84	2	1309	2643.68	99	104
S102	38240	0	382.4	1	382	0	1	0	76.48	101	1

CURRICULUM VITAE

Name Surname : **Sina SAM**

EDUCATION :

- **B.Sc.** : 2016, University of Tanriz, Civil Engineering.

- **M.Sc.** : 2019, Istanbul Technical University, Civil Engineering, Hydraulics and Water Resources Engineering.

PUBLICATIONS, PRESENTATIONS AND PATENTS ON THE THESIS:

- **Sam, S., & Özger, M.** (2025). A multi-method and multi-duration trend analysis of temperature and precipitation in Istanbul, Turkey, by using meteorological records, MERRA-2 reanalysis, and IMERG estimations. *HydroResearch*, 8, 209-222. https://doi.org/https://doi.org/10.1016/j.hydres.2024.11.005
- **Sam, S., & Özger, M.** (2025). İstanbul İçin Çok Yöntemli Sıcaklık ve Yağış Eğilim Analizi. *11'inci Türkiye Kuvaterner Sempozyumu.*
- **Sam, S., & Özger, M.** (2025-Under review). An integrated framework based on AHP and auto-calibration of SWMM for implementing and assessing LID practices. *(Natural Hazards Journal).*

OTHER PUBLICATIONS, PRESENTATIONS AND PATENTS:

- **Samouei, S., & Özger, M.** (2020). Evaluating the performance of low impact development practices in urban runoff mitigation through distributed and combined implementation. *Journal of Hydroinformatics*, 22(6), 1506-1520. https://doi.org/10.2166/hydro.2020.054

- **Samouei, S., & Özger, M.** (2020). A Rainfall-Runoff model for highly urbanized areas: A case study at Istanbul Technical University main campus. *IOP Conference Series: Materials Science and Engineering*, 737(1), 012163. https://doi.org/10.1088/1757-899X/737/1/012163